DESIGN AND SIMULATION OF VARIANTS OF KOCH MODELS FOR FRACTAL ANTENNA

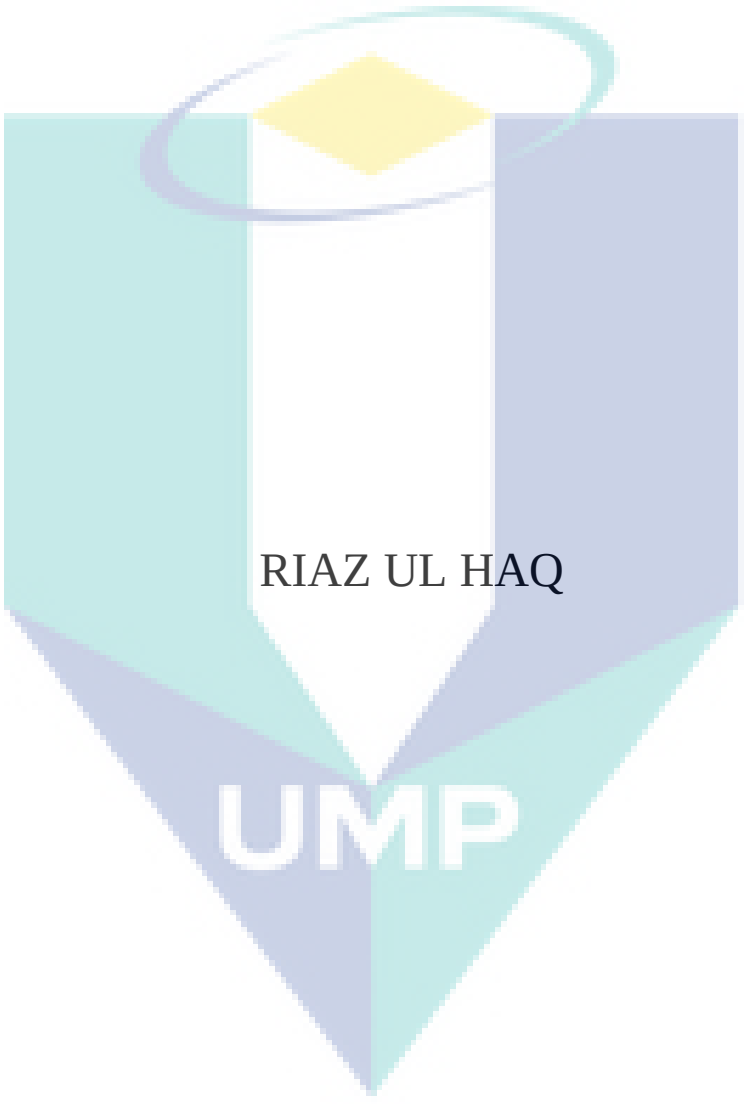

RIAZ UL HAQ

Faculty of Computer Systems and Software Engineering
UNIVERSITI MALAYSIA PAHANG

SUPERIOR FRACTAL ANTENNAS

RIAZ UL HAQ

Thesis submitted in fulfillment of the requirements for the award of the degree of Master of Science (Computer Science)

UNIVERSITI MALAYSIA PAHANG

JUL 2011

SUPERVISOR'S DECLARATION

I hereby declare that I have checked this thesis and in my opinion, this thesis is satisfactory in terms of scope and quality for the award of the degree of Master of Science in Computer Science.

Name of Supervisor: DR. NORROZILA SULAIMAN
Position: SENIOR LECTURER
Date:

Name of Co-Supervisor: DR. MAMTA RANI
Position: ASSOCIATE PROFESSOR

STUDENT'S DECLARATION

I hereby declare that the work in this thesis is my own except for quotations and summaries, which have been duly acknowledged. The thesis has not been accepted for any degree and is not concurrently submitted for award of other degree.

Name: RIAZ UL HAQ
ID Number: MCC 09003
Date:

To my parents

ACKNOWLEDGEMENT

In the name of all mighty Allah the most gracious & merciful, who provides me guidance, strength and enabled me to complete this desertion, I pay my all gratitude to Allah.

Completion of the thesis involves support and help of numerous persons. I would like to take this opportunity to express my gratitude to my supervisor Dr. Norrozila Sulaiman for her constant guidance, encouragement and help during the whole research work. I thank her for her continuous valuable comments and suggestions.

I express my deep gratitude to my co-supervisor Dr. Mamta Rani for her technical guidance in research. I remember our long technical discussion sessions whenever I stuck at certain points. I thank her for her valuable suggestions during the preparation of the thesis.

I would like to thank Dr. Jasni Mohammad Zain, Dean, Faculty of Computer Systems & Software Engineering, Dr. Adzhar Kamaluddin, Deputy Dean (Academics), Dr. Mazlina Abdul Mazid, Deputy Dean (Research) and Mr. Aziman Abdullah for their administrative help. Furthermore, I extend my many thanks to FSKKP admin staff Ms. Fauziah, Ms. Nor Aftalina and Ms. Rohaiyya for the support. I thank to all the FSKKP, UMP staff.

At this point, I would like to thank Mr. Ilzam (RMC), Mr. Iskandara (RMC), Mr. Abdurrahmaan (RMC), Mr. Ramli (Finance), and whole CGS and International Office staff for the help in their own ways. I extend my deep thanks to Mr. Shapon Anwar, Lecturer, Faculty of Electrical & Communication, UTHM and my friend Inam Abbasi for their help in performing the simulation work.

My special thanks to my friend Hemin Mohyoddin for his continuous motivation and fruitful discussions during the course. He was always there whenever I used to be in low spirit. I thank to all my friends in hostel who provided me homely environment in Malaysia.

Last but not the least, I express my indebtedness to my parents for their prayers, endless support and encouragement during the course of a long and tedious struggle to accomplish the work in time.

ABSTRACT

Fractal antennas are multi-resonant, wideband and smaller in size and have good applications in areas like mission-oriented activities. Many fractal shapes work better as antenna than circular antenna. A good antenna is mainly measured in terms of return loss (RL), Voltage Standing Wave Ratio (VSWR) and bandwidth. The performance of a fractal antenna is directly related to its dimension. Koch curve and many of its variants have been studied widely as fractal antennas and their antenna characteristics have been improved. There is a continuous need to improve the performance of fractal antenna in terms of reduced size, lesser VSWR, lesser RL and wider bandwidth. For improved performance, shapes of further lesser dimensions with smaller sizes are required. It is also required to have more flexibility in design of fractal antennas of smaller sizes. The self-similarity dimension of the Koch curve geometry can be varied by changing the generator used in the recursive Iterated Function System (IFS). In the research work, new variants of Koch models have been generated by dividing the initiator into unequal parts and their mathematical properties have been analyzed. Many of the new variants of Koch models are of reduced size. One of the reduced-sized Koch model have been simulated and it was found that it has better performance than the von Koch curve in terms of RL, VSWR and bandwidth. One of the new variants, which is of the same size and dimension as conventional Koch curve but with different design, have been generated, simulated and compared with the conventional Koch curve. It was found that the two curves of the same size and dimension performed differently due to different designs.

ABSTRAK

Antena fraktal mempunyai pelbagai salunan, berjalur lebar dan bersaiz lebih kecil serta mempunyai aplikasi yang baik dalam bidang yang berorientasikan misi. Kebanyakkan antena yang berbentuk fractal berfungsi lebih baik daripada antena berbentuk bulat. Antenna yang baik diukur dari segi *return loss (RL)*, *Voltage Standing Wave Ratio (VSWR)* dan jalurlebar. Prestasi antena fraktal berkait secara langsung dengan dimensinya. Pelbagai jenis lengkung *Koch* telah dikaji secara meluas sebagai antena fractal dan ciri-ciri antenna telah bertambah baik. Terdapat keperluan yang berterusan untuk meningkatkan prestasi antena fraktal dari segi saiz yang lebih kecil, *VSWR* yang kurang, *RL* yang lebih rendah dan jalurlebar yang lebih luas. Untuk prestasi yang lebih baik, bentuk dimensi yang kurang serta saiz yang lebih kecil diperlukan. Reka bentuk antena fraktal yang bersaiz lebih kecil juga memerlukan lebih fleksibiliti. Dimensi diri keserupaan geometri lengkung *Koch* boleh diubah dengan menukar penjana yang digunakan dalam fungsi sistem berintegrasi yang rekursif. Dalam kerja penyelidikan yang dijalankan, varian baru model *Koch* telah dihasilkan dengan membahagikan pemula ke beberapa bahagian yang tidak sama dan sifat matematiknya telah dianalisa. Kebanyakan varian baru model Koch bersaiz lebih kecil. Salah satu daripada model *Koch* yang bersaiz lebih kecil telah disimulasi dan ianya didapati lebih baik daripada lengkung *von Koch* dimana *RL* berkurangan, *VSWR* lebih rendah dan jalurlebar yang lebih luas. Salah satu varian baru, yang bersaiz dan dimensi yang sama dengan lengkung *Koch* konvensional tetapi dengan reka bentuk yang berlainan telah dihasilkan, disimulasi dan dibandingkan dengan lengkung *Koch* konvensional. Didapati bahawa kedua-dua lengkung yang bersaiz dan berdimensi sama, mempunyai keupayaan yang berbeza kerana reka bentuk yang berlainan.

TABLE OF CONTENTS

LIST OF TABLES

LIST OF FIGURES

LIST OF ABBREVIATIONS

CST	Computer Simulation Technology
dB	Decibel
HPBW	Half Power Bandwidth
IFS	Iterated Function System
SO	Superior Iterates
VSWR	Voltage Standing Wave Ratio

CHAPTER 1

INTRODUCTION

1.1 INTRODUCTION

Modern telecommunication systems require antennas with wider bandwidths and smaller sizes than conventional antennas. This had initiated antenna research in various directions, one of which is by using fractal shaped antenna elements. In recent years of development in antenna area for communication, fractal geometry has occupied front of interest. All the basic trigonometric shapes are already utilized in antenna design and their radiation mechanisms have been well explored in communication. Use of fractals as antennas offers better radiation pattern in communication and offers more controlling parameters to designer.

1.1.1 Fractal Geometries in Antenna

Several antenna configurations based on fractal geometries have been reported in recent years. Antennas with reduced size have been obtained using Hilbert curve fractal geometry. Furthermore, more design equations for these antennas are obtained in terms of its geometrical parameters such as fractal dimension. Antenna properties have also been linked to fractal dimension of the geometry.

Fractal antennas are multi-resonant and smaller in size. Qualitatively, multi-band characteristics have been associated with the self-similarity of the geometry and Hausdorff dimensions are associated with size. Extensive researches are going on towards quantitative relation between antenna properties and fractal parameters in

communication. Any variation in fractal parameters has direct impact on the primary resonant frequency of the antenna, input resistance at primary resonant frequency, and the ratio of the first two resonant frequencies. In other words, these antenna features can be quantitatively linked to the fractal dimension of the geometry. Fractal antennas with less self-similarity dimension give better radiation pattern. This finding can lead to increased flexibility in designing antennas for communication using fractal geometries. These results have been experimentally validated by the researchers (Vinoy et al., 2003, 2004).

1.1.2 The von Koch Curve

Initiator of the von Koch curve is a straight line. Fractal dimension of the von Koch curve is ≈ 1.262. The Koch curve is a graphical curve, which is continuous everywhere but not differentiable at any point. The length of Koch curve is infinite. When Koch curve is generated on initiator triangle, Koch snowflake curve will be obtained. The beauty of the Koch snowflake is that its perimeter is infinite but area is compact and equal to $\frac{6\sqrt{3}}{5}r^2$, where r denotes the radius of the circle which accommodates the Koch snowflake. This geometrical property makes the Koch fractal as better antenna in place of circular antenna (Falconer, 2003).

1.1.3 Superior Fractals

In 2002 (Rani), two-step feedback machine have been implemented in fractal graphics via superior iterations and generated superior fractals. Since then a few fractal models have been improved based on the idea of unequal division of an initiator and thus the gallery of superior fractals have been enriched. New fractal carpets, fractal plants and superior Cantor sets are examples of superior fractals generated by unequal division of initiator.

Above mentioned superior fractal models suggest that there exists a whole gallery of fractal models for the same kind of problem rather than one model, and they have different fractal dimensions. For example, there used to exist a Cantor set and recently many superior Cantor sets have been suggested. In this new gallery of Cantor

sets, most of the objects have different fractal dimensions. Kumar (2010) gave a detailed study on superior fractals in his Master thesis and in future work, he suggested generation of superior Koch curves and their use as antenna.

1.2 MOTIVATION

The von Koch curve has been rigorously analyzed and widely used as fractal antenna. The performance of a fractal antenna is directly related to its dimension. Antennas of lesser dimension give better performance. To improve the antenna characteristics of the Koch curve, a few variants of Koch curve of lesser dimension has been given. Barcellos (1984) gave variants of Koch curve by dividing the initiator into 4 equal parts. These curves have a fixed dimension. Further, there was no suggestion to obtain the curves of lesser dimension. Vinoy, Jose and Vardan (2002) generated new shapes of Koch antenna by varying its indentation angle. All these variants have lesser dimension than the conventional Koch antenna. The curves given by Vinoy et al. occupy more area than the conventional Koch curve. So there is a need to propose Koch shapes of lesser dimension and compact size for better performance with compact in size. Also, there is a curiosity left in the literature whether the two different shapes with the same dimension will have the same performance as antenna or not.

1.3 PROBLEM STATEMENT

Fractal antennas are smaller in size, multi-resonant and wideband. Koch curve and many of its variants have been rigorously studied as fractal antennas and gradually their antenna characteristics have been improved. Few variants have a fixed lesser dimension and few variants have variable lesser dimensions but their area is wider than the conventional Koch curve. There is a continuous need to improve the performance of fractal antenna. For improved performance, shapes of further lesser dimensions with smaller sizes are required. In addition, it is required to have more flexibility in design of fractal antennas of smaller sizes.

1.4 OBJECTIVES OF THE STUDY

The objectives of the study are

i. To propose new design of Koch models by unequal division of the initiators, and measure their geometrical properties to be used as fractal antennas.

ii. To simulate the performance of the new design shapes as antenna.

1.5 OUTCOMES OF THE STUDY

The outcomes of the study are as follows:

i. Design of new variants of Koch curves and Koch snowflakes, and their classification.

ii. Rewriting systems for generation of new variants of Koch curves.

iii. Formulas to measure the geometrical properties of new variants of Koch fractals.

iv. A better Koch fractal antenna will be obtained.

1.6 ORGANIZATION OF THESIS

The thesis has been organized as follows:

Chapter 1 is introductory in nature. It explains the problem statement, objective of the work and related details of Koch curve.

Chapter 2 provides the basic concepts and literature review of fractals and antennas, which forms the basis of the research work.

In chapter 3, new antenna geometries that are new examples of superior fractals have been proposed and their productions rules have been defined. Also, new formulas have been given to measure the geometrical properties of new fractals.

In chapter 4, two new fractal antenna designs have been simulated and compared with the conventional antennas.

Finally, the research work has been concluded in Chapter 5. Also, future work has been suggested.

CHAPTER 2

LITERATURE REVIEW

2.1 INTRODUCTION TO FRACTALS

Large number of people believes that the geometry of nature is centered on simple figures such as a lines, circles, conic sections, polygons, sphere, quadratic surfaces and so on. For example, tyres of the vehicle are circular, solar system moves around the sun in elliptical orbit. Poles are cylindrical, etc. Have we ever thought, what is the shape of a mountain? Can we describe the structure of animals and plants? How can the networks of veins that supply blood be described by classical geometry? Many objects in nature are so complicated and irregular that it is hopeless to use classical geometry to model them. To analyze many of these questions fractals and mathematical chaos are the appropriate tools.

2.1.1 Definition

Benoît Mandelbrot coined the term “fractal” in 1975. The term “fractal” is derived from the Latin word “fractus”, which means "broken" or "fractured". A fractal is defined as a rough or fragmented geometric shape that can be divided into smaller parts and each of the parts is a reduced-size copy (or at least approximately) of the whole (Mandelbrot, 1982; Crownover, 1995). A mathematical fractal is based on an equation that undergoes iteration, a form of feedback based on recursion (Briggs, 1992).

Since, fractals are scale invariant, i.e., fractals appear similar at all levels of magnification, fractals are often considered to be infinitely complex objects (in informal terms). Examples of natural objects that are approximate fractals are: various vegetables (cauliflower and broccoli), coastlines, animal coloration patterns, clouds, snowflakes, mountain ranges, lightning bolts. However, not all self-similar objects are fractals. For example, the real line (a straight line) is formally self-similar but fails to have other fractal characteristics. It is irregular enough to be described in Euclidean terms (Crilly, 1991; Edgar, 1990).

A fractal often has the following features:

i. A fractal can not be described by traditional Euclidean geometric language as it is too irregular.
ii. It is self-similar (at least approximately).
iii. It is scale invariant, i.e., It has a fine structure at arbitrarily small scales.
iv. It has dimension in fractions.
v. It has a simple and recursive definition.

2.1.2 Backbone of the Fractals

Whole fractal theory is based on the feedback process. Feedback processes are fundamental in all sciences and has become backbone of fractal theory. Sir Issac Newton and Gotfried W. Leibnitz, first, introduced feedback processes independently about 300 years ago in the form of dynamical law. It is simple in principle. The same process is performed repeatedly with new input (Petigen et al., 2004). The output of a function at some iteration is the input for the next iteration. It can be easily understood by the following Figure 2.1.

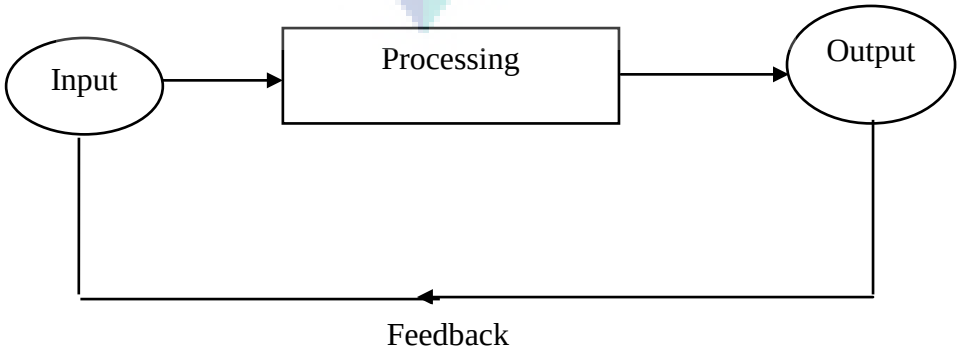

Figure 2.1: Feedback Process (Peitgen et. al., 2004)

2.1.3 Generation

There are four common techniques for generation of fractals:

i. Escape-time fractals: These are also known as "orbits" fractals, and defined by a complex functions. Mandelbrot sets, Julia sets, Burning Ship fractal, Nova fractal, the Lyapunov fractal, Biomorphs etc. are some popular examples of escape-time fractals. A Julia set, an example of escape-time fractal is shown in Figure 2.2 (Peitgen et. al., 2004).

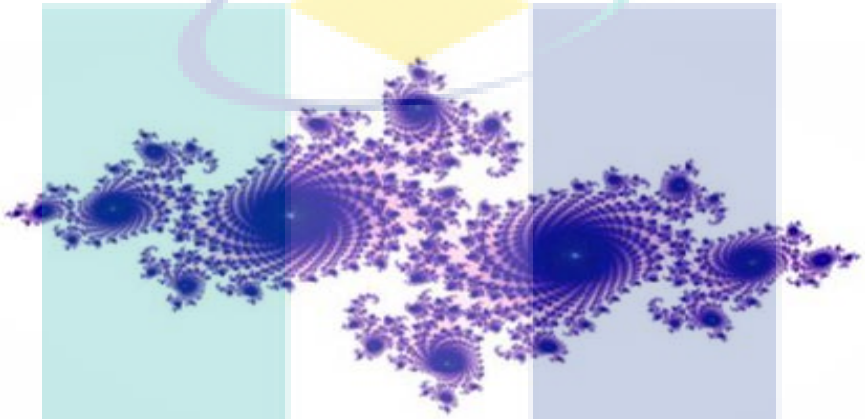

Figure 2.2: A Julia Set: An Example of Escape Time Fractal (Peitgen et. al., 2004)

ii. Iterated function systems (IFS): These fractals have a fixed geometric replacement rule. Examples of this type are the Cantor sets, fractal carpets, Sierpinski gaskets, Peano curve, Koch snowflakes, Harter-Highway dragon curve, T-square and Menger sponge. An example of IFS fractal is shown in Figure 2.3 (Crownover, 1995).

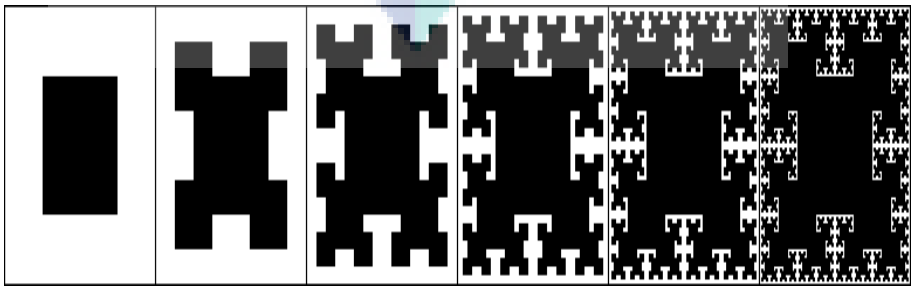

Figure 2.3: T-Square Fractal: An Example of IFS Fractal (Crownover, 1995)

iii. Random fractals: Random fractals are generated by stochastic rather than deterministic processes. Examples of these types are trajectories of the Brownian motion, Lacvy flight, fractal landscapes and the Brownian tree. A fractal landscape is shown in Figure 2.4 (Crownover, 1995).

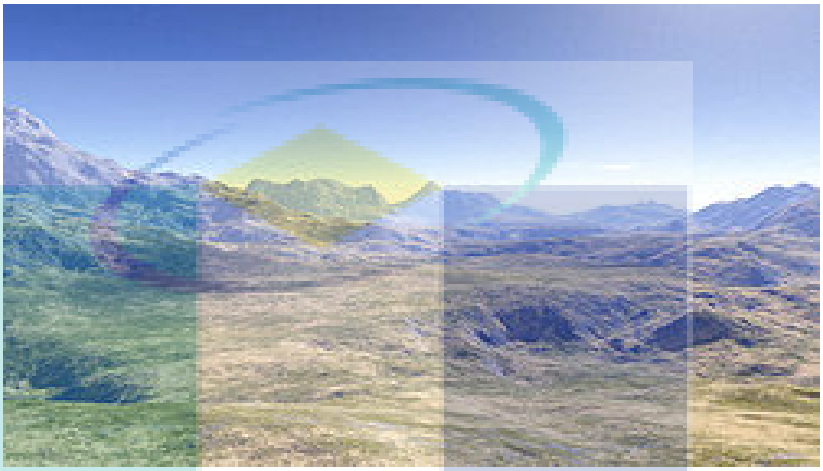

Figure 2.4: Fractal Landscape: An Example of Random Fractal (Crownover, 1995)

iv. Strange attractors: These kind of fractals are generated by iterating a map or the solution of a system obtained by iterating initial-value differential equations that exhibit chaos. See a strange attractor in Figure 2.5 (Peitgen et al., 2004).

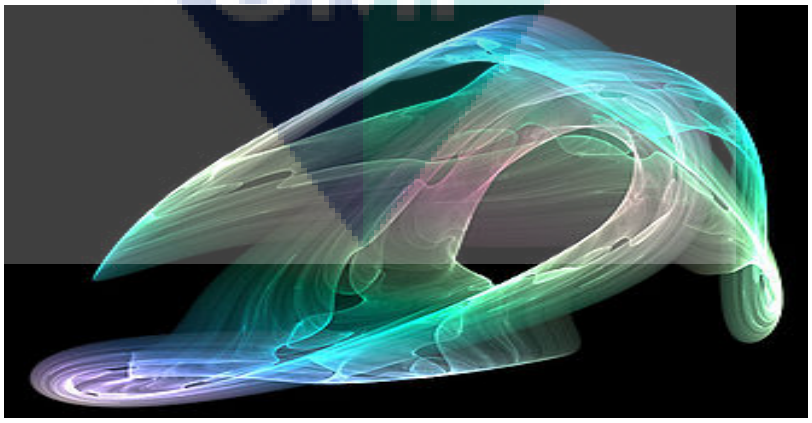

Figure 2.5: Visual Representation of a Strange Attractor (Peitgen et al., 2004)

2.1.4 Classification

Fractals can be classified according to their self-similarity. There are three types of self-similarity found in fractals (Peitgen et al., 2004; Crownover, 1995 and Schroeder, 1991):

i. Exact self-similarity
ii. Quasi-self-similarity
iii. Statistical self-similarity

Table 2.1: Self-Similarity Classification

	Exact self-similarity	**Quasi-self-similarity**	**Statistical self-similarity**
Form of self-similarity	The strongest type of self-similarity	Loose form of self-similarity	The weakest type of self-similarity
Self-similarity at scales	Fractal appears identical at different scales.	Fractal appears approximately (but not exactly) identical at different scales. Quasi-self-similar fractals contain small copies of the entire fractal in distorted and degenerate forms.	Fractal has numerical or statistical measures which are preserved across scales.
Example	Fractals defined by iterated function systems often display exact self similarity.	Fractals defined by recurrence relations are usually quasi-self-similar but not exactly self-similar.	Random fractals are examples of fractals which are statistically self-similar, but neither exactly nor quasi-self-similar.

2.1.5 Applications

The best thing about fractals is the variety of their applications, e.g., fractal antenna (Cohen, 1996), fractals in nature (Mandelbrot, 1982; Barnsley, 2006), fractals in olden days as Meru or Pascal triangle (Patwardhan, Naimpally & Singh, 2001; Rani, 2005), fractal architecture (Jackson, 2004), fractal weapon (Rani & Kumar, 2002), fractal noise (Rani & Agarwal, 2010), fractals image coding (Wohlberg & Jager, 1999) etc. The applications of fractals are found in every small or large parts of the universe, i.e., from bacteria cultures to galaxies to our body. Barnsley and Hawley (1993) wrote a book "Fractals Everywhere" in which they suggested applications of fractals in a lot of areas.

A list of application areas of fractals apart from the above mentioned areas are diffusion, economy, fractal art, fractal music, landscapes, Newton's method, special effects, weather, galaxies, rings of Saturn, bacteria cultures, chemical reactions, human anatomy, molecules, Botany, population growth, clouds, coastlines and borderlines, Chemistry, medical science, film industry, wavelet theory, nanotechnology etc (see for instance, Bunde, Armin & Havlin, 1994, Peitgen, Henriques, Penedo, 1991; Peitgen & Richter, 1986 and Petigen & Saupe, 1988).

2.2 FRACTAL DIMENSION

At the turn of the nineteenth century, it was one of the major problems in science to determine what dimension means and which properties it has. Mathematicians have come up with ten different notions of dimension: self-similarity dimension, box-counting dimension, Hausdorff dimension, topological dimension, fractal dimension, information dimension, capacity dimension and more. Some of them make sense in certain situations but not in other situations. However, in certain situations, they all make sense and all are the same. Some are used very often and easily in fractal theory. However, all the different dimensions are special forms of Mandelbrot's fractal dimension (Peitgen, Jurgen & Saupe, 2004, p. 202). Here, self-similarity dimension is explained in brief, which is one of the most popular dimension methods in fractal graphics.

Self-Similarity Dimension

This is generally used in calculating dimension of self-similar figures. There is a nice power relation between the number of pieces *n* of an object and the reduction factor *s* as shown in Eq. (2.1) and Eq. (2.2).

$$n = 1/s^D \tag{2.1}$$

where *n* is the number of pieces of an object,
D is the dimension of the object and
s is the scaling factor.

From Eq. (2.1), following equation is obtained:

$$\log n = D\log(1/s) \tag{2.2}$$

For example, in following square, apply $s = 1/3$ then $n = 9$

So log 9 = D log 3 and D = 2. Thus the dimension of square is 2.

2.3 FRACTAL ANTENNAS

In today's world of wireless communications, there has been an increasing need for more compact and portable communications systems. Just as the size of circuitry has evolved to transceivers on a single chip, there is also a need to evolve antenna

designs to minimize the size. Currently, many portable communications systems use a simple monopole with a matching circuit. However, if the monopole was very short compared to the wavelength, the radiation resistance decreases, the stored reactive energy increases, and the radiation efficiency would decrease. As a result, the matching circuitry can become quite complicated. As a solution to minimizing the antenna size while keeping high radiation efficiency, fractal antennas can be implemented. The fractal antenna not only has a large effective length, but the contours of its shape can generate a capacitance or inductance that can help to match the antenna to the circuit. Fractal antennas can take on various shapes and forms. For example, a quarter wavelength monopole can be transformed into a similarly shorter antenna by the Koch fractal (Vinoy, 2002).

2.4 CLASSICAL FRACTAL GEOMETRIES IN ANTENNA

Here, few fractal geometries from its classical gallery (Peitgen et al., 2004) are given that has been used as antenna in wireless communication.

2.4.1 The Koch Curve

Swedish mathematician Helge von Koch introduced what is now called Koch curve. Initiator of the Koch curve is a straight line it will be partitioned into three equal parts. Middle part will be replaced by an equilateral triangle. This is the basic step and the reduced figure will have four equal lines joined with each other. This new figure is known as a generator. The same operation will be repeated be on each of the four lines (Falconer, 2003). Iterative construction of the Koch curve is given in Figure 2.6 (a-d).

When initiator is a triangle and the same procedure is applied, Koch snowflake curve is obtained. Iterative construction of the Koch snowflake curve is shown in Figure 2.7 (a-d) (Falconer, 2003; Peitgen Jurgen & Saupe, 2004; Shroeder, 1991).

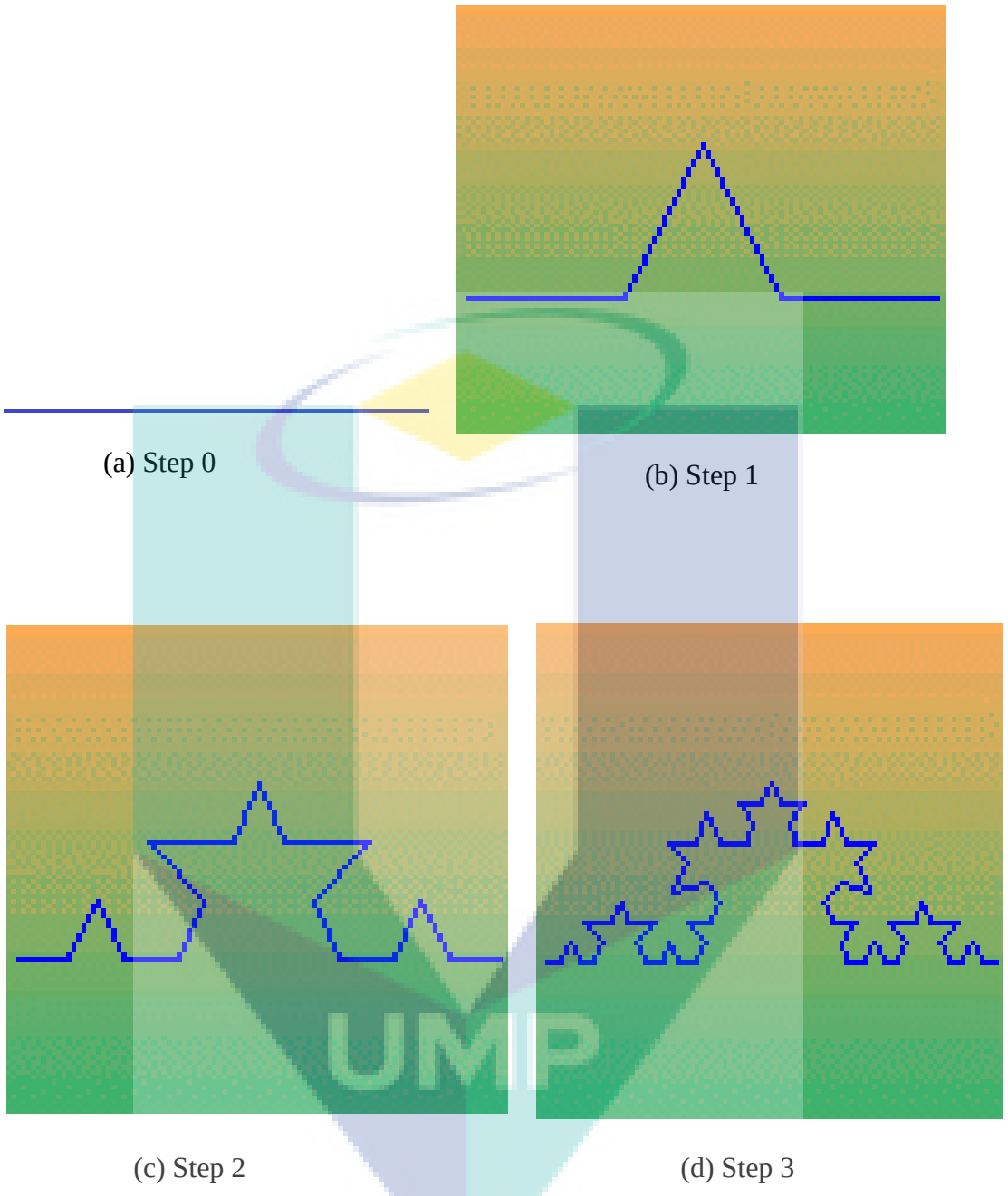

Figure 2.6: Iterative Construction of Koch Curve (Shroeder, 1991)

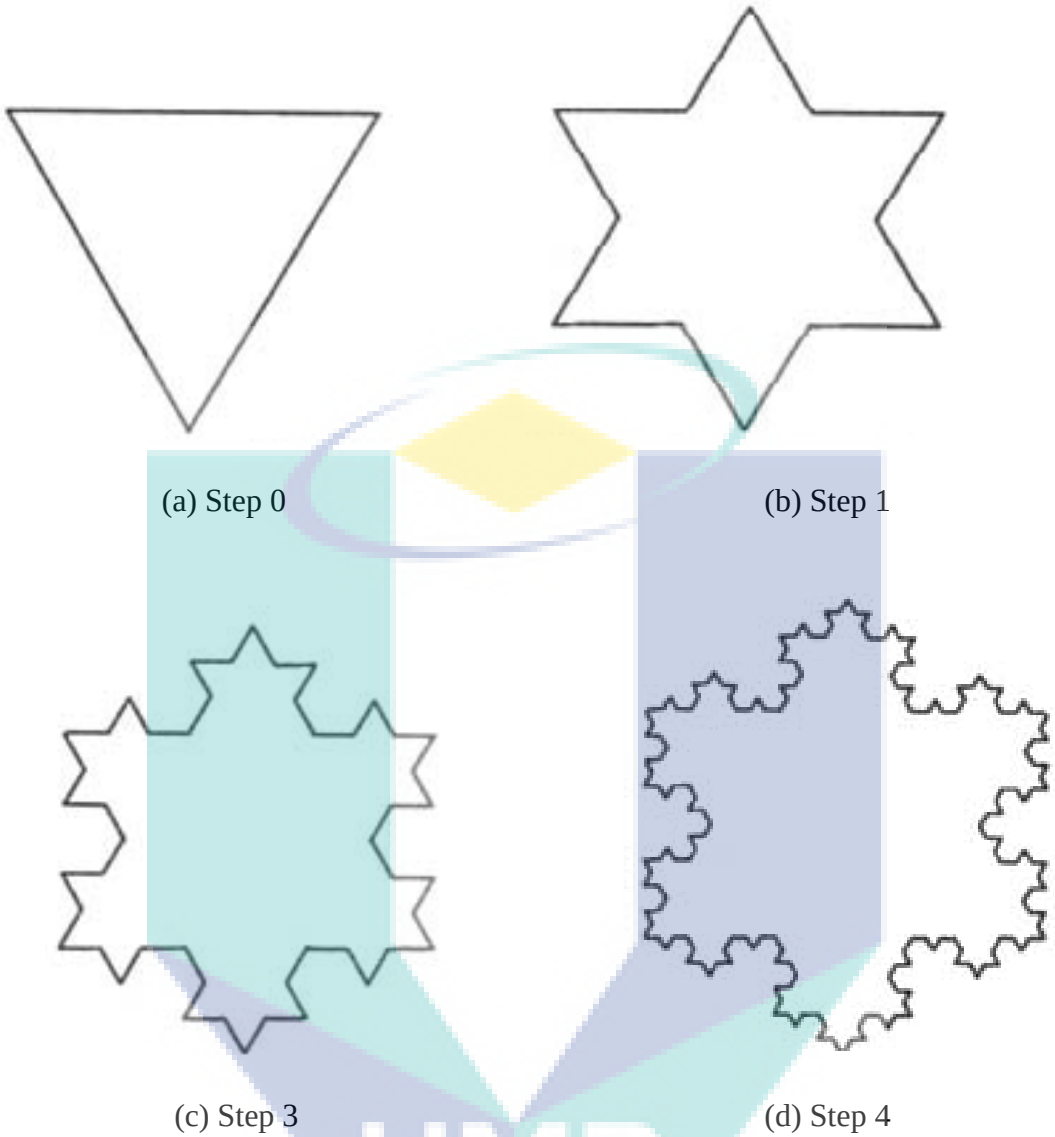

Figure 2.7: Iterative Construction of Koch Snowflake (Shroeder, 1991)

2.4.2 Fractal Tree

The Pythagoras Tree is a plane fractal, invented by the Dutch mathematics teacher Albert E. Bosman. The construction of the Pythagoras tree begins with a square. Upon this square, two squares are constructed, each scaled down by a linear factor of ½√2, such that the corners of the squares coincide pairwise. The same procedure is then applied recursively to the two smaller squares. The illustration in Figure 2.8 (a-e) shows that the first few iterations in the construction process of Pythagoras tree (Peitgen Jurgen & Saupe, 2004).

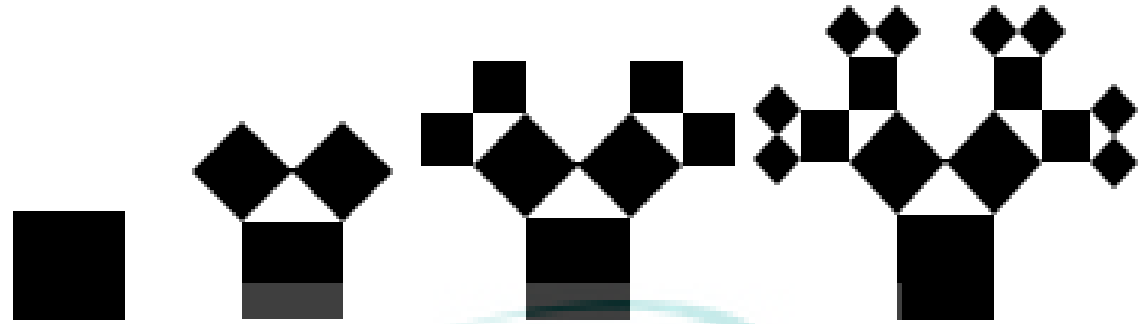

(a) Order 0 (b) Order 1 (c) Order 2 (d) Order 3

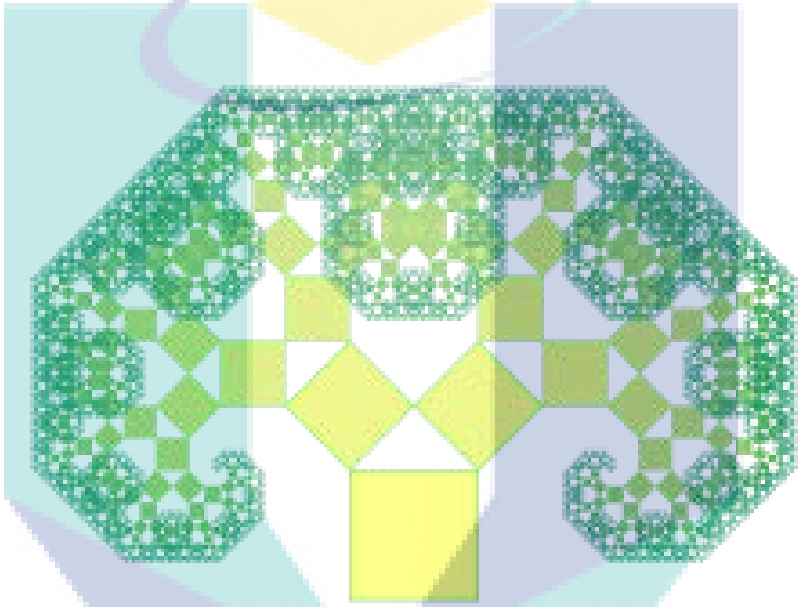

(e)

Figure 2.8: Iterative Construction of Pythagoras Tree (Peitgen Jurgen & Saupe, 2004)

2.4.3 Hilbert Curve

A Hilbert curve (also known as a Hilbert space-filling curve) is a continuous fractal space-filling curve. It was, first, described by the German mathematician David Hilbert in 1891, as a variant of the space-filling curves discovered by Giuseppe Peano in 1890. Its stepwise construction is shown in Figure 2.9 (a-e) (Peitgen Jurgen & Saupe, 2004).

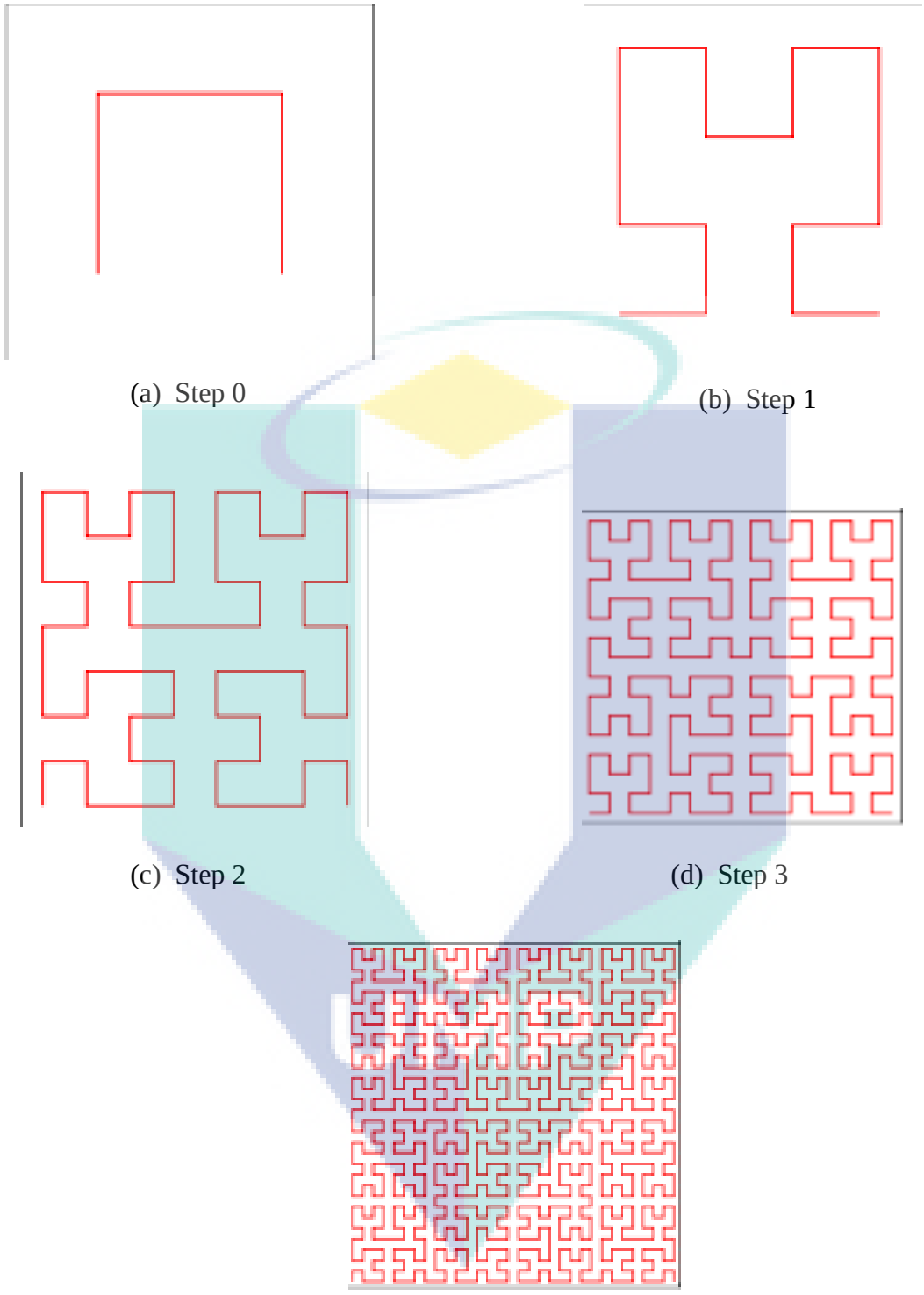

Figure 2.9: Iterative Construction of Hilbert Curve (Falconer, 2003)

2.4.4 Sierpinski Gasket

Triangle is the initiator for construction of Sierpinski Gasket. Triangle is divided into four congruent triangles, and middle small triangle is dropped as shown in Figure 2.10(a). The same procedure continues recursively on three remaining small triangles. Iterative construction of Sierpinski gasket is shown in Figure 2.10 (a-e) (Peitgen Jurgen & Saupe, 2004).

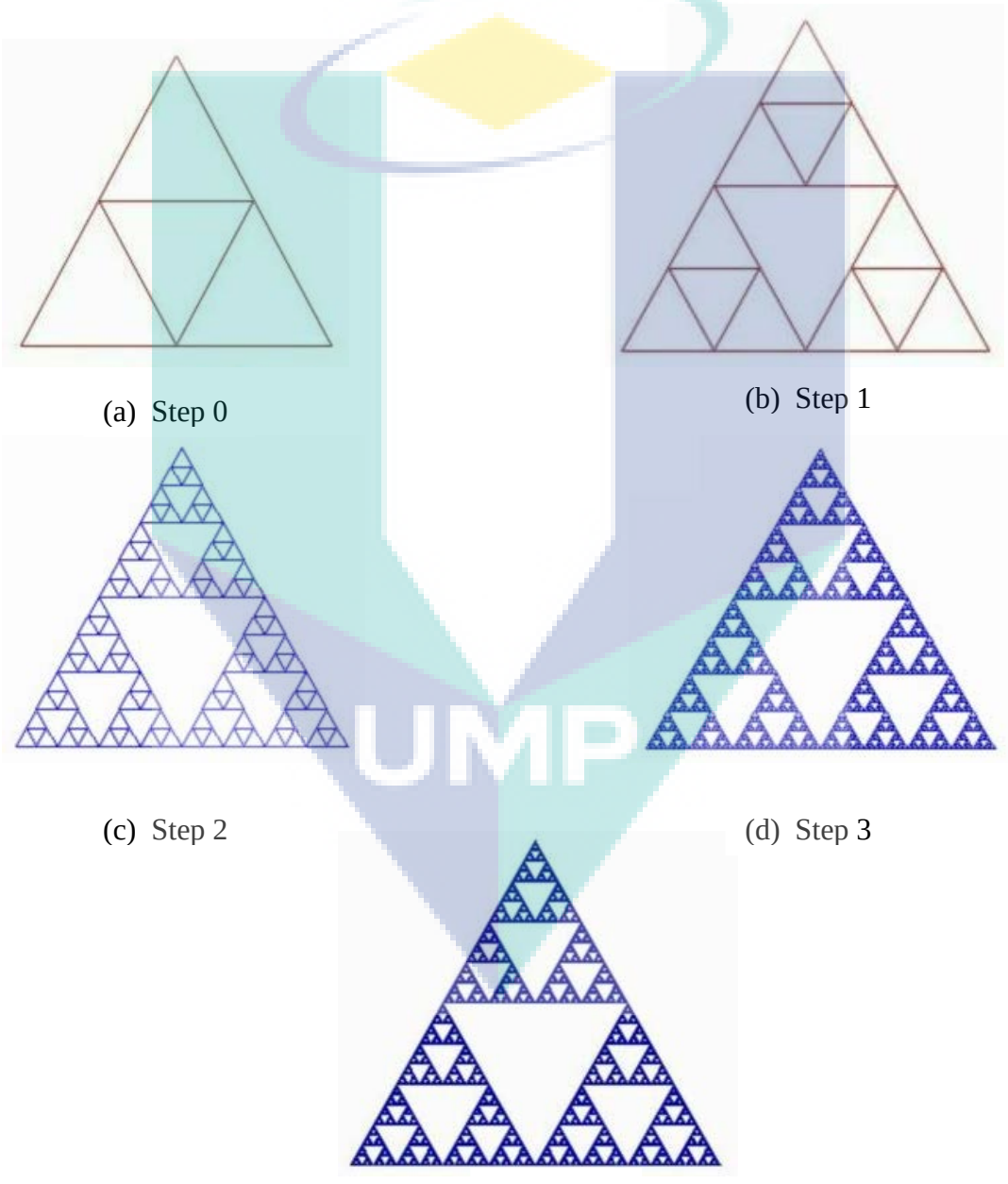

(a) Step 0 (b) Step 1

(c) Step 2 (d) Step 3

(e) Step 4

Figure 2.10: Iterative Construction of Sierpinski Gasket (Peitgen Jurgen & Saupe, 2004)

2.4.5 Sierpinski Carpet

Polish mathematician Waclaw Sierpinski (1882-1969) presented the Sierpinski carpet in 1916. Besides being credited for being one of the most brilliant creations among the historical fractals, it has enjoyed a great importance in Topology (Peitgen Jurgen & Saupe, 2004).

In order to construct the Sierpinski carpet as shown in Figure 2.11d, a square is used as the initiator. It is subdivided into nine congruent squares and the center square is dropped. With each remaining square, same process will be repeated. After sufficient number of iterations, Sierpinski carpet is obtained. In first guess, Sierpinski carpet looks a variation of Sierpinski gasket, while both are entirely different in nature (Peitgen Jurgen & Saupe, 2004).

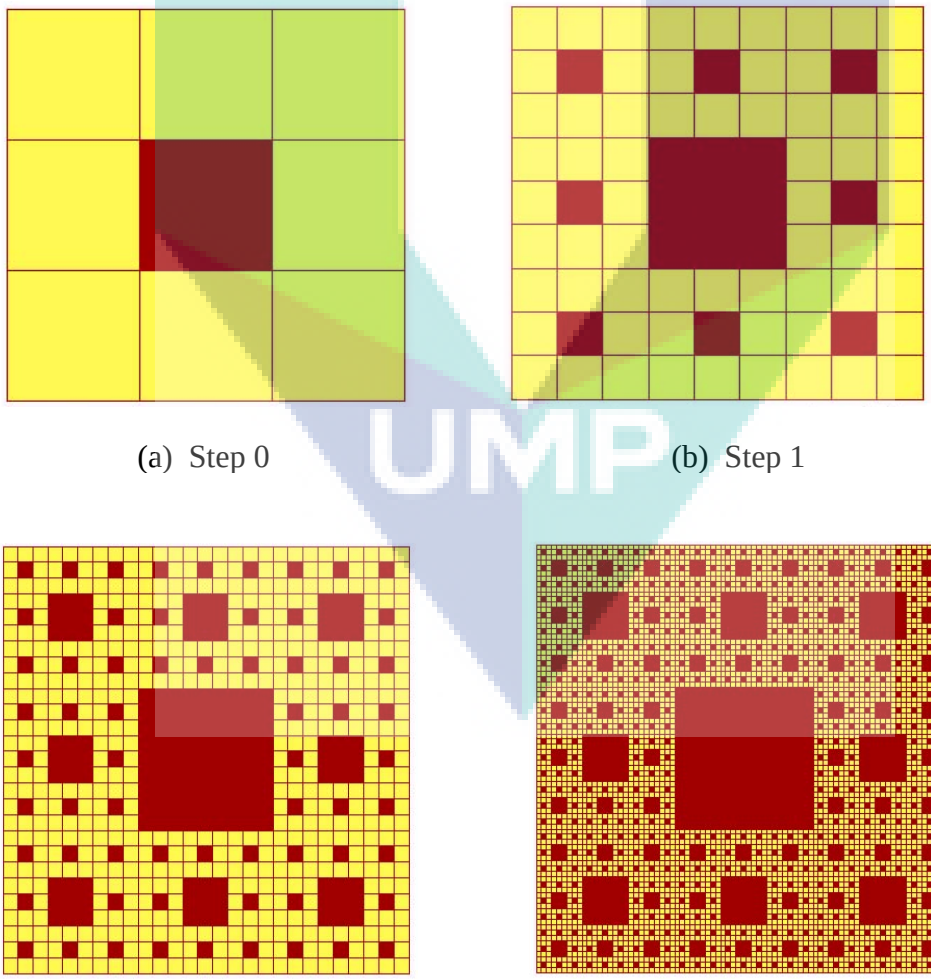

(a) Step 0 (b) Step 1

(c) Step 2 (d) Step 3

Figure 2.11: Iterative construction of fractal carpet (Peitgen Jurgen & Saupe, 2004)

2.5 KOCH FRACTAL ANTENNA

The Koch snowflake (also known as the Koch star and Koch island) is a mathematical curve. It is based on the Koch curve, which appeared in 1904 in a paper titled "On a continuous curve without tangents, constructible from elementary geometry" (original French title: "Sur une courbe continue sans tangente, obtenue par une construction géométrique élémentaire") by the Swedish mathematician Helge von Koch (Falconer 2003). It has following properties (Shroeder, 1991):

i. It is continuous everywhere but differentiable nowhere.
ii. It is a bounded curve of infinite length.
iii. It is self-similar.

Fractal dimension of Koch curve is calculated by using Eq. 2.2 (see at Page 11). When s = 1/3, the Koch curve breaks down into four parts, i.e., n = 4 (Figure 2.6b at Page 13) and $D = \log 4/\log 3 \approx 1.2619$.

2.6 ANTENNA CHARACTERISTICS AND PARAMETERS

In this section, a few antenna characteristics and parameters have been discussed in brief that has been used in the thesis (Best, 2005).

2.6.1 Radiation Pattern

The radiation pattern is graphical depiction of the relative field strength transmitted from or received by the antenna. It is a 3D plot of an antenna radiation far from source. It provides the information that describes how the antenna directs the energy it radiate. Antenna radiation patterns are taken at one frequency, one polarization and one plane cut. Figure 2.12 shows radiation pattern of a dipole antenna.

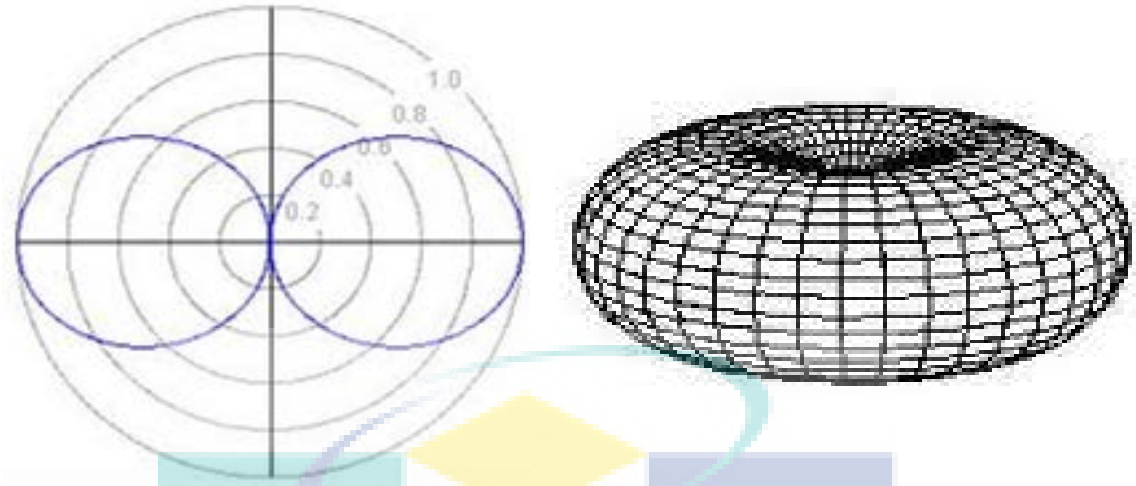

(a) (b)

Figure 2.12: Radiation pattern of a dipole antenna (a) 2Dview (b) 3D view (Best, 2005)

2.6.2 Directivity and gain or power gain

The directivity or gain of an antenna is a measure of the concentration of the radiated power in a particular direction. It is a ratio of radiation intensity in a given direction to the average radiation intensity. The directivity D of the antenna defined by:

$$D(\theta,\phi) = \frac{\text{Radiation intesity of antenna in direction}}{\text{Average radiation intensity in all direction}} \quad (2.3)$$

The power gain G or simply the gain of an antenna is the ratio of its radiation intensity to that of an isotropic antenna radiating the same total power as accepted by the real antenna. It is the product of efficiency, directivity and accounts for the fact that loss reduces the power density radiated in a given direction.

$$G(\theta,\phi) = eD(\theta,\phi)\ [\text{dBi}] \quad (2.4)$$

where

e is Radiation efficiency

D is Directivity.

2.6.3 Impedance and Voltage Standing Wave Ratio (VSWR)

For efficient transfer of energy, the impedance ratio of the antenna, and impedance ratio of the transmission line connecting the radio to the antenna must be the same. Radios typically are designed for 50Ω impedance and coaxial cables (transmission lines) used with them also have 50Ω impedance. Efficient antenna configurations often have impedance other than 50Ω. Some sort of impedance matching technique is then required to transform the antenna impedance to 50Ω.

The Voltage Standing Wave Ratio (VSWR) is an indication of how good the impedance match is. A high VSWR is an indication that the signal is reflected prior to being radiated by the antenna. Higher VSWR gives a greater mismatch. A VSWR of 2.0 or less is considered good. The VSWR is formulated as:

$$VSWR = \frac{1+|\Gamma|}{1-|\Gamma|} \tag{2.5}$$

where Γ is called the reflection coefficient.

2.6.4 Return Loss

The Return loss is a parameter, which indicates the amount of power that is lost to the load and it does not return as a reflection. Return loss is a parameter similar to the VSWR to indicate how well the matching between the transmitter and antenna is. The return loss, denoted by RL, is given by

$$\mathrm{RL} = -20\log_{10}|\Gamma| \quad [\mathrm{dB}] \tag{2.6}$$

If Γ= 0 and RL = ∞, it means no power would be reflected back, whereas when Γ = 1 and RL = 0 dB, all the incident the power is reflected.

2.6.5 Bandwidth

The bandwidth of an antenna expresses its ability to operate over a wide frequency range. It is often defined as the range over which the power gain is maintained within 3dB of its maximum value or the range over which the VSWR is not greater than 2. The bandwidth is, usually, given as a percentage of the nominal operating frequency. The radiation pattern of an antenna may change dramatically outside its specified operating bandwidth. A VSWR ≤ 2 with RL $\leq$ -10dB ensures good performance.

2.7 SUPERIOR FRACTALS

Basically, there are two types of feedback machines: one-step machine, and two-step machine (Peitgen, Jurgen & Saupe, 2004). Both types of the machines can be characterized by iterative procedures. Iteration methods are one way to achieve the self-similarity. One-step feedback machines are characterized by Peano-Picard iterations (generally called Picard or function iterations) formula $x_{n+1} = f(x^n)$, where f(x) can be any function of x.

Picard Orbit

Definition 2.1: Let X be a non-empty set of numbers and f: X $\rightarrow$ X. For a point x_0 in X, the Picard orbit (generally called orbit of f) is the set of all iterates of a point x_0, that is:

$$O(f, x_0): = \{x_n: \ x_n = f(x_{n-1}), n = 1, 2, \dots \} \quad (2.7)$$

The orbit $O(f, x_0)$ of f at the initial point x_0 is the sequence $\{f_n(x_0)\}$ (Rani, 2002).

In two-step feedback machines, output is computed by the formula $x_{n+1} = g(x_n, x_{n-1})$. It requires two numbers as input and returns a new number (Peitgen,

Jurgen and Saupe, 2004). For example, the Fibonacci numbers are generated by the iterative procedure $g(x_n, x_{n-1}) = x_n + x_{n-1}$.

In all the literature, whole fractal theory was based on one-step feedback machine. All the fractal models were being studied in Picard orbit until two-step feedback machine was introduced in the study of fractal models by Rani in 2002. The author characterized two-step feedback machine by superior iterates in fractal graphics and generated superior fractals. It was a new approach in computation, visualization and analysis of fractal models. Following is the definition of superior iterates:

Superior Iterates

Definition 2.2: Let X be a non-empty set of numbers and f: X $\rightarrow$ X. For an $x_0 \in X$, construct a sequence $\{x_n\}$ in the following manner:

$$x^1 = \beta_1 f(x_0) + (1 - \beta_1)x_0,$$
$$x_2 = \beta_2 f(x_1) + (1 - \beta_2)x_1,$$
$$x_n = \beta_n f(x^n) + (1 - \beta_n)x_{n-1},$$

where $0 < \beta_n \leq 1$ and $\{\beta_n\}$ is convergent away from 0.

The sequence $\{x_n\}$ constructed above was called as superior sequence of iterates, denoted by *SO*(f, x_0, β_n). At $\beta_n = 1$, *SO*(f, x_0, β_n) reduces to O(f, x_0) (cf. Definition 2.1).

This procedure was, essentially, given by Mann (1953). Since the results obtained in fractal modeling via Mann iterates are the super set of their corresponding fractal models in Picard orbit, therefore, Rani called it as superior iterates. At $\beta_n = 1$, superior iterates behave as one-step feedback machine (Chandra & Rani, 2009; Rani & Agarwal, 2010; Rani & Goel, 2009; Rani & Kumar, 2004a, 2004b, 2004c; Rani & Prasad, 2010). Many escape-time fractals and few strange attractors were generated in *SO*. Rani and Agarwal (2010) discussed few good applications of fractals in *SO*. A comprehensive review of literature on superior fractals that are constructed using superior iterates, is given by Kumar (2010).

From superior iterates, Rani and Kumar (2004a) got the idea of generation of fractal models via unequal division of the initiator. This concept has been applied on Sierpinski carpet (Rani & Kumar, 2004; Rani, 2005; Rani & Goel, 2009), Cantor set and Devil's staircase (Rani & Prasad, 2010), and fractal plants (Chandra & Rani, 2009). Thus, there exists now a big gallery of each of these fractals. For example, see a superior fractal carpet, superior fractal plant and superior Cantor set with its Devil's staircase in Figure 2.13, Figure 2.14 and Figure 2.15 respectively, generated by unequal division of the initiators.

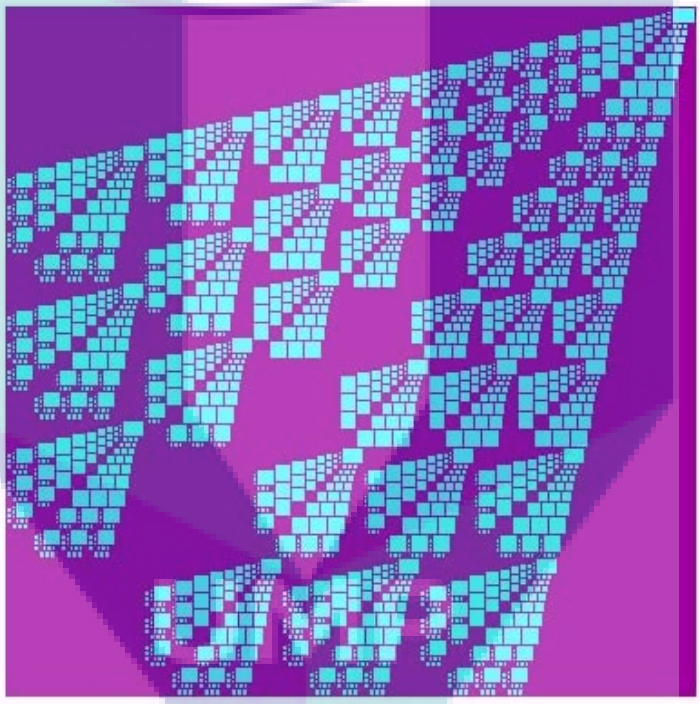

(a)Vinod carpet

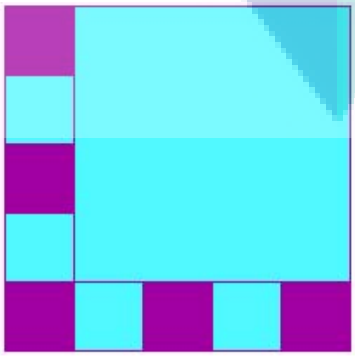

(b) Generator of Vinod carpet

Figure 2.13: Vinod carpet, an example of the fractal obtained by unequal division of the initiator (Rani & Kumar, 2004).

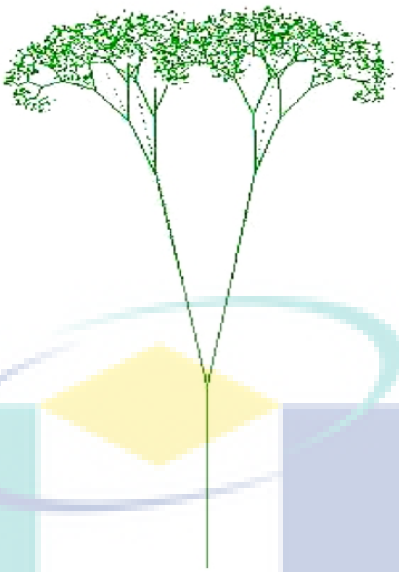

Figure 2.14: Fractal plant at (s; θ) = (1/2; 30°, 45°, 60°) (Chandra & Rani, 2009)

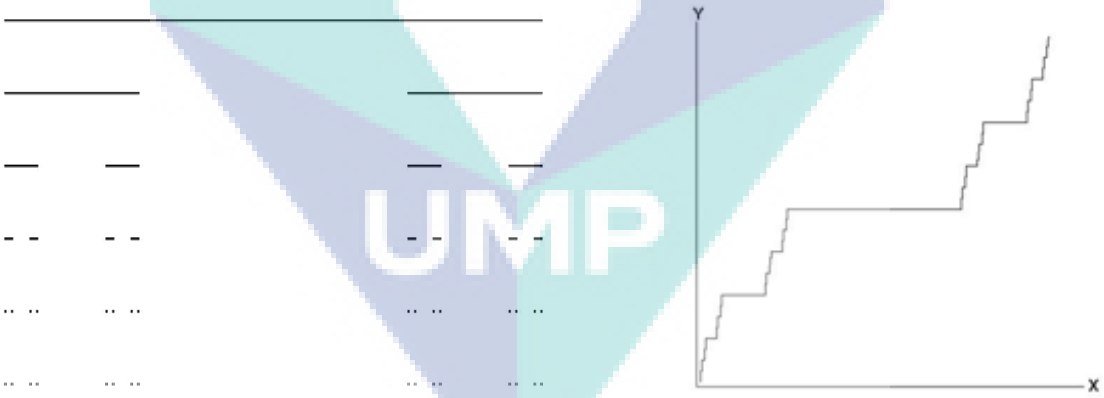

(a) Cantor middle one-half set (b) Superior Devil's staircase

Figure 2.15: Superior Cantor set and Devil's staircase obtained by dividing the initiator into unequal segments (Rani & Prasad, 2010).

2.8 DISCUSSION ON KOCH FRACTAL ANTENNA

Koch snowflake is used as fractal antenna in wireless communications. Cohen (1996, 1997) explicitly explained useful applications of fractal antenna in defense services because of its compact size and multiband characteristic.

Poor behavior of antenna is also, due to the inefficient way that these shapes fill up the volume that encloses them. On the other hand, the fractal counterparts of these antennas having a larger fractal dimension are more efficient in filling up the space. Balirada (2000) analyzed the Koch monopole numerically and experimentally and results showed that as the number of iterations on the small fractal Koch monopole increases, the antenna approaches the fundamental limit for small antennas. In a large number of applications, and especially those involving mobile terminals, the reduction of the antenna size is an ultimate goal.

These results are contradicting to the results of Vinoy, Jose and Vardan (2004) as they showed that fractal antennas with smaller dimension have better multiband-resonance.

This means that there must be a trade off between dimension and size of antenna to make a balance between small size and better multiband characteristic of an antenna. The possibility to employ antennas that fit in smaller volumes, but still have an efficient behavior, is certainly appealing.

Strycek and Hertl (2007) presented advantages and disadvantages of fractal elements implementation into antenna structure. The reduction of transversal dimensions is the main reason for using log periodic antenna with fractal elements instead of the common structure. The axial length is reduced for fractal antenna in comparison to common LPA. Both antennas are similar in term of impedance matching, but fractal antenna has slightly higher reactance. Fractal log periodic antenna has one large disadvantage also in comparison with Euclidean log periodic antenna that its gain is smaller.

Harish & Joshi (2007) performed studies on application of fractal based geometries in printed antenna structures and found that the fractals can be used to reduce the size of the antenna. By coupling two structures having different sizes but with close resonance frequencies, it is possible to enhance the bandwidth of the antenna. Also, fractal structures, if used as parasitic elements, can bring in appreciable flexibility to modify the performance of antennas. By introducing irregularity in the fractal structure, it is possible to further enhance the performance of the antenna.

Elkamchouchi and Mustafa (2007) performed experiment on the 3D-fractal rectangular Koch dipole and the 3D fractal Hilbert dipole antennas and found that 3Dfractal shaped wire antennas can give resonance compression and multiband behavior. The 3D-self-similarity fractal antennas have acceptable resonant resistance and constant input impedance at the high frequency bands. The 3D-fractal technique is suitable for designing compact antennas with multiple resonances.

McClure (2008) has discussed the vibrational modes of a drum, shaped like Koch snowflake. Vibrational modes are computed using a fairly standard finite difference technique, which has been applied to a discrete approximation to the snowflake. Epstien & Adeeb (2008) derived stiffness of the Koch curve. The calculation is based on structural mechanics principles and a physically motivated similarity criterion, which is assumed as a postulate.

Kordzadeh and Kashani (2009) proposed rectangular Koch microstrip antenna proposed. Using this the surface current path is lengthened and thus they found that the resonance frequency is decreased to a great deal. When compared with an antenna of the same resonance frequency, a reduction of about 85% is achieved in antenna size. By adding a matching network to the antenna feed, bandwidth is increased to an acceptable value. This antenna can be used in applications where the overall volume of the structure is an important factor, such as mobile terminals, etc.

Ghatak et al. (2009) simulated the performance of V-Koch antenna and analyzed its characteristics. Hohlfeld & Cohen (1999) explained geometric requirements of frequency dependent antenna. Krishna et al. (2009) design of a compact wideband Koch

fractal printed slot antenna, suitable for WLAN 2.4/5.2/5.8 GHz and WiMAX 2.5/3.5/5.5 GHz operations. Mirzapour and Hassani (2009) confirmed that there is a 49% increase in bandwidth and about 70% reduction in radiating surface size in Koch snowflake antenna compared with the ordinary Koch antenna are achievable.

Tang (2000) has studied antenna characteristic of many fractal geometries. Also, Werner, Haupt & Werner (1999), Werner and Ganguly (2003) and Zhang et al., (2006) gave a review on different shaped fractal antenna engineering.

A few patents have also been searched and it was found that in designing of an actual fractal antenna, for reduction of size and enhancement of multiband characteristic, some tips are given (see Vardan et. al., 2003; Veerasamy, 2003; Almong et. al., 2006; Cohen, 2006; Chang et. al., 2007). For more studied on Koch antenna one may further refer to Fractus (2000), Song et al. (2008) and several cross references thereof.

Variants of Koch fractal antenna:

Barcellos (1984) gave variants of Koch curve by dividing the initiator into 4 equal parts. These curves have a fixed dimension. Further, there was no suggestion to obtain the curves of lesser dimension. Vinoy, Jose and Vardan (2002) generated new shapes of Koch antenna by varying its indentation angle. All these variants have lesser dimension than the conventional Koch antenna and gave a formula to calculate their fractal dimension. The curves given by Vinoy et al. occupy more area than the conventional Koch curve.

2.9 SUMMARY

From the above discussion it is concluded that there is need to propose Koch shapes of lesser dimension and compact size for better performance with compact size. Beside this one should have flexibility in designing of antenna for a certain performance. Also, there is a curiosity left in the literature whether the two different shapes having same dimension will have same performance as antenna or not.

For the above requirements and seeing the success of superior fractals, it is proposed to generate new Koch models of lesser dimension and smaller size (compared to Koch models of Vinoy et. al., 2002) by dividing the initiator into unequal parts.

CHAPTER 3

NEW KOCH MODELS: DESIGN, CLASSIFICATION, REWRITING SYSTEM AND GEOMETRY

3.1 INTRODUCTION

The von Koch curve, a classical fractal model, is generated by dividing the initiator into three equal parts. There exist a few numbers of variants of Koch curve in literature as discussed in previous chapter. These variants are of lesser dimension than the von Koch curve, so have better multiband characteristic when used as antenna. On the other hand, these variants are of larger size than the size of von Koch curve, while a fractal antenna should be compact. It is required to have Koch models of lesser dimension (for improved multiband characteristic) and should be smaller in size (compact). In this chapter, a few new Koch models are presented that are of lesser dimension and smaller size than the von Koch model, so are expected to perform better as antenna. In the series of superior fractals, superior Koch curves were developed. A few numbers of new shapes of Koch curve were computed by dividing initiator into the line segments of unequal length, and new design of antennas are proposed. With the increase in size of the set of Koch curves, there is a need of classification of Koch family for their systematic generation. The classification is based on their method of generation. The models are classified into different categories. Further, rewriting rules for superior Koch curves have been developed, and formulas for calculation of their fundamental mathematical properties are given.

3.2 GENERATION OF NEW KOCH ANTENNA DESIGNS

Inspired by superior iterates (given in Chapter 2), new Koch curves were computed using C++. To learn the programming concepts in C++, one may refer to Dietel & Dietel (2005), Gotfried (1996) and Kanetkar (2008). These curves are new examples of superior fractals.

3.2.1 Koch Left One-Third Curve

Koch left one-third curve is generated by dividing the initiator line into three equal parts. The left line segment was replaced by an equilateral triangle, and the base of triangle was removed. After this basic step, generator was produced in which reduced Figure has four equal lines joined with each other. The same operation was repeated on each of the remaining line segment many times (ideally infinitely). Koch left one-third curve with its generator is shown in Figure 3.1(a). When the same generation is applied on initiator triangle, a snowflake is generated as shown in Figure 3.1 (b).

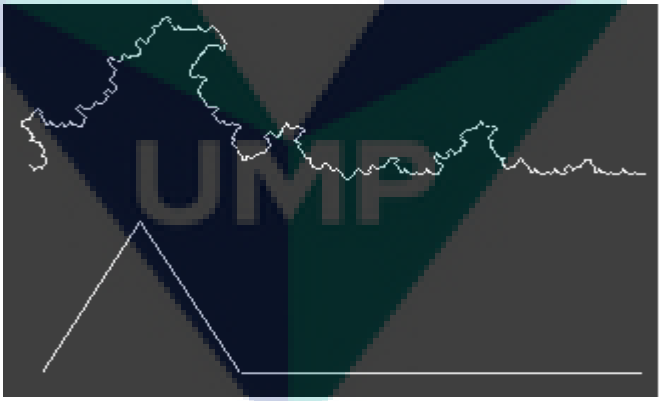

(a) Koch left one-third curve with Generator

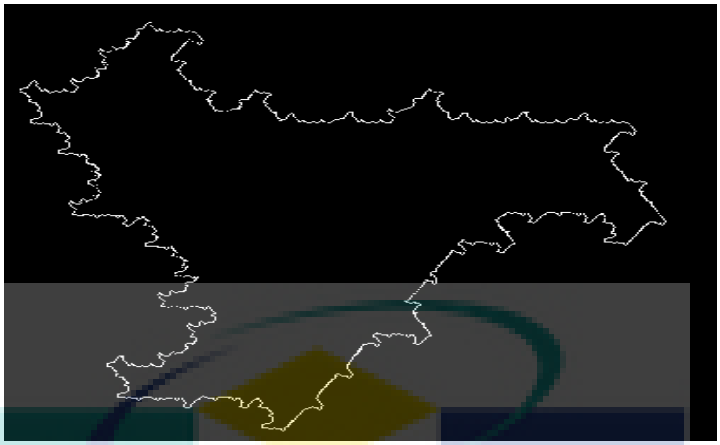

(b) Koch left one-third Snowflake

Figure 3.1: Koch Left One-Third Curve and Koch Snowflake for (r1, r2, r3) = (1/3,1/3,1/3)

Algorithm 3.1. Following is the algorithm to compute the Koch left one-third curve:

```
void koch (int x1, int y1, int x2, int y2)
{
        int x3,y3,x4,y4,x,y;
        float r1=0.33,r2=0.33;
         if (abs(x2-x1)>=5)
        {
                setcolor(WHITE);
                line (x1,y1,x2,y2);
                x3=x1+(x2-x1)*r1;
                y3=y1+(y2-y1)*r1;
                x4=x1+(x2-x1)*(r1+r2);
                y4=y1+(y2-y1)*(r1+r2);
                x=(x3-x1)*cos(-1.05)-(y3-y1)*sin(-1.05)+x1;
                y=(y3-y1)*cos(-1.05)+(x3-x1)*sin(-1.05)+y1;
                line(x1,y1,x,y);
                line(x3,y3,x,y);
                setcolor(BLACK);
                line(x1,y1,x3,y3);
```

```
            koch(x1,y1,x,y);
            koch(x,y,x3,y3);
            koch(x3,y3,x4,y4);
            koch(x4,y4,x2,y2);
        }
}
```

3.2.2 Koch Right One-Third Curve

Following the pattern of Koch left one-third curve, Koch right one-third curve may also be computed by dividing the initiator line into 3 equal parts and manipulating the right line segment. By applying the same construction method on initiator triangle, Koch right one-third snowflake may be generated.

Following the same method of nomenclature, the conventional Koch curve was renamed as Koch middle one-third curve. All the three Koch curve (left one-third, right one-third, and middle one-third) have same fractal dimension, which is ≈ 1.262.

Algorithm 3.2. The algorithm to compute the Koch right one-third curve is given below.

```
void koch (int x1, int y1, int x2, int y2)
{
        int x3,y3,x4,y4,x,y;
        float r1=0.33,r2=0.33;
         if (abs(x2-x1)>=5)
        {
                setcolor(WHITE);
                line (x1,y1,x2,y2);
                x3=x1+(x2-x1)*r1;
                y3=y1+(y2-y1)*r1;
                x4=x1+(x2-x1)*(r1+r2);
                y4=y1+(y2-y1)*(r1+r2);
                x=(x2-x4)*cos(-1.05)-(y2-y4)*sin(-1.05)+x4;
```

```
            y=(y2-y4)*cos(-1.05)+(x2-x4)*sin(-1.05)+y4;
            line(x4,y4,x,y);
            line(x2,y2,x,y);
            setcolor(BLACK);
            line(x4,y4,x2,y2);
            koch(x1,y1,x3,y3);
             koch(x3,y3,x4,y4);
            koch(x4,y4,x,y);
            koch(x,y,x2,y2);
        }
}
```

3.2.3 Koch Right Half Curve

To draw the Koch right half curve (Figure 3.2(a)), the initiator line was divided into three parts such that left and middle line segments are one-fourth and right line segment is half of the initiator respectively. Now, the right line segment was manipulated as shown in Figure 3.2(a). The same process was repeated on the remaining four segments sufficient number of times. To compute the Koch right half curve, (r1, r2) is set to (0.25, 0.25) in Algorithm 3.2. Fractal dimension of the Koch right half curve is calculated as follows:

Dimension of Koch right half curve = (log 6) / log (4) ≈ 1.2925,

Dimension of Koch right half curve is greater than the von Koch curve dimension. Koch right half snowflake (Figure 3.2(b)) was obtained by applying the above process on triangle.

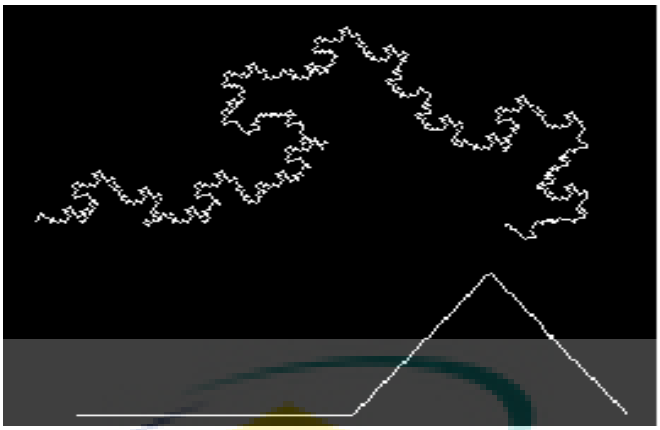

(a) Koch right half curve with generator

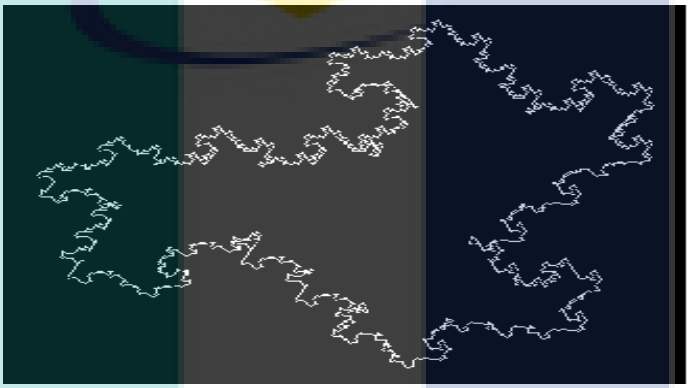

(b) Koch right half snowflake

Figure 3.2: Koch right half curve and snowflake for (r1, r2, r3) = (1/4, 1/4, 1/2)

3.2.4 Koch Middle Half Curve

The initial line segment is divided into three parts such that the left and right line segments are ¼, and the middle is ½ of the initial line segment, and then the middle line segment is manipulated in the same way as in Koch curve. The same procedure is repeated with the remaining lines and thus Koch middle-half curve is obtained (Figure 3.3(a)). The fractal dimension of the new superior Koch curve is given by the same as Koch right half curve. Furthermore, Koch middle half snowflake was obtained by applying the same method on initiator triangle (Figure 3.3(b)).

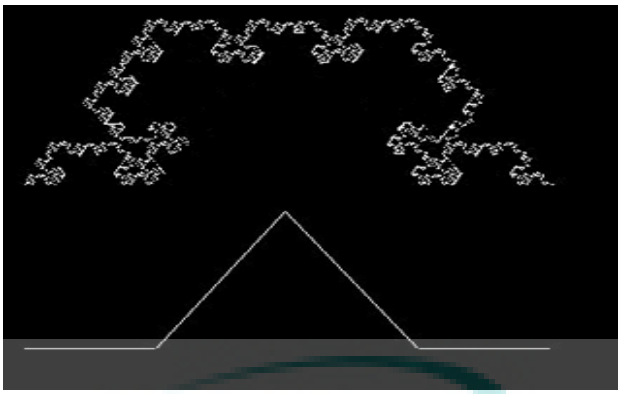

(a) Koch middle half curve with its generator

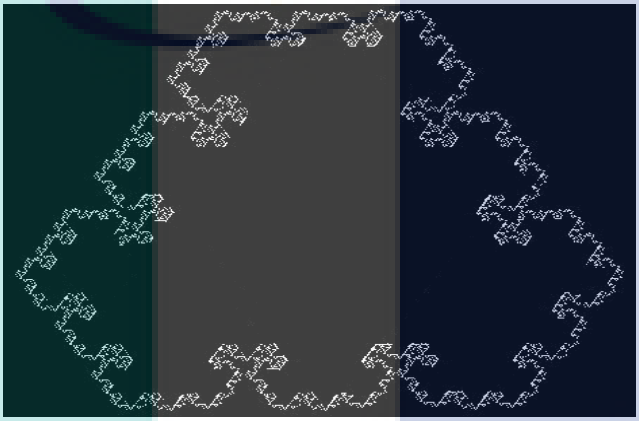

(b) Koch middle half snowflake

Figure 3.3: Koch middle half curve and snowflake for (r1, r2, r3) = (1/4, 1/2, 1/4)

Algorithm 3.3. Following is the algorithm to compute the Koch middle half curve. The von Koch curve may also be generated by the same algorithm by setting (r1, r2) to (0.33, 0.33).

```
void koch (int x1, int y1, int x2, int y2)
{
        int x3,y3,x4,y4,x,y;
        float r1=0.25,r2=0.5;
         if (abs(x2-x1)>=5)
        {
                setcolor(WHITE);
                line (x1,y1,x2,y2);
```

```
            x3=x1+(x2-x1)*r1;
            y3=y1+(y2-y1)*r1;
            x4=x1+(x2-x1)*(r1+r2);
            y4=y1+(y2-y1)*(r1+r2);
            x=(x4-x3)*cos(-1.05)-(y4-y3)*sin(-1.05)+x3;
            y=(y4-y3)*cos(-1.05)+(x4-x3)*sin(-1.05)+y3;
            line(x3,y3,x,y);
            line(x4,y4,x,y);
            setcolor(BLACK);
            line(x3,y3,x4,y4);
            koch(x1,y1,x3,y3);
             koch(x3,y3,x,y);
            koch(x,y,x4,y4);
            koch(x4,y4,x2,y2);
        }
}
```

3.2.5 Koch Middle One-Fifth curve

The initiator line is divided into three unequal parts in which the left and right line segments are 2/5, and the middle line segment is 1/5 of the initiator. The middle line segment is manipulated the same way as it is done in the von Koch curve. By applying the same method on remaining line segments, the Koch middle one–fifth curve is obtained (Figure 3.4 (a)). Koch middle one-fifth curve may be computed by setting (r1, r2) to (0.4, 0.2) in Algorithm 3.3. Fractal dimension of this new superior Koch curve is given by:

Dimension of Koch middle one-fifth curve = (log 6) / log (5) ≈ 1.113

which is lesser than the dimension of the von Koch curve. Further, Koch middle one-fifth snowflake is shown in Figure 3.4(b).

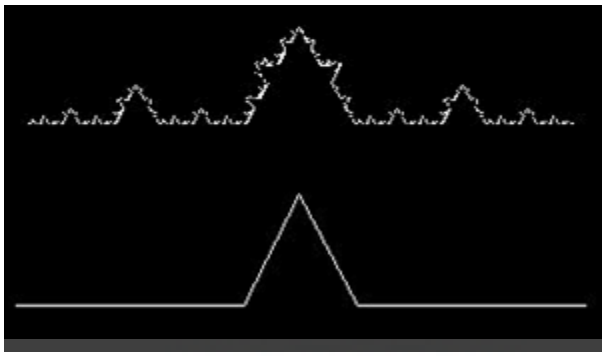

(a) Koch middle one-fifth curve with its initiator

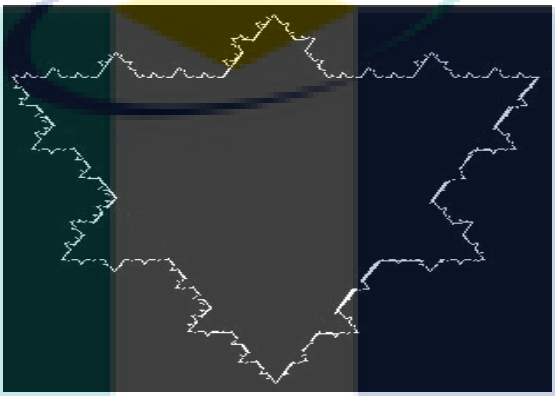

(b) Koch middle one-fifth snowflake

Figure 3.4: Koch Middle one-fifth curve and snowflake for (r1, r2, r3) = (2/5, 1/5, 2/5)

3.2.6 Koch Middle One-Sixth Curve

To draw the Koch middle one-sixth curve (Figure 3.5(a)), the initiator line was divided into three parts such that left, middle and right line segments are 1/3, 1/6 and 1/2 of the initiator. Now, the middle line segment was manipulated as shown in Figure 3.5(a). The same process was repeated on the remaining four-line segments sufficient number of times. Koch middle one-sixth curve may be computed by setting (r1, r2) to (0.33, 0.167). Fractal dimension of the Koch middle one-sixth curve is given by:

$$\text{Dimension of Koch middle one-sixth curve} = (\log 7) / \log (6) \approx 1.086$$

which is less than the von Koch curve. Koch middle one-sixth snowflake (Figure 3.5(b)) was obtained by applying the above process on triangle.

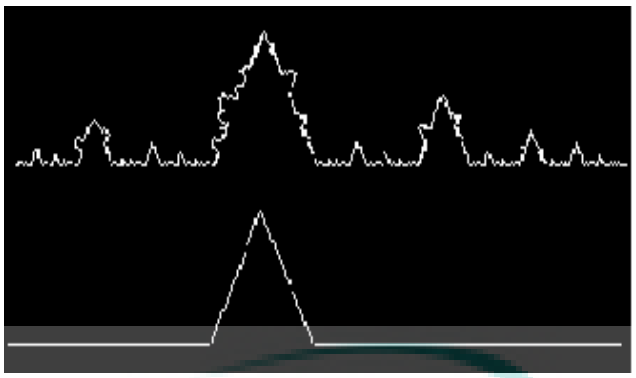

(a) Koch middle one-sixth curve with its generator

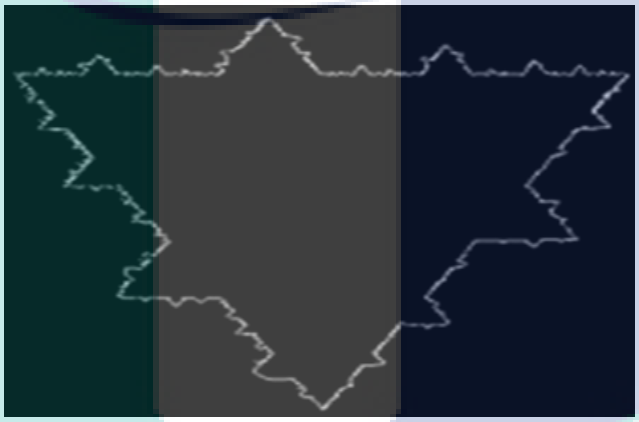

(b) Koch middle one-sixth snowflake curve

Figure 3.5: Koch middle one-sixth curve and snowflake for (r1, r2, r3) = (1/3, 1/6, 1/2)

3.3 CLASSIFICATION

With the increased number of Koch curves in the literature, now there is a need to systematize them into different categories to understand the methodology of their generation. There are various ways to classify the fractal objects. The proposed classification is based on the method of division of initiator. Different variants of Koch curve have been classified into two categories: generation by equal division and generation by unequal division.

3.3.1 Category 1: Generation by equal division.

In this category, we divide the initiator was divided into three equal parts and one of the segments was manipulated. The same process was repeated on the remaining segments sufficient number of times. Conventional Koch curve (Figure1.2), Koch left one-third curve (Figure 3.1) and Koch right one-third curve fall into Category 1.

There are many other variants of Koch curve available in literatures that are fit into Category 1. Barcellos (1984) generated variants of Koch curve of dimension between 1 and 2 by dividing the initiator into four equal parts. The author manipulated middle two segments such that one can obtain 3, 4, 5 or 6 components; each of them is of length ¼ of the initiator. As the number of components of equal length increases in Barcello's Koch curves, their dimension increase. As per the nomenclature method followed, Barcello's Koch curves is named as Koch middle two one-fourth curves. Vinoy et. al. (2002), also, modified the Koch curve modified by altering its indentation angle, which are fit in Category 1.

3.3.2 Category 2: Generation by unequal division.

Now, Koch curves obtained by unequal division of the initiators are categorized into two cases.

Case 1: In this case, an initiator is divided into three parts such that two parts are equal in length and 3rd part is unequal, and one of the segment is manipulated iteratively. Koch right half curve (Figure 3.2), Koch middle half curve (Figure 3.3) and Koch middle one-fifth curve (Figure 3.4) are examples of Case 1. Sengufta (2005) gave few variations of Koch curve. Out of his collection, Koch middle one-forth (name as per our nomenclature) belong to Case 1.

Case 2: In this case, an initiator is divided into three parts such that the all parts are unequal in length. Koch middle one-sixth curve (Figure 3.5) is example of Case 2. Sengufta's (2005) Koch middle one-eighth curves (name as per our nomenclature) is also fit in Case 2.

3.4 REWRITING SYSTEM FOR KOCH MIDDLE ONE-THIRD CURVE

An L-system or Lindenmayer system is a parallel rewriting system, namely a variant of a formal grammar. It is most famously used to model the growth processes of plant development, but also able to model the morphology of a variety of organisms. Using L-system, almost all the fractals can be generated. An L-system consists of an alphabet of symbols that can be used to make strings, a collection of production rules which expand each symbol into some larger string of symbols, an initial "axiom" string from which to begin construction, and a mechanism for translating the generated strings into geometric structures (Garcia, 2005).

Construction of the Koch curve (Figure 2.6) is well known. It can be expressed by following rewrite system (L-system) (Garcia, 2005):

Alphabet: F
Constants: +, −
Axiom: F
Production rule: F → F + F - - F + F (3.1)

Here, F means "draw forward", + means "turn left 60°", and − means "turn right 60°". To draw a Koch snowflake curve, the Prod. Rule 4.1 will be applied on the axiom " F - - F - - F".

3.5 REWRITING SYSTEM FOR NEW KOCH CURVES

In this section, general production rules to draw superior Koch curves have been developed. The production rules for Koch curves have been divided into two parts according to their scaling factors. All the symbols used in the following rewriting systems carry similar meanings as in that of Koch curve. A line is the initiator in all the generations.

3.5.1 Case 1

Koch curves at scaling factor $s = \frac{1}{n}$, where n is an odd number.

Let $s = \frac{1}{5}$, then one of the possible Koch curves is shown in Figure 3.4(a). The following is the rewriting system for such a Koch curve:

Scaling factor: $s = \frac{1}{5}$

Alphabet: F

Constants: +, −

Axiom: F

Production rule: F → F F + F - - F + F F (3.2)

At $s = \frac{1}{7}$, rewriting system for Koch middle one-seventh curve is as follows:

Scaling factor: $s = \frac{1}{7}$

Alphabet: F

Constants: +, −

Axiom: F

Production rule: F → F F F + F - - F + F F F (3.3)

The general rewriting system for Koch curves at $s = \frac{1}{n}$, where n = 3, 5, 7, 9, …, which can be derived from Prod. Rule 1, 2, and 3 is as follows:

Scaling factor $s = \frac{1}{n}$, where n is an odd natural number and $n \geq 3$.

Alphabet: F

Constants: +, −

Axiom: F

Production rule: F → ((n-1)/2)F + F - - F + ((n-1)/2)F (3.4)

Eq. (3.4) can be used to produce Koch middle one-third curve and Koch middle one-fifth curve via L-system. Further, Koch middle one-seventh curve, Koch middle one-ninth curve etc. can be produced by using Eq. (3.4).

3.5.2 Case 2

Koch curves at scaling factor $s = \frac{1}{n}$, where n is an even number.

Let the scaling factor be $\frac{1}{4}$, then rewriting system for the two possible Koch middle one-fourth curves (see the generators in Figure 3.6 is given below.

Scaling factor: $s = \frac{1}{4}$

Alphabet: F

Constants: +, −

Axiom: F

Production rule: F → F + F - - F + F F

or F → F F + F - - F + F (3.5)

(a) Generator at (r1, r2, r3) = (1/4, 1/4, 1/2) (b) Generator at (r1, r2, r3) = (1/2, 1/4, 1/4)

Figure 3.6: Generators of two possible Koch middle one-fourth curves

At the scaling factor $s = \frac{1}{6}$, rewriting system for two possible Koch middle one-sixth curves (Figure 3.7) is as follows:

Scaling factor: $s = \frac{1}{6}$

Alphabet: F

Constants: +, −

Axiom: F

Production rule: F → F F + F - - F + F F F

or F → F F F + F - - F + F F (3.6)

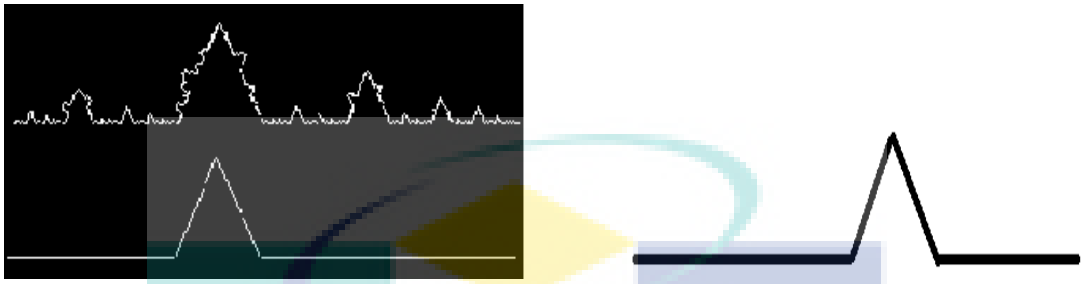

(a) At generator (r1, r2, r3) = (1/3, 1/6, 1/2) (b) at generator (r1, r2, r3) = (1/2, 1/6, 1/3)

Figure 3.7: Generators of two possible Koch middle one-sixth curves

The general rewriting system for Koch curves at $s = \frac{1}{n}$, where n = 4, 6, 8, 10, …, which can be derived from Prod. Rule 5 and 6 is as follows:

Scaling factor: $s = \frac{1}{n}$, where n is an even natural number, and $n \geq 4$

Alphabet: F

Constants: +, −

Axiom: F

Production rule: F → (n/2 - 1)F + F - - F + (n/2)F

or F → (n/2)F + F - - F + (n/2 - 1)F (3.7)

Eq. (3.7) can be used to produce Koch middle one-fourth curve and Koch middle one-sixth curve via L-system. Further Koch middle one-eight curve, Koch middle one-tenth curve etc. can be produced by using Eq. (3.7).

3.6 FRACTAL ANTENNA PROPERTIES

Superior Koch curves generated at scaling factors $s = \frac{1}{n}$, for $n \geq 4$. Koch loop can be generated by applying Prod. Rule 4 or 7 on the axiom "F - - F - - F". Following

are some of the basic properties of a Koch loop. Here, r denotes the radius of the circle which accommodates the Koch loop.

The general formula to calculate the area of a Koch loop is given by

$$\text{Area}_{\text{Koch Loop}} = \frac{3\sqrt{3}}{4} r^2 \left(1 + \frac{3}{n^2 - 4}\right), \; n \in N \text{ and } n \geq 3 \tag{3.8}$$

Therefore,

$$\text{Area}_{\text{Koch Loop}} = \lim_{n \to \infty} \frac{3\sqrt{3}}{4} r^2 \left(1 + \frac{3}{n^2 - 4}\right)$$

$$= \frac{3\sqrt{3}}{4} r^2 .$$

Thus smaller the scaling factor, lesser the area of the Koch loop.

The general formula to calculate the perimeter of a Koch loop is given by

$$\text{Perimeter}_{\text{Koch Loop}} = 3\sqrt{3}\, r + \frac{9\sqrt{3}}{n} r \left((4/3)^m - 1\right), \; m, n \in N, \text{and } n \geq 3 \tag{3.9}$$

where m is the total number of iterations.

Considering $\lim_{m \to \infty} 3\sqrt{3}\, r + \frac{9\sqrt{3}}{n} r \left((4/3)^m - 1\right)$,

It can be seen that $\text{Perimeter}_{\text{Koch Loop}} = \infty$.

Theoretically, a Koch loop can accommodate wire of infinite length. However, with the reducing scaling factor, growth rate of the perimeter decreases.

The general formula to calculate the dimension of a Koch curve is given by

$$\text{Dimension}_{\text{Koch curve}} = \frac{\log(n+1)}{\log n}, \; n \in N, \text{and } n \geq 3 . \tag{3.10}$$

From (3.10), it can be calculated that the dimension of Koch curves at n = 4, 5 and 6 is approximately 1.16, 1.113 and 1.086 respectively. According to Vinoy et al. (2002, 2004) since fractal antennas having smaller dimensions show better multi-band characteristics, Koch antennas at $s = \frac{1}{n}$, for $n \geq 4$, shall exhibit better multiband characteristics.

Theoretically, superior Koch loops, generated at $s = \frac{1}{n}$, for $n \geq 4$, are more suitable as antennas than the Koch antenna at $s = \frac{1}{3}$, as they are more compact in size (Kordzades, Kashani & Hojat, 2001) and can accommodate long length of wire (Krisha

et al., 2009), and therefore will have better multiband characteristics due to smaller fractal dimension (McClure, 2008).

3.7 SUMMARY

Using the idea of division of initiator into unequal parts, a few variants of Koch curve have been presented in this chapter. These Koch curves are new examples of superior fractals. Different variants of Koch curve have been classified into two categories. Category 1 includes the Koch curves that are generated by dividing the initiator into equal parts and category 2 includes Koch curves that are generated by the division of initiator into unequal parts. In both categories, using the given ideas, many Koch curves can be generated. In this chapter, different types of variants for Koch curve have been surveyed and made them fit into the proposed classification

Further, the formulas for calculation of perimeter, area and dimension for geometrical analysis of new variants of Koch curves have been derived. Theoretically, the curves having lesser dimension are more suitable as antenna. The performance of new curves as antenna shall be evaluated experimentally in next chapter.

Further, few curves have same dimension, but their main antenna portions are at different positions (e.g., Koch middle one-third curve and Koch left one-third curve). Does such kind of curves perform similar as antenna or the position of main antenna portion contribute in performance? This curiosity shall also be answered in next chapter.

CHAPTER 4

RESULTS AND DISCUSSIONS

4.1 INTRODUCTION

In this chapter, the antenna characteristics of the new Koch geometries (given in Chapter 3) will be analyzed experimentally. For this, two shapes Koch middle one-fifth and the Koch left one-third curves are chosen out of the given new designed shapes. Koch middle one-fifth curve will represent the curves of lesser dimension than the conventional Koch curve. It is proposed in Chapter 3 that due to lesser dimension, Koch middle one-fifth curve will perform, theoretically, better than the conventional Koch curve. In this chapter, this phenomenon will be verified experimentally.

Also, it is also required to check whether the two Koch fractals having same dimension will perform similar. For this reason, Koch left one-third curve is chosen, whose dimension is equal to the conventional Koch curve. In this chapter, antenna characteristics of Koch left one-third curve will be analyzed and compared with the conventional Koch curve.

Both the above said new shapes are simulated using Micro Wave Studio package of Computer Simulation Technology (CST) 2009. In addition, first, the Koch middle one-third curve will be simulated, so that the antennas may be compared to find the strong points of new antennas

To understand the antenna properties of the shapes, simulation has been divided into three sections: Koch middle one-third antenna, Koch middle one-fifth antenna, and Koch left one-third antenna. Each design of the antenna have been simulated at Iteration 1, 2 and 3. Table 4.1 shows values of common parameters that have been taken in all the simulations:

Table 4.1: Parameters in antenna simulation

Parameters	Values
End to end length	28 mm
Height	0.16 mm
Thickness of the wire	0.07 mm
Port type	Discrete

4.2 KOCH MIDDLE ONE-THIRD ANTENNA

4.2.1 First Iteration

To design the Koch middle one-third antenna at iteration 1, coordinates and its design in CST are shown in Appendix A1. Figure 4.1 shows the return loss (S11) for frequency swept from 0 GHz to 10 GHz for the first iteration of Koch middle one-third antenna. It can be seen that the shape works as antenna on two frequencies 2.16 GHz and 6.63 GHz.

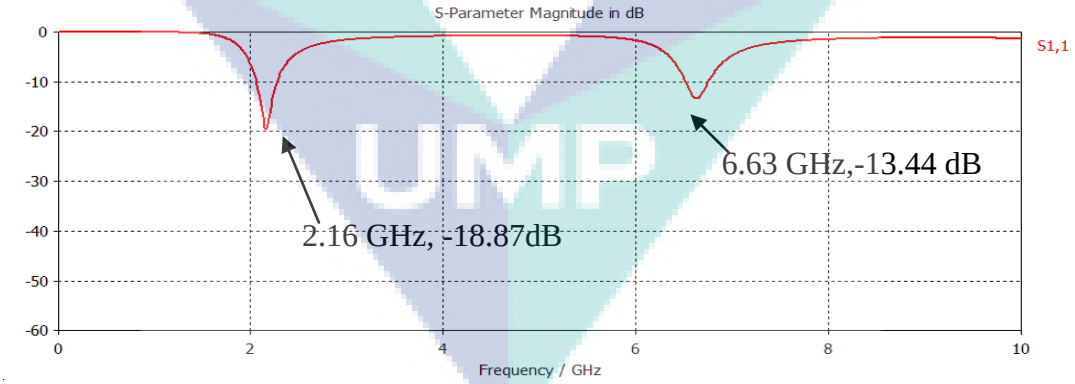

Figure 4.1: Return Loss (S11) at 2.16 GHz and 6.63 GHz

Another important measurement of antenna is voltage standing wave ratio (VSWR), which shows the value of electric field intensity of standing wave. For a good antenna, the value of VSWR should be ≤ 2. Figure 4.2 shows that VSWRs at 2.16 GHz and 6.63 GHz are 1.25 and 1.54 respectively.

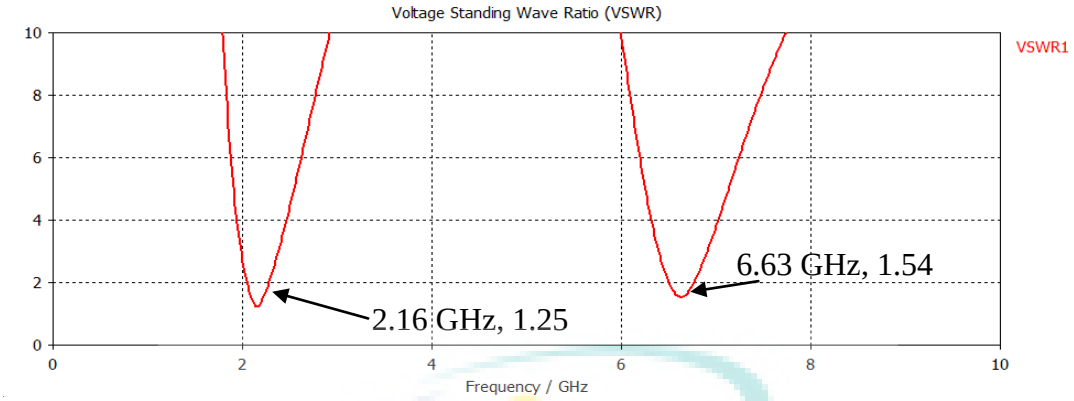

Figure 4.2: VSWR at 2.16 GHz, and 6.63 GHz

Radiation Pattern and Antenna Gain

In the CST Micro wave studio, the radiation pattern is obtained from far field monitors. The radiation pattern at 2.16 GHz is 270 degree (theta angle) in the main lobe direction, with the angular width [3dB] 81 degrees. The radiation pattern in E-plane and H-plane is shown in Figure 4.3a and Figure 4.3b. In addition, the radiation pattern in 3D at frequency 2.16 GHz is shown in Figure 4.4. Here, gain is 1.948 dB.

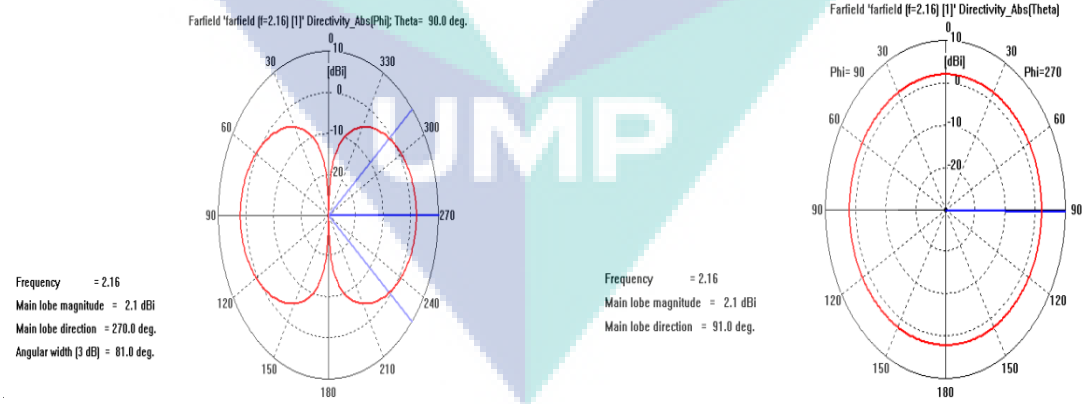

Figure 4.3: Radiation Pattern (a) E-plane, and (b) H-plane at 2.16 GHz

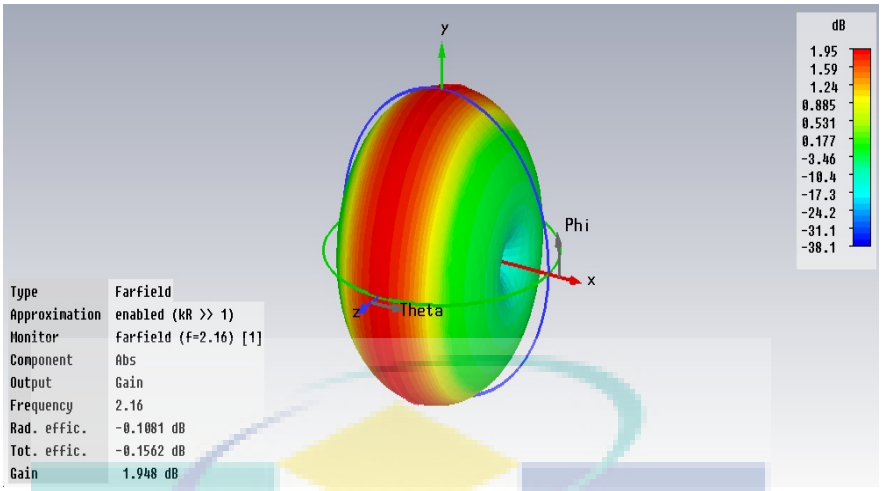

Figure 4.4: 3-D Radiation Pattern at 2.16 GHz

The radiation pattern at 6.63 GHz is 320 degree (theta angle) in the main lobe direction, with the angular width [3dB] 34 degrees. The radiation patterns in E-plane and H-plane are shown in Figure 4.5a and Figure 4.5b respectively. Also, the radiation pattern in 3D at frequency 6.63 GHz is given in Figure 4.6. Here, gain is 3.445 dB.

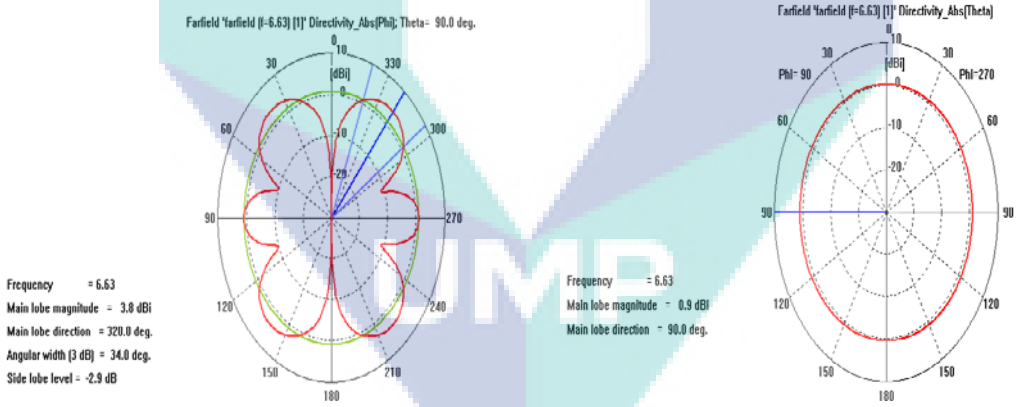

Figure 4.5: Radiation Pattern (a) E-Plane, and (b) H-Plane at 6.63 GHz

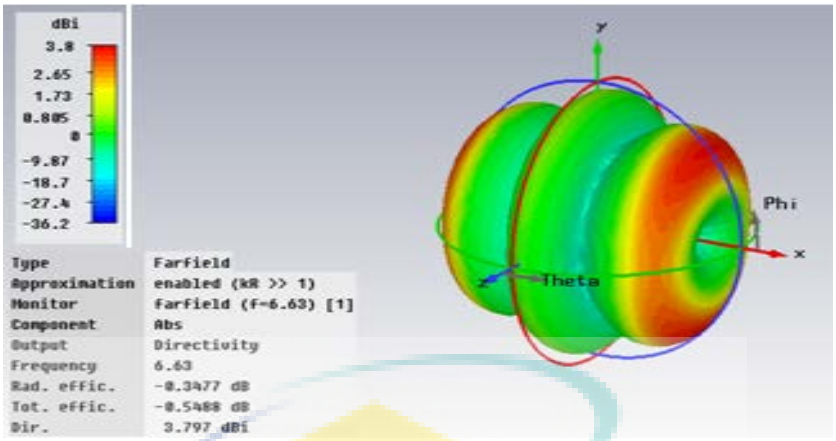

Figure 4.6: 3-D Radiation Pattern at 6.63 GHz

Table 4.2 shows the summary of results and Table 4.3 shows the summary of radiation patterns at both the resonant frequencies.

Table 4.2: 1st Iteration, Koch Middle One-Third Antenna

n-resonant frequency	**F (GHz)**	**S11 (dB)**	**VSWR**	**%BW (fH-fL)/fC**	**Ratio of resonant freq. f-2/f-1**
1	2.16	-18.87	1.25	10	3.05
2	6.63	-13.44	1.54	3.5	

Table 4.3: 1st Iteration, Radiation Pattern of Koch Middle One-Third Antenna

Frequency (GHz)	HPBW (degree)	Gain (IEEE) (dB)	Dir. (dBi)
2.16	81	1.948	2.056
6.63	34	3.445	3.797

4.2.2 Second Iteration

To design the Koch middle one-third antenna at Iteration 2, coordinates and its design in CST are shown in Appendix A2. Figure 4.7 shows the return loss (S11) for frequency swept from 0 GHz to 10 GHz for the 2nd iteration of Koch middle one-third antenna. It can be seen that the shape can work as antenna on three frequencies 2.01 GHz (with return loss of -35.84dB), 5.9 GHz (with return loss -38.37dB), i.e., the antenna has multi-band characteristics.

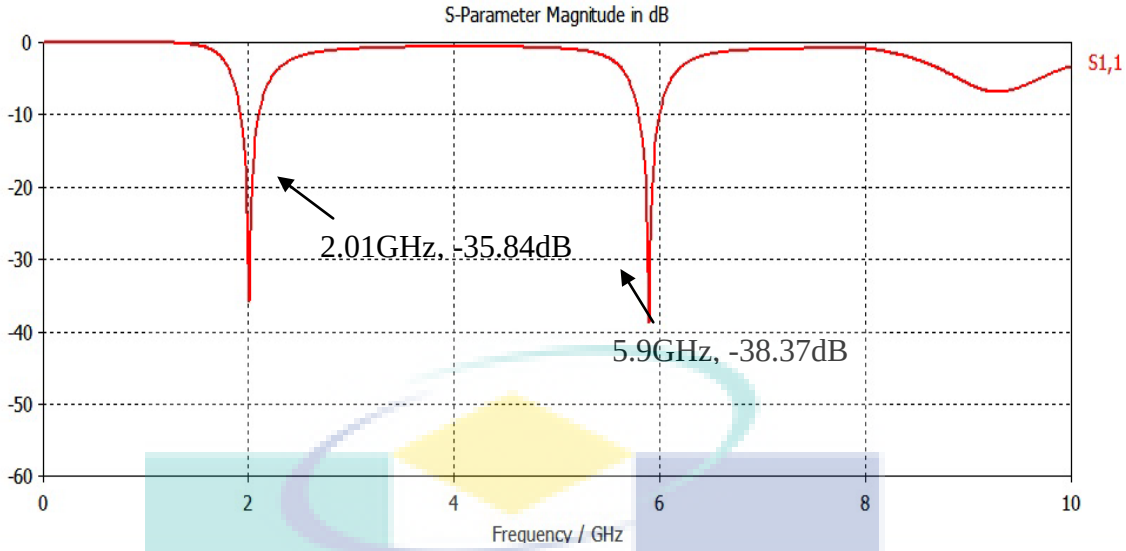

Figure 4.7: Return Loss (S11) at 2.01 GHz and 5.9 GHz

Figure 4.8 shows the simulated VSWRs, from 0-10 GHz is 1.032 at 2.01GHz and 1.02 at 5.9 GHz.

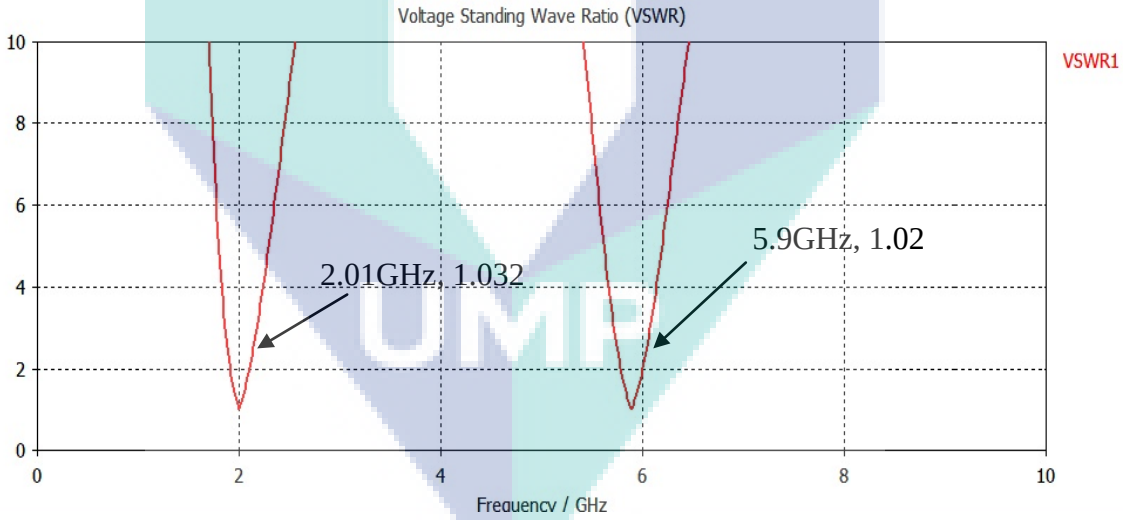

Figure 4.8: VSWR at 2.01 GHz and 5.9 GHz

Radiation Pattern and Antenna Gain

The radiation pattern at 2.01 GHz is 270 degree (theta angle) in the main lobe direction, with the angular width [3dB] 82.2 degrees. The radiation pattern in E-plane and H-plane are shown in Figure 4.9a and Figure 4.9b respectively. Also, the radiation pattern in 3D at frequency 2.01 GHz is shown in Figure 4.10. Gain is 1.778 dB.

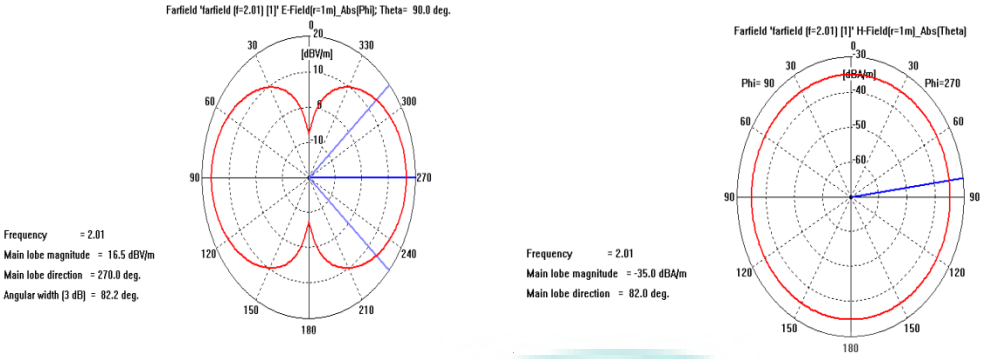

Figure 4.9: Radiation Pattern (a) E-plane, and (b) H-plane at 2.01 GHz

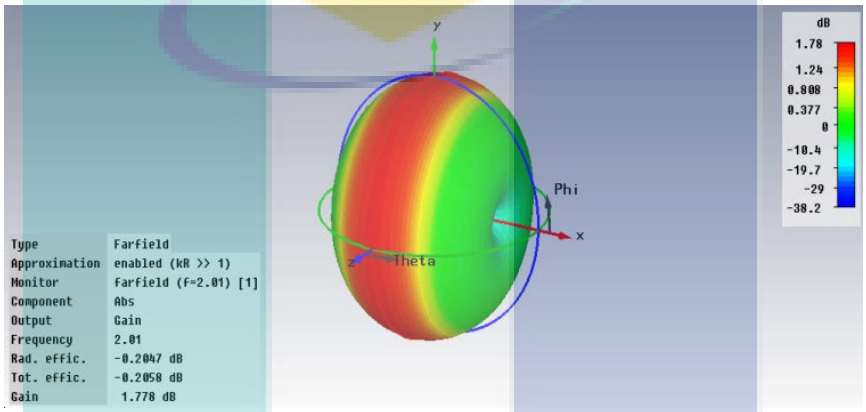

Figure 4.10: 3-D radiation Pattern at 2.01 GHz

The radiation pattern at 5.69 GHz is 34 degree (theta angle) in the main lobe direction, with the angular width [3dB] 37.7 degrees. The radiation patterns in E-plane and H-plane are shown in Figure 4.11a and Figure 4.11b respectively. In addition, the radiation pattern in 3D at frequency 5.9 GHz is shown in Figure 4.12. Gain is 2.067 dB.

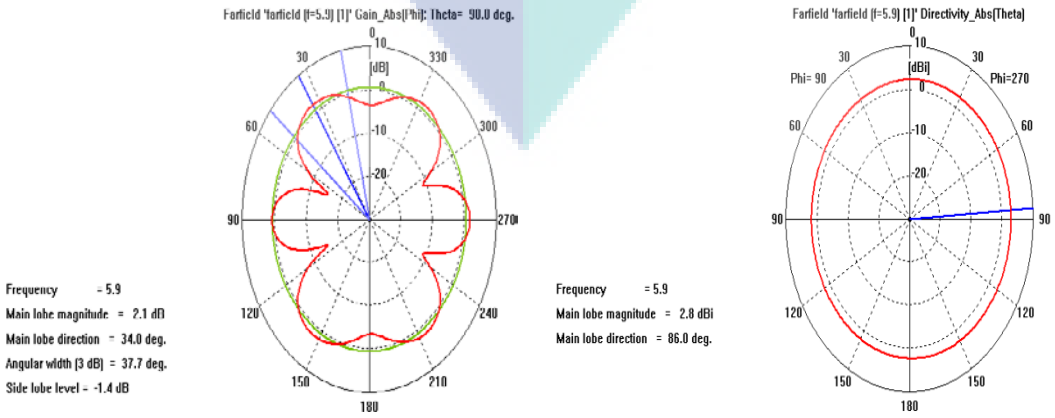

Figure 4.11: Radiation Pattern (a) E-plane, and (b) H-plane at 5.9 GHz.

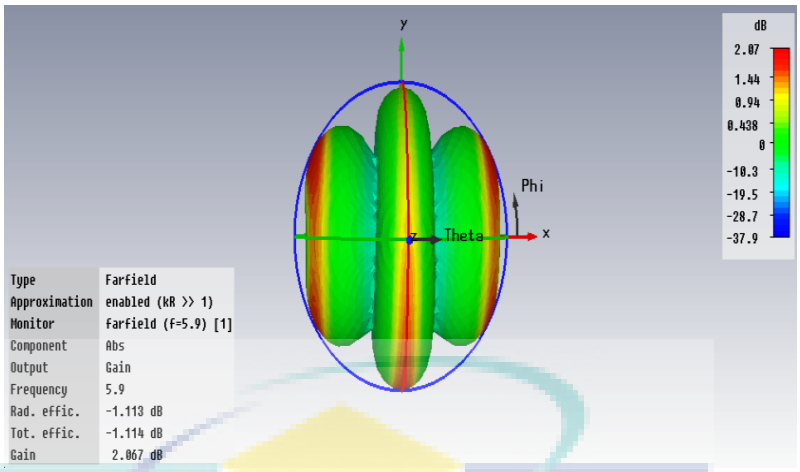

Figure 4.12: 3-D Radiation Pattern at 5.9 GHz

Table 4.4 shows the summary of results and Table 4.5 shows the summary of radiation patterns.

Table 4.4: 2nd iteration, Koch middle one-third antenna

n-resonant frequency	**F (GHz)**	**S11 (dB)**	**VSWR**	**%BW (fH- fL)/fC**	**Ratio of resonant freq. f-2/f-1**
1	2.01	-35.842	1.032	8.9	
2	5.90	-38.37	1.02	3.4	2.93

Table 4.5: 2nd Iteration, Radiation Pattern of Koch Middle One-Third Antenna

Frequency (GHz)	HPBW (degree)	Gain (IEEE) (dB)	Dir. (dBi)
2.01	82.2	1.778	1.98
5.9	37.7	2.067	3.181

4.2.3 Third Iteration

To design the Koch middle one-third antenna at Iteration 3, coordinates and its design in CST are shown in Appendix A3. Figure 4.13 shows the return loss (S11) for frequency swept from 0 GHz to 10 GHz for the Koch middle one-third antenna at third (3rd) iteration. It can be seen that the shape works as antenna at three frequencies 1.93

GHz (with the return loss of -36.27dB) and 5.69 GHz (with the return loss of -14.86 dB), and 9.63 GHz (with return loss -25.98dB) i.e., the antenna has multi-band characteristics.

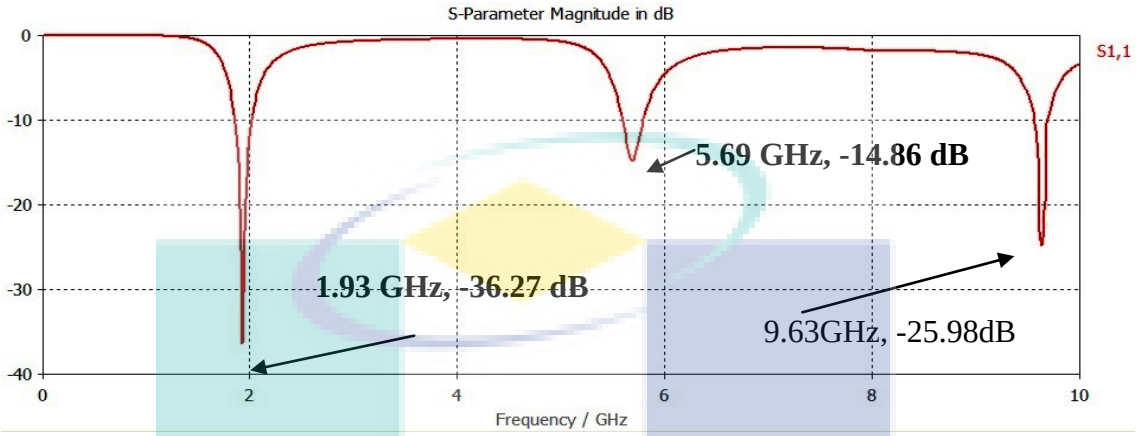

Figure 4.13: Return Loss (S11) at 1.93 and 5.69 GHz

Figure 4.14 shows the simulated VSWR from 0-10 GHz. VSWR is 1.03 at 1.93 GHz, 1.43 at 5.69 GHz and 1.105 at 9.63 GHz.

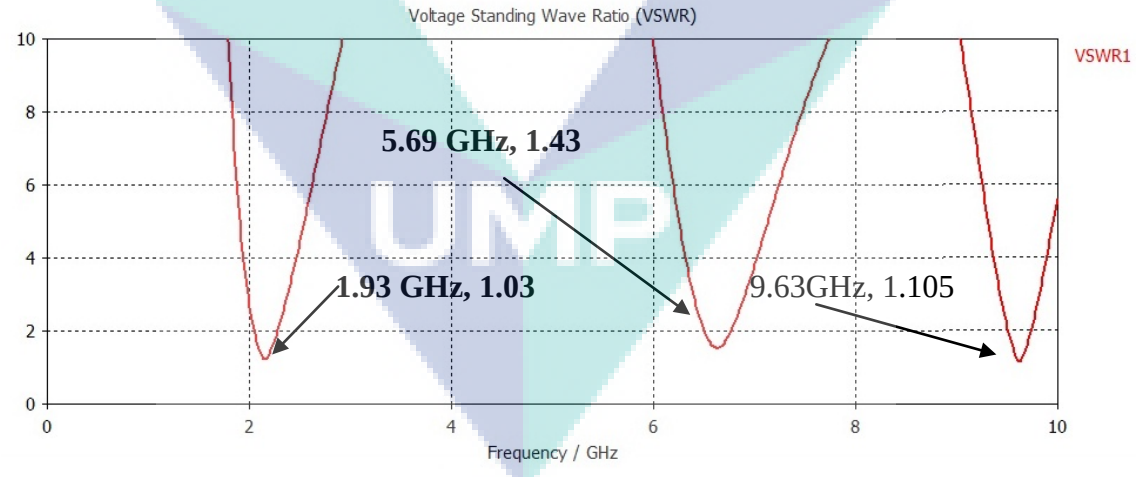

Figure 4.14: VSWR at 1.93 GHz, 5.69 GHz and 9.63 GHz

Radiation Pattern and Antenna Gain

The radiation pattern at 1.93 GHz is 90 degree (theta angle) in the main lobe direction, with the angular width [3dB] 83.0 degrees. The main lobe magnitude is 1.9dB. The radiation patterns in E-plane and H-plane are shown in Figure 4.15a and

Figure 4.15b respectively. In addition, the radiation pattern in 3D at frequency 1.93GHz is shown Figure 4.16. Gain at 1.93 GHz is 1.962dB.

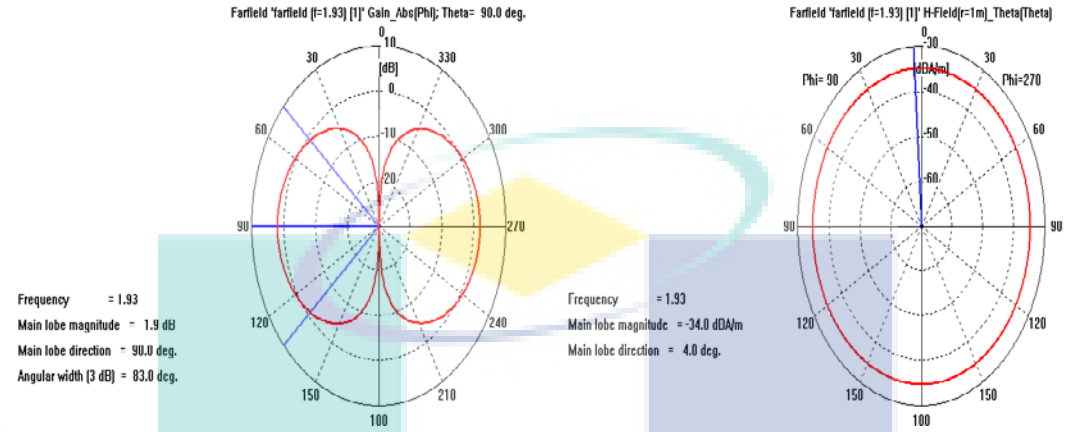

Figure 4.15: Radiation Pattern (a) E-plane, and (b) H-plane at 1.93 GHz.

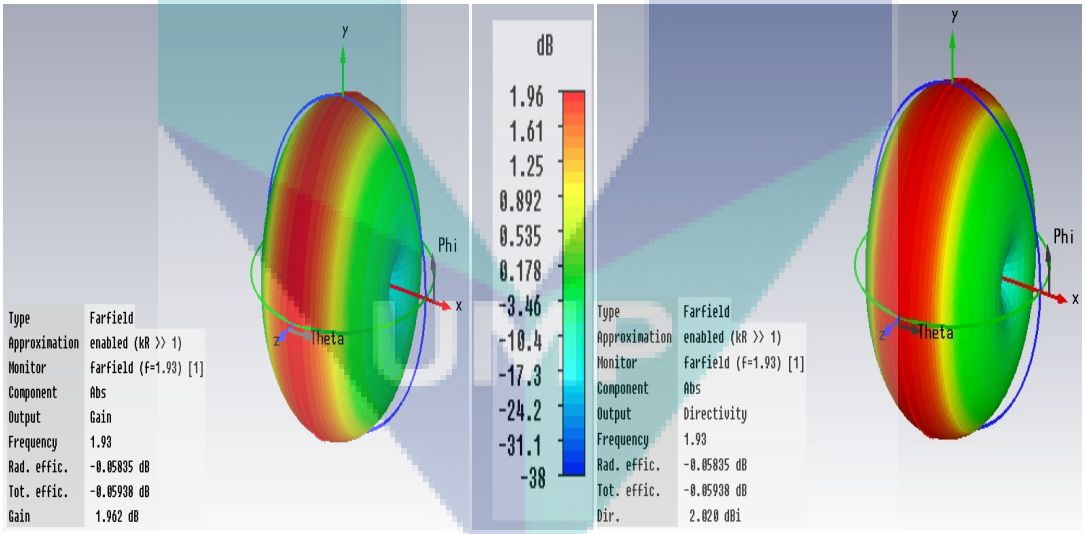

Figure 4.16: 3-D Radiation Pattern at 1.93 GHz

The radiation pattern at 5.69 GHz is 217 degree (theta angle) in the main lobe direction, with the angular width [3dB] 43.2 degrees. The radiation patterns in E-plane and H-plane are shown in Figure 4.17a and Figure 4.17b respectively. Also, the radiation pattern in 3D at frequency 5.69GHz is shown Figure 4.18.

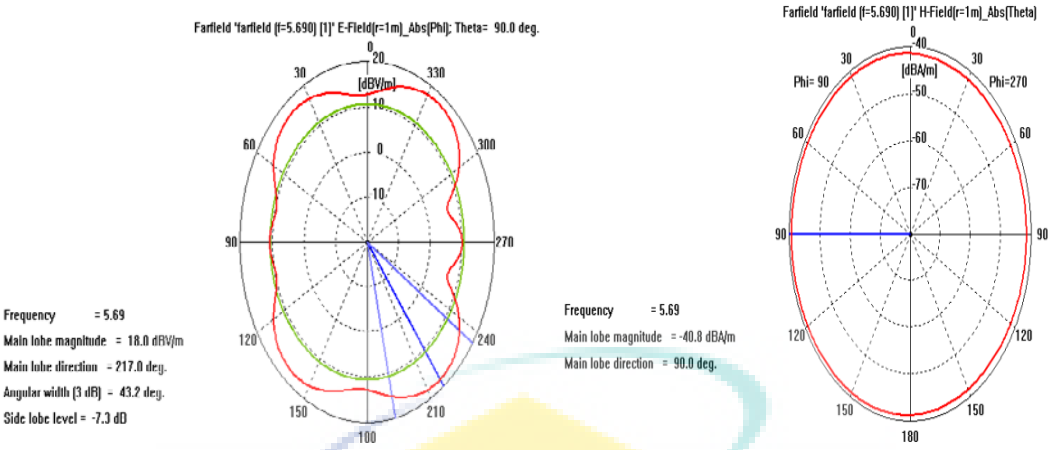

Figure 4.17: Radiation Pattern (a) E-plane, and (b) H-plane at 5.69 GHz.

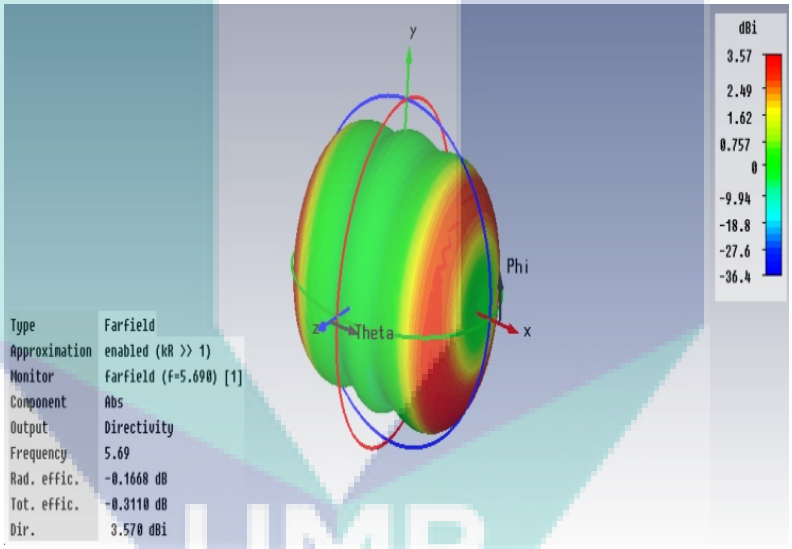

Figure 4.18: 3-D Radiation Pattern at 5.69 GHz

The radiation pattern at 9.63 GHz is 160 degree (theta angle) in the main lobe direction, with the angular width [3dB] 52.7 degrees. The radiation patterns in E-plane and H-plane shown are in Figure 4.19a and Figure 4.19b respectively. Also, the radiation pattern in 3D at frequency 9.63 GHz, is shown in Figure 4.20. Here, gain is 2.665 dB.

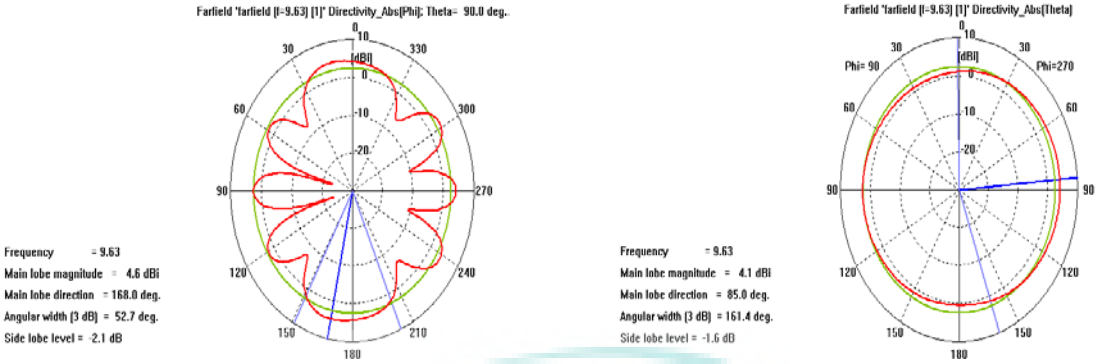

Figure 4.19: Radiation Pattern (a) E-plane, and (b) H-plane at 9.63 GHz.

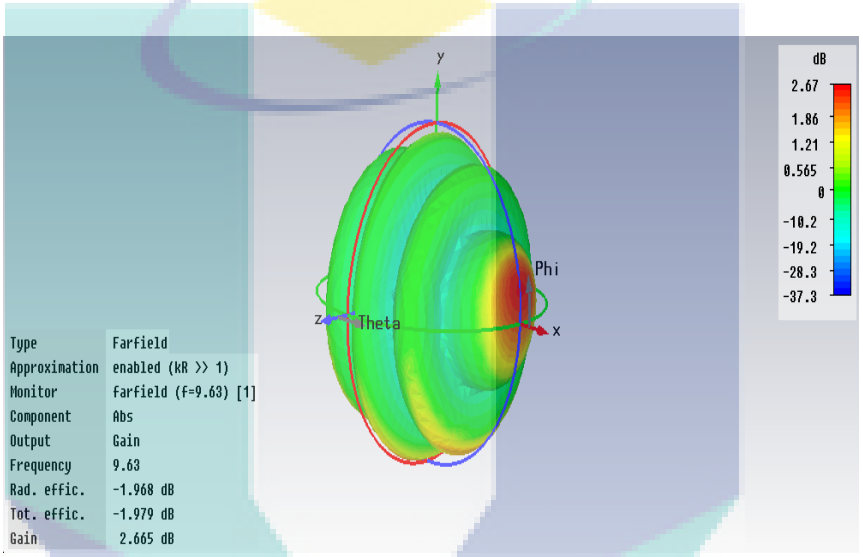

Figure 4.20: 3-D Radiation Pattern at 9.63 GHz

Table 4.6 shows the summary of results and Table 4.7 shows the summary of radiation patterns.

Table 4.6: 3rd iteration, Koch middle one-third antenna

n-resonant frequency	F (GHz)	S11 (dB)	VSWR	%BW (fH- fL)/fC	Ratio of resonant freq. f-2/f-1	Ratio of resonant freq. f-3/f-2
1	1.93	-36.27	1.03	8.8	2.94	1.69
2	5.69	-14.86	1.43	3.5		
3	9.63	-25.98	1.105	2.2		

Table 4.7: 3rd iteration, Radiation pattern of Koch middle one-third antenna

Frequency (GHz)	HPBW (degree)	Gain (IEEE) (dB)	Dir. (dBi)
1.93	83	1.9	2.02
5.69	43.2	3.54	3.57
9.63	52.7	2.66	4.633

4.2.4 Comparative study of the antenna at all three iterations

Comparison of return losses shown for Koch middle one-third antenna at Iteration 1, 2 and 3 has been shown Figure 4.21. VSWR comparison graph for all the three iterations is shown in Figure 5.22.

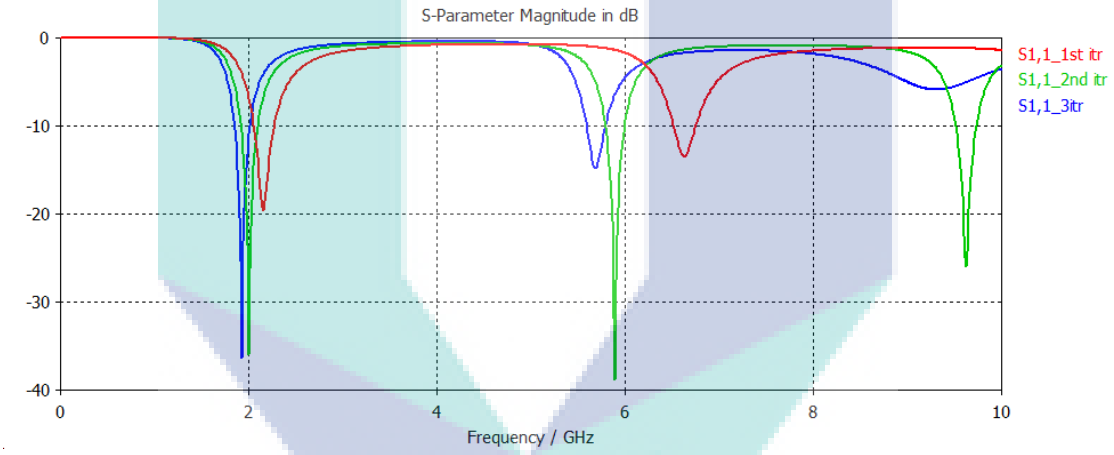

Figure 4.21: Return Losses for Koch middle one-third antenna at Iteration 1, 2 and 3

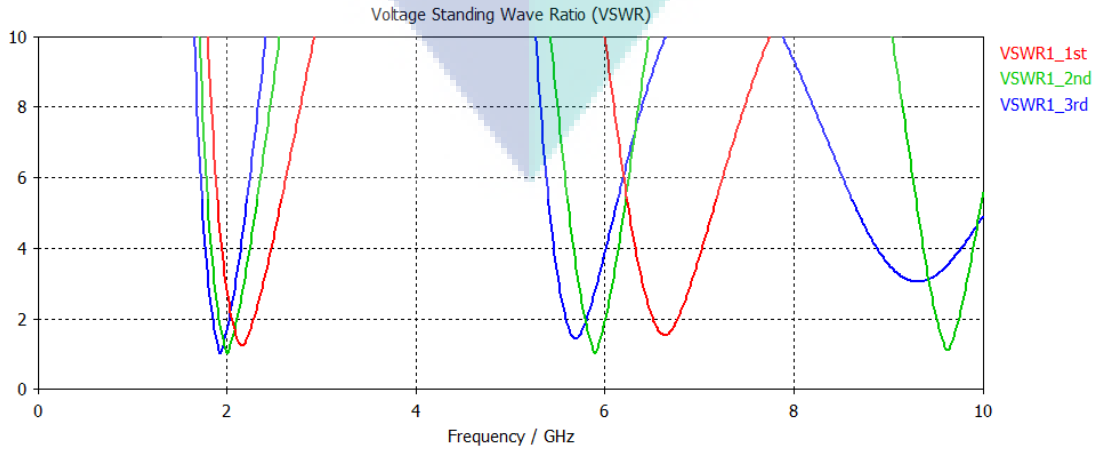

Figure 4.22: VSWRs, at Iteration 1, 2 and 3

It is clear from the graph plotted in Figure 4.21 that the return loss is minimum at iteration 2. Also, it can be seen in the graph plotted in Figure 4.22 that VSWR is minimum at iteration 2. This shows that Koch middle one-third antenna performs the best when designed for second iteration.

4.3 KOCH MIDDLE ONE-FIFTH ANTENNA

4.3.1 First Iteration

To design the Koch middle one-fifth antenna at Iteration 1, the coordinates and its design in CST are shown in Appendix B1. Figure 4.23 shows the return loss (S11) for frequency swept from 0 GHz to 10 GHz for the Koch middle one-fifth antenna at 1st iteration. It can be seen that the shape works as antenna at two frequencies 2.17 GHz (with the return loss of -18.45dB) and 6.79 GHz (with the return loss of –13.60 dB). The antenna has multi-band characteristics.

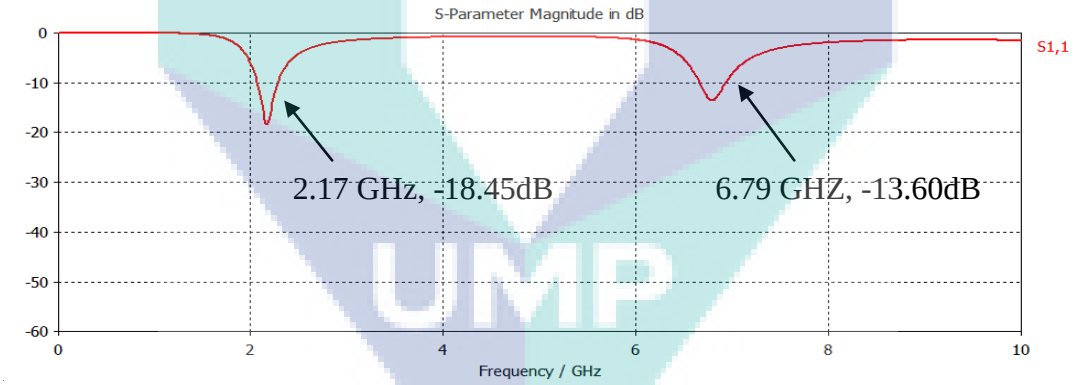

Figure 4.23: Return Loss S11 at 2.17 GHz and 6.79 GHz

Figure 4.24 shows the simulated VSWR from 0-10 GHz. VSWR is 1.271at 2.17 GHz and 1.527 at 6.79 GHz .

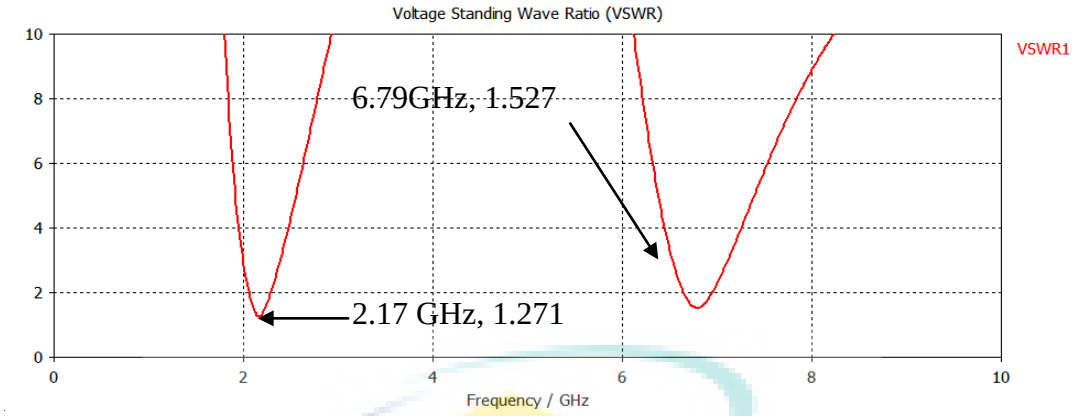

Figure 4.24: VSWR, at 2.17 GHz and 6.79 GHz

The radiation pattern at 2.17 GHz is 91.8 degree (theta angle) in the main lobe direction, with the angular width [3dB] 80.8 degrees. The radiation patterns in E-plane and H-plane are shown in Figure 4.25a and Figure 4.25b respectively. In addition, the radiation pattern in 3D at frequency 2.17GHz is shown Figure 4.26.

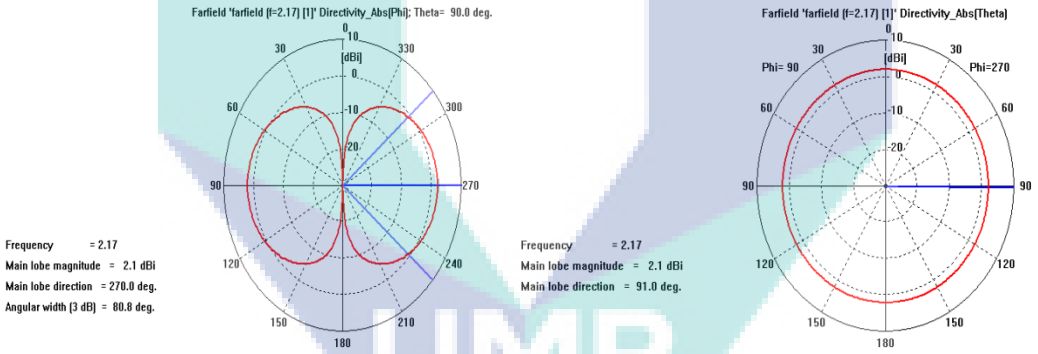

Figure 4.25: Radiation Pattern (a) E-Plane, and (b) H-Plane at 2.17 GHz

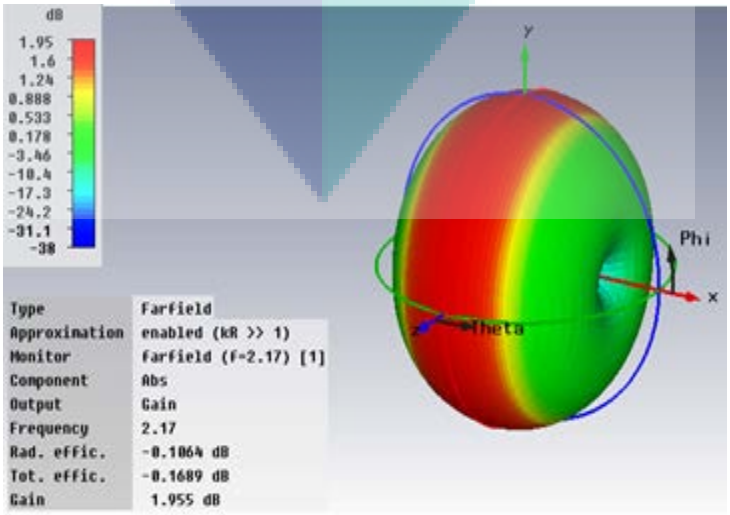

Figure 4.26: 3-D Radiation Pattern at 2.17 GHz

The radiation pattern at 6.79 GHz is 91.8 degree (theta angle) in the main lobe direction, with the angular width [3dB] 34.3 degrees. The radiation patterns in E-plan and H-plane are shown in Figure 4.27a and Figure 4.27b respectively. In addition, the radiation pattern in 3D at frequency 6.79GHz is shown Figure 4.28.

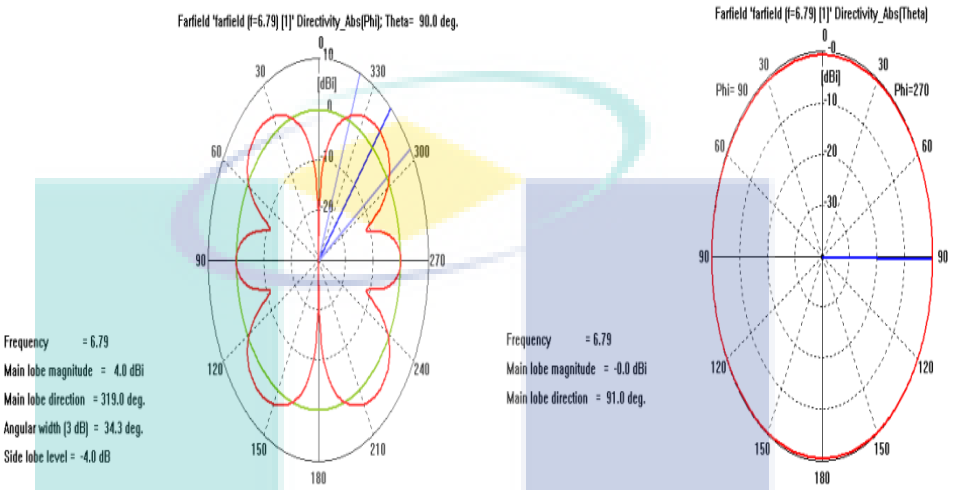

Figure 4.27: Radiation Pattern (a) E-Plane, and (b) H-Plane at 6.79GHz

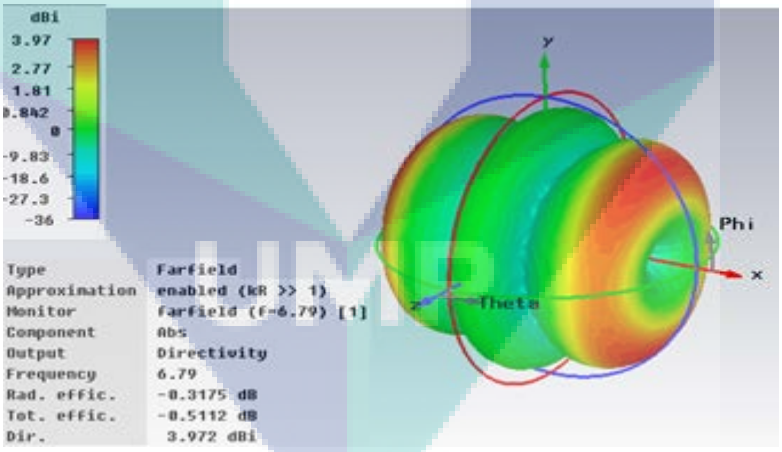

Figure 4.28: 3-D Radiation Pattern at 6.79 GHz

Table 4.8 shows the summary of results and Table 4.9 shows the summary of radiation patterns.

Table 4.8: 1st Iteration, Koch Middle One-Fifth Antenna

n-resonant frequency	F (GHz)	S11 (dB)	VSWR	%BW (fH-fL)/fC	Ratio of resonant freq. f-2/f-1
1	2.17	-18.45	1.271	9.8	3.13
2	6.79	-13.60	1.527	3.7	

Table 4.9: 1st Iteration, Radiation Pattern of Koch Middle One-Fifth Antenna

Frequency (GHz)	HPBW (degree)	Gain (IEEE) (dB)	Dir. (dBi)
2.17	80.8	1.955	2.06
6.79	34.3	3.65	3.97

If Koch middle one-fifth antenna at iteration 1 is compared with the Koch middle one-third antenna at iteration 1, it can be observed that overall return loss and overall gain become poor while overall bandwidth remains unchanged.

4.3.2 Second Iteration

To design the Koch middle one-fifth antenna at Iteration 2, coordinates and its design in CST are given in Appendix B2. Figure 4.29 shows the return loss (S11) for frequency swept from 0 GHz to 10 GHz for the Koch middle one-fifth antenna at 2nd iteration. The shape works as antenna at two frequencies 2.13 GHz (with the return loss of -23.33dB) and 6.45GHz (with the return loss of –16.20 dB). This shows that the antenna has multi-band characteristics.

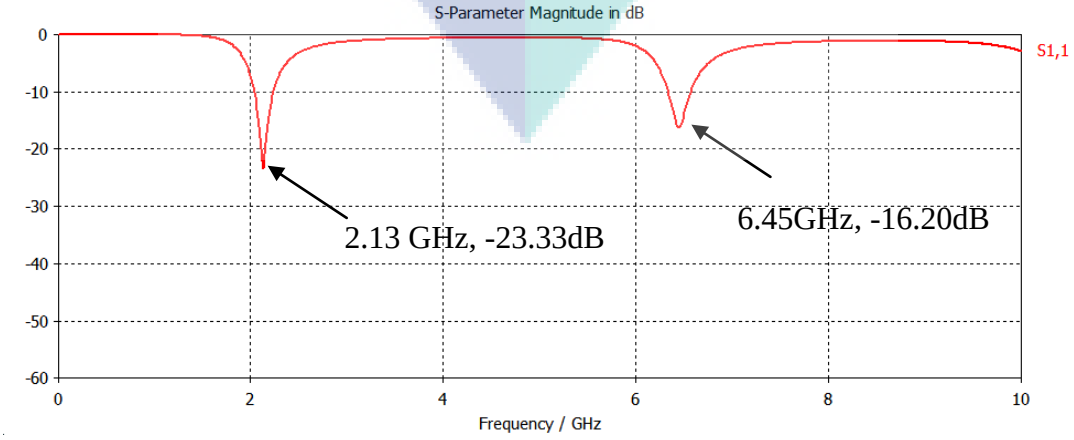

Figure 4.29: Return Loss S11 at 2.13 GHz and 6.45 GHz

Figure 4.30 shows the simulated VSWR from 0-10 GHz. VSWR is 1.146 at 2.13 GHz, 1.366 at 6.45 GHz.

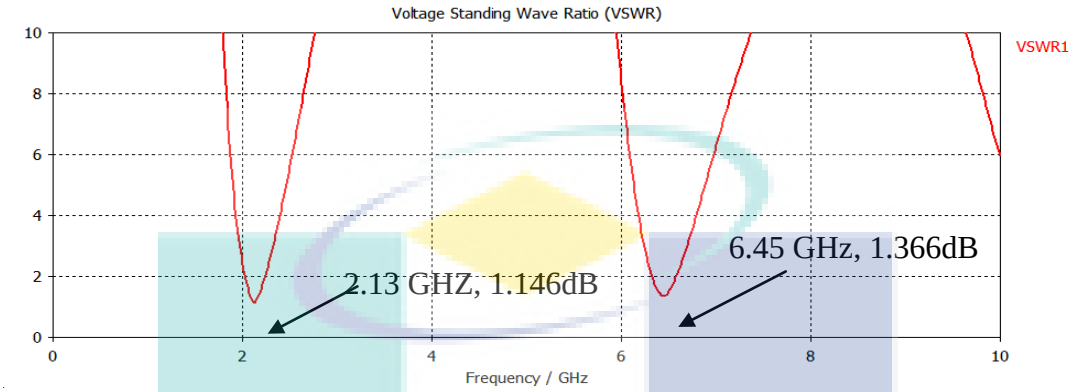

Figure 4.30: VSWR, at 2.13 GHz and 6.45 GHz

Radiation Pattern and Antenna Gain

The radiation pattern at 2.13 GHz is 90.0 degree (theta angle) in the main lobe direction, with the angular width [3dB] 81.5 degrees. The radiation patterns in E-plane and H-plane are shown in Figure 4.31a and Figure 4.31b. In addition, the radiation pattern in 3D at frequency 2.13GHz is shown Figure 4.32.

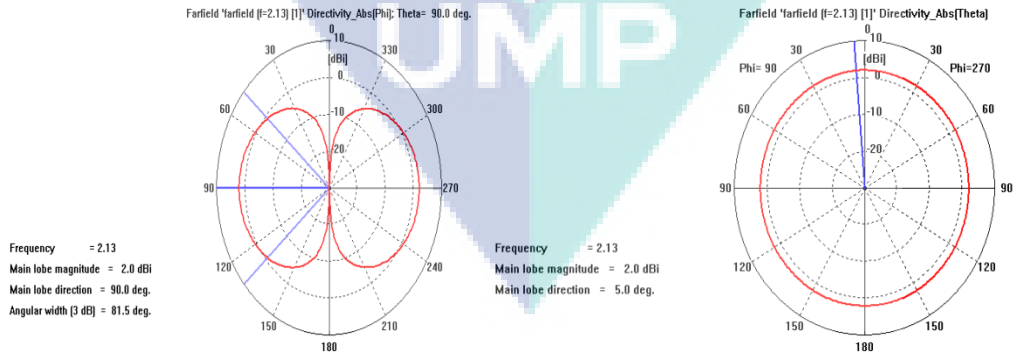

Figure 4.31: Radiation Pattern (a) E-plane, and (b) H-plane at 2.13 GHz

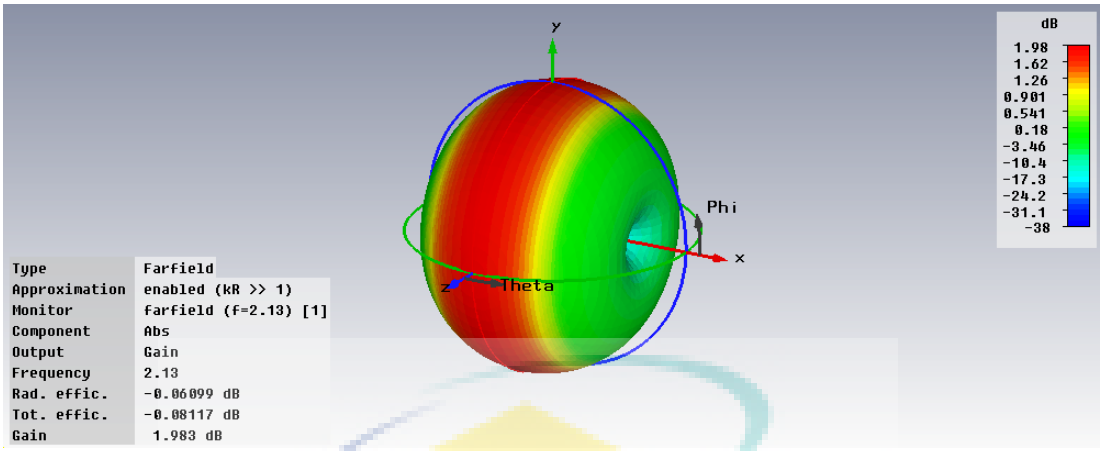

Figure 4.32: 3-D Radiation Pattern at 2.13 GHz

The radiation patterns at 6.45 GHz in E-plane and H-plane are shown in Figure 4.33a and Figure 4.33b. In addition, the radiation pattern in 3D at frequency 6.45GHz is shown Figure 4.34.

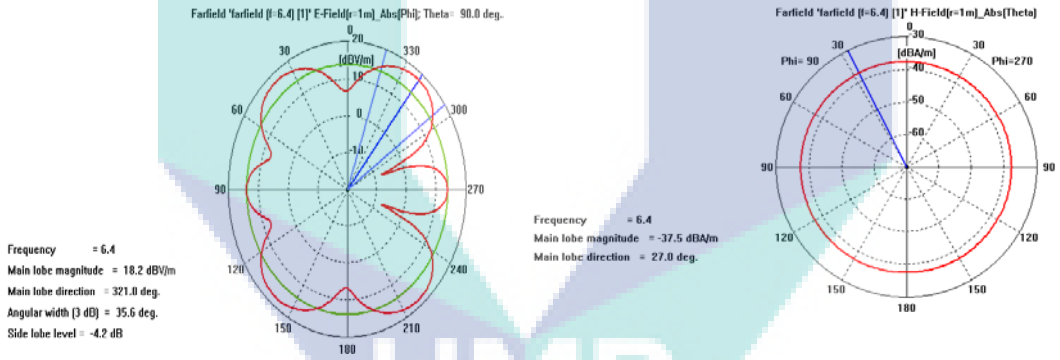

Figure 4.33: Radiation Pattern (a) E-Plane, and (b) H-Plane at 6.45 GHz

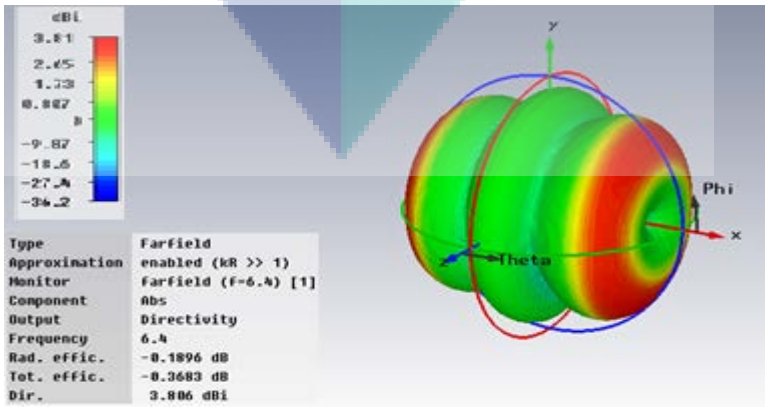

Figure 4.34: 3-D Radiation Pattern at 6.45 GHz

Table 4.10 shows the summary of results and Table 4.11 shows the summary of radiation patterns. The return losses and VSWRs obtained from Table 4.11 are much poor than that of at 2nd iteration of Koch middle one-third antenna, while bandwidth becomes wider here.

Table 4.10: 2nd Iteration, Koch Middle One-Fifth Antenna

n-resonant frequency	F (GHz)	S11 (dB)	VSWR	%BW (fH-fL)/fC	Ratio of resonant freq. f-2/f-1
1	2.13	-23.33	1.146	9.3	3.20
2	6.45	-16.20	1.366	3.6	

Table 4.11: 2nd Iteration, Radiation Pattern of Koch Middle One-Fifth Antenna

Frequency (GHz)	HPBW (degree)	Gain (IEEE) (dB)	Dir. (dBi)
2.13	81.5	1.983	2.04
6.45	35.6	3.611	3.80

4.3.3 Third Iteration

To design the Koch middle one-fifth antenna at Iteration 3, coordinates and its design in CST are shown in Appendix B3. Figure 4.35 shows the return loss (S11) for frequency swept from 0 GHz to 10 GHz for the Koch middle one-fifth antenna at third (3rd) iteration. It can be seen that the shape works as antenna at three frequencies 1.96 GHz (with the return loss of -45.44dB), 5.78 GHz (with the return loss of -34.3dB) and 9.31 GHz (with the return loss of -13.81dB).i.e. the antenna has multi-band characteristics.

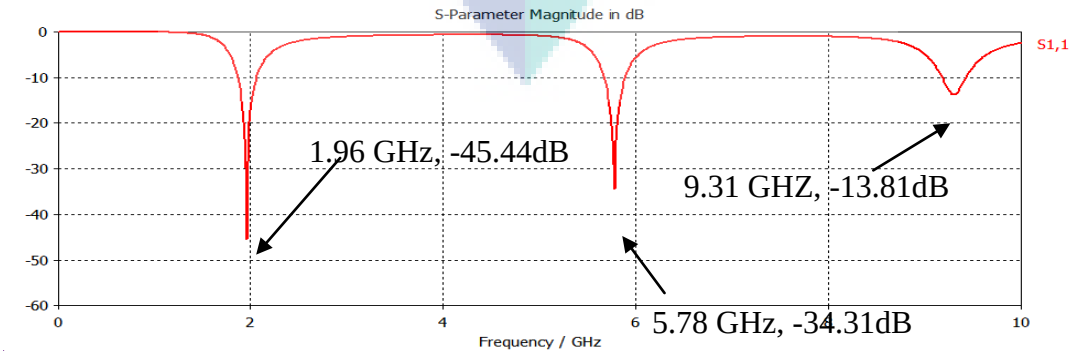

Figure 4.35: Return Loss S11 at 1.96, 5.78 and 9.31GHz

Figure 4.36 shows the simulated VSWR from 0-10 GHz. VSWR is 1.01 at 1.96 GHz, 1.039 at 5.78 GHz and 1.51 at 9.31GHz.

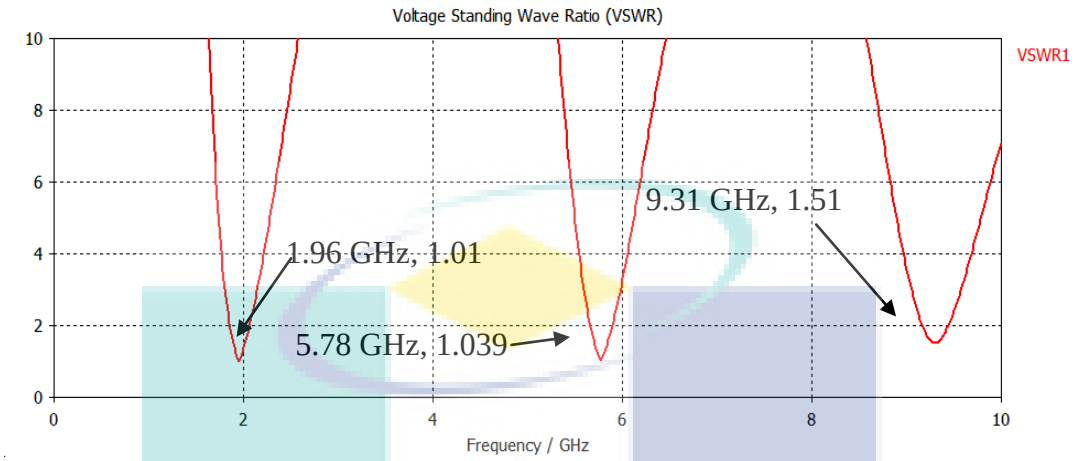

Figure 4.36: VSWR at 1.96 GHz, 5.78 GHz and 9.31GHz

Radiation Pattern and Antenna Gain

The radiation patterns at 1.96 GHz in E-plane and H-plane are shown in Figure 4.37a and Figure 4.37b. Also, the radiation pattern in 3D at frequency 1.96 GHz is shown Figure 4.38.

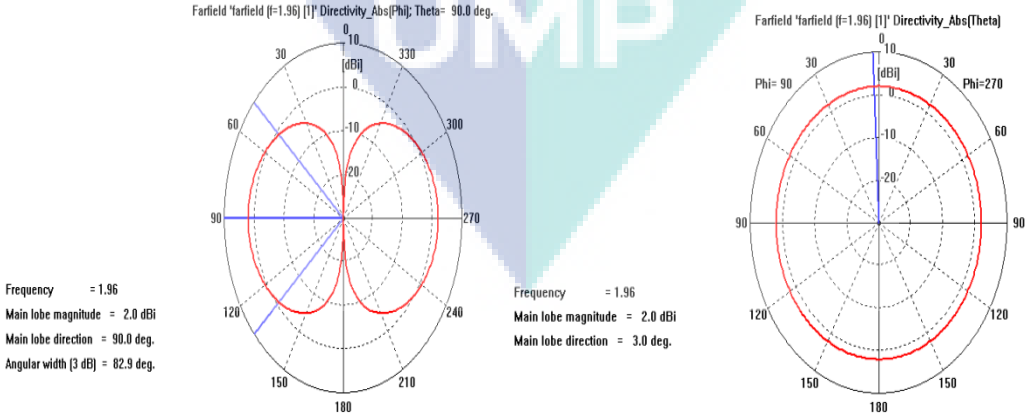

Figure 4.37: Radiation Pattern (a) E-plane, and (b) H-plane at 1.96 GHz

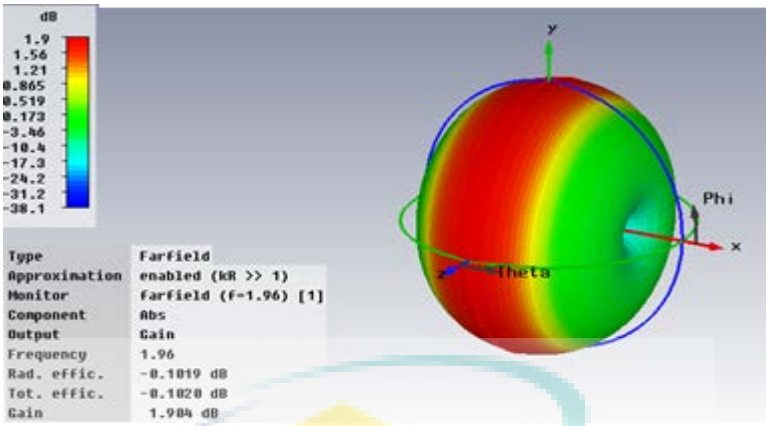

Figure 4.38: 3-D Radiation Pattern at 1.96 GHz

The radiation patterns at 5.78 GHz in E-plane and H-plane are shown in Figure 4.39a and Figure 4.39b. In addition, the radiation pattern in 3D at frequency 5.78 GHz is shown Figure 4.40.

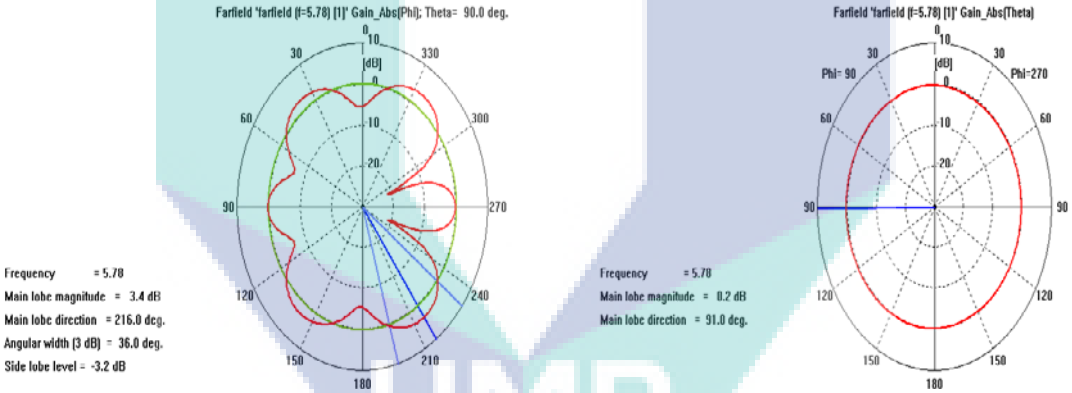

Figure 4.39: Radiation Pattern (a) E-Plane, and (b) H-Plane at 5.78 GHz

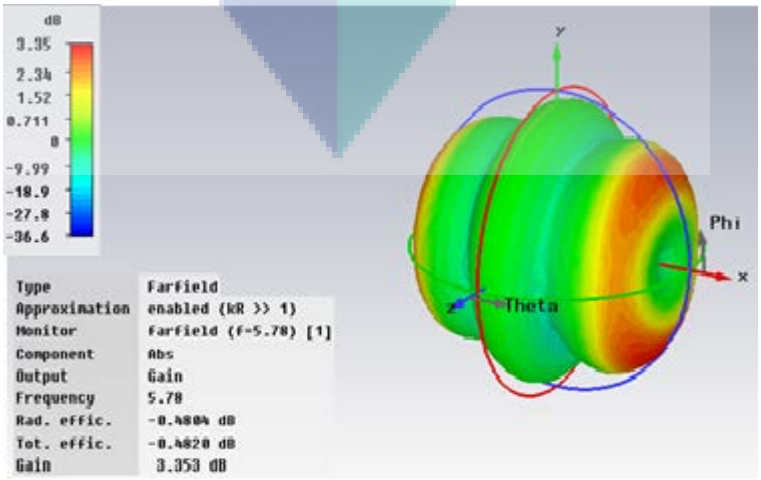

Figure 4.40: 3-D Radiation Pattern at 5.78 GHz

The radiation pattern at 9.31 GHz in E-plane and H-plane is shown in Figure 4.41a and Figure 4.41b. The radiation pattern in 3D at frequency 9.31GHz is shown Figure 4.42.

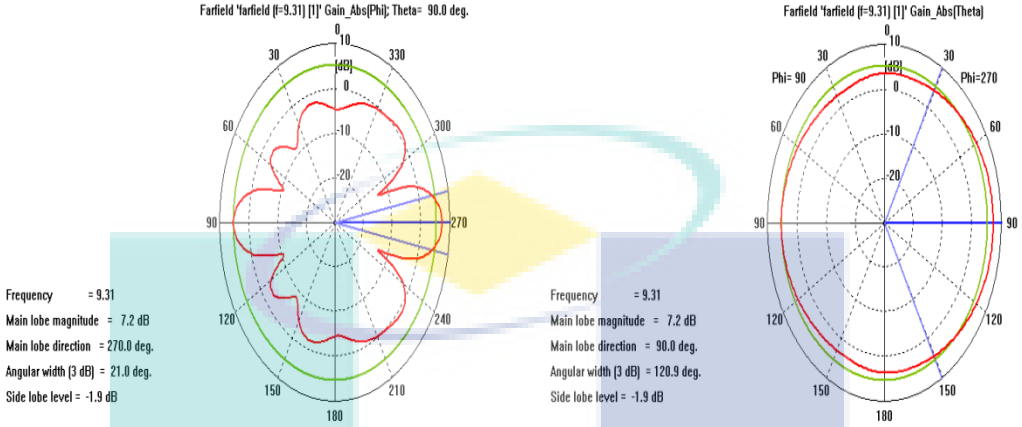

Figure 4.41: Radiation Pattern (a) E-Plane, and (b) H-Plane at 9.31GHz

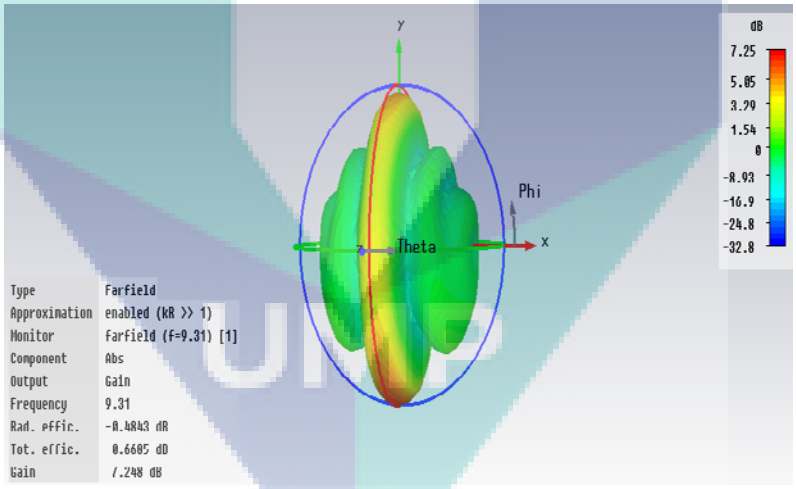

Figure 4.42: 3-D Radiation Pattern at 9.31 GHz

Table 4.12 shows the summary of results and Table 4.13 shows the summary of radiation patterns. Here, return losses and VSWRs at lower and middle resonant frequency are significantly improved, but poor for higher resonant frequency as compared to Koch middle one-third antenna at iteration 3. Bandwidth gets wider here.

Table 4.12: 3rd Iteration, Koch Middle One-Fifth Antenna

n-resonant frequency	F (GHz)	S11 (dB)	VSWR	%BW (fH-fL)/fC	Ratio of resonant freq.f-2/f-1	Ratio of resonant freq.f-3/f-2
1	1.96	-45.44	1.01	9.8	2.94	1.610
2	5.78	-34.31	1.039	13.8		
3	9.31	-13.81	1.51	2.6		

Table 4.13: 3rd iteration, Radiation pattern of Koch middle one-fifth antenna

Frequency(GHz)	HPBW (degree)	Gain (IEEE) (dB)	Dir. (dBi)
1.96	82.9	1.904	2.05
5.78	36	3.353	3.83
9.31	21	7.248	7.73

4.3.4 Comparative Study of Antenna at All Three Iterations

Return loss comparison S11 is shown for Koch middle one-fifth iteration at Iteration 1, 2 and 3 in Figure 4.43. VSWR comparison graph for all the three iterations is shown in Figure 4.44.

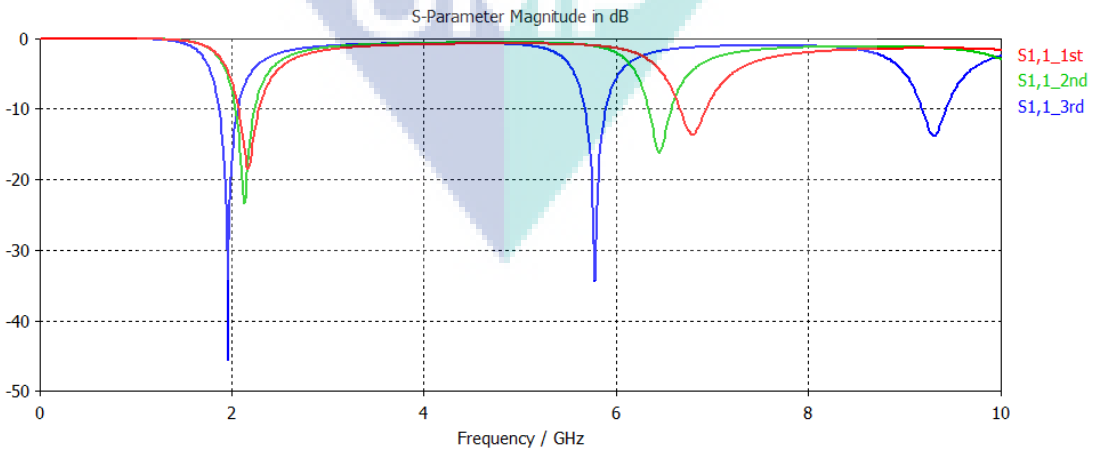

Figure 4.43: Return Losses, S11 at Iteration 1, 2 and 3

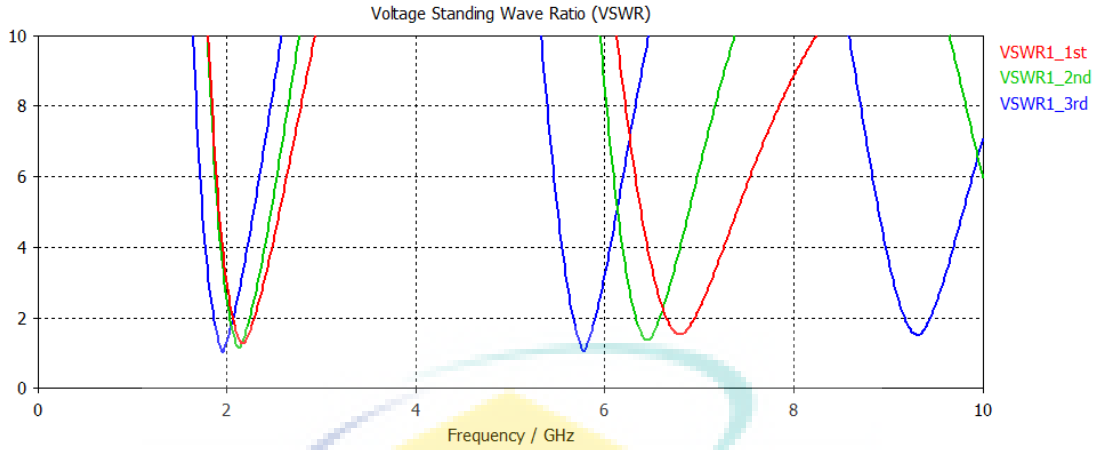

Figure 4.44: Combined VSWRs at Iteration 1, 2 and 3

The minimum return loss and VSWR is obtained at Iteration 3. This shows that Koch middle one-fifth antenna performs best when designed for third iteration, unlike Koch middle one-third antenna, which performs best when designed at iteration 2.

4.4 KOCH LEFT ONE-THIRD ANTENNA

4.4.1 First Iteration

To design the Koch left one-third antenna at Iteration 1, coordinates and its design in CST are given in Appendix C1. Figure 4.45 shows the return loss (S11) for frequency swept from 0 GHz to 10 GHz for the Koch left one-third antenna at 1st iteration. It can be seen that the shape works as antenna at three frequencies 1.99 GHz (with the return loss of -19.0dB), 6.03GHz (with the return loss of -15dB), the antenna has multi-band characteristics.

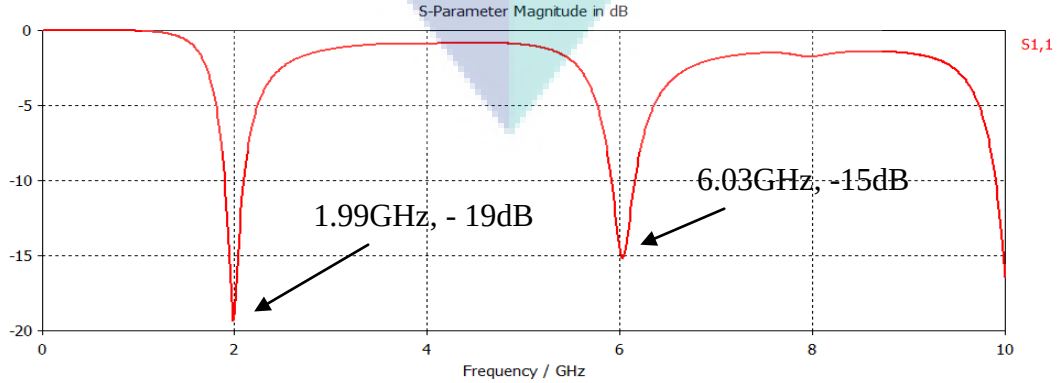

Figure 4.45: Return Loss S11 at 1.99 GHz and 6.03 GHz

Figure 4.46 shows the simulated VSWR from 0-10 GHz. VSWR is 1.19 at 1.99 GHz, 1.39 at 6.03 GHz.

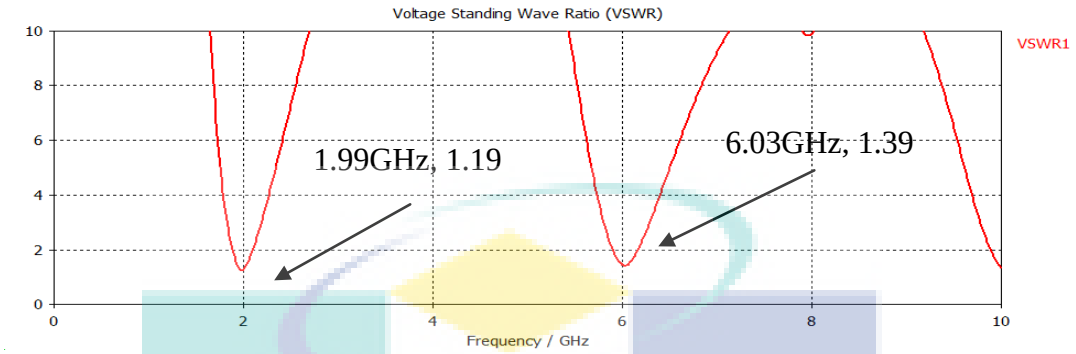

Figure 4.46: VSWR at 1.99 GHz and 6.03 GHz

Radiation Pattern and Antenna Gain

The radiation pattern at 1.99 GHz in E-plane and H-plane is shown in Figure 4.47a and Figure 4.47b. The radiation pattern in 3D at frequency 1.99GHz is shown Figure 4.48.

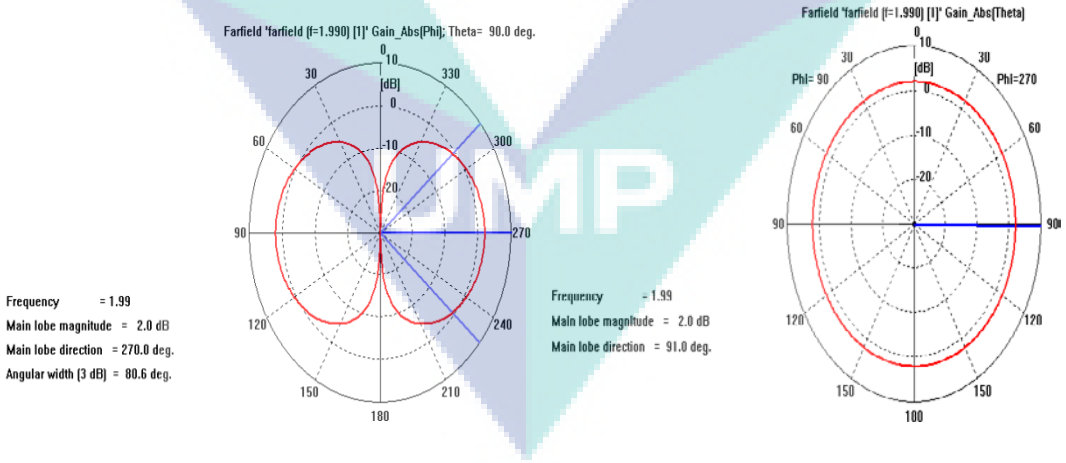

Figure 4.47: Radiation Pattern (a) E-Plane, and (b) H-Plane at 1.99GHz

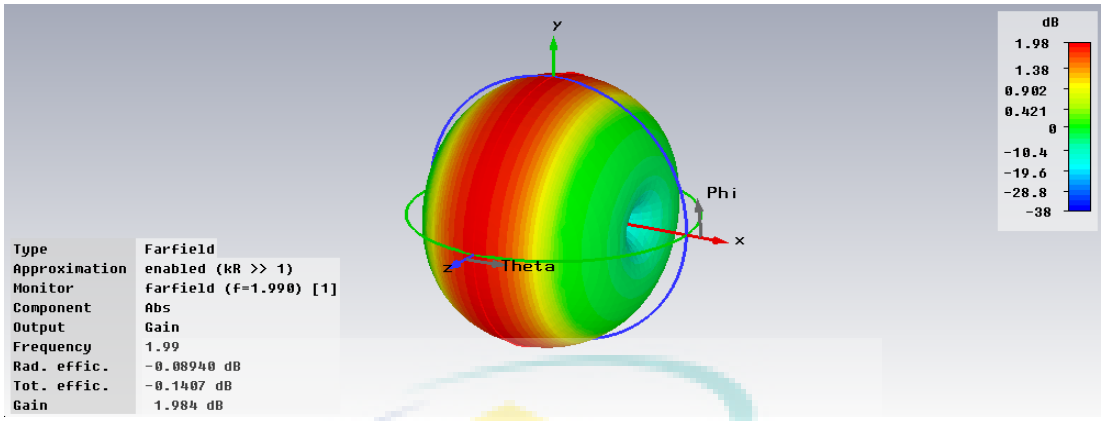

Figure 4.48: 3-D Radiation Pattern at 1.99 GHz

The radiation pattern at 6.03GHz in E-plane and H-plane is shown in Figure 4.49a and Figure 4.49b. The radiation pattern in 3D at frequency 6.03GHz is shown Figure 4.50.

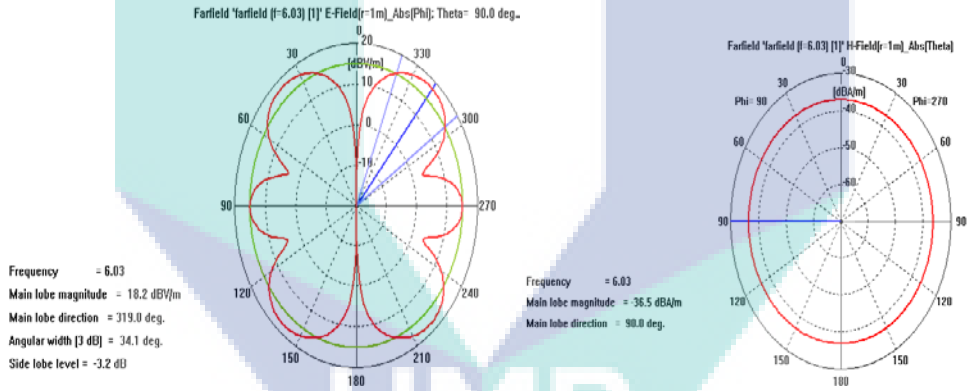

Figure 4.49: Radiation Pattern (a) E-Plane, and (b) H-Plane at 6.03GHz

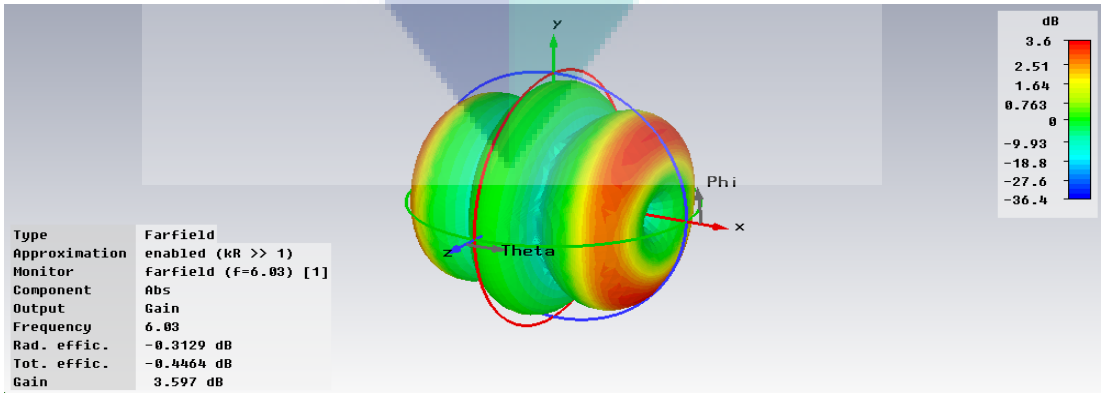

Figure 4.50: 3-D Radiation Pattern at 6.03 GHz

Table 4.14 shows the summary of results and Table 4.15 shows the summary of radiation patterns.

Table 4.14: 1st iteration, Koch left one-third antenna

n-resonant frequency	F (GHz)	S11 (dB)	VSWR	%BW (fH-fL)/fC	Ratio of resonant freq. f-2/f-1
1	1.99	-19	1.19	10.00	3.03
2	6.03	-15	1.39	3.9	

Table 4.15: 1st iteration, Radiation pattern of Koch left one-third antenna

Frequency (GHz)	HPBW (degree)	Gain (IEEE) (dB)	Dir. (dBi)
1.99	80.6	1.984	2.073
6.03	34.1	3.597	3.91

When these results are compared with the results obtained in first iteration of the Koch middle one-third antenna, it is found that there is decrease in VSWR and return loss. Also, bandwidth gets slightly wider. Thus, Koch left one-third antenna shows its superiority on Koch middle one-third antenna at first iteration.

4.4.2 Second Iteration

To design the Koch left one-third antenna at Iteration 2, coordinates and its design in CST are given in Appendix C2. Figure 4.51 shows the return loss (S11) for frequency swept from 0 GHz to 10 GHz for the Koch left one-third antenna at 2nd iteration. It can be seen that the shape works as antenna at three frequencies 1.93GHz (with the return loss of -23.50dB), 5.64GHz (with the return loss of -32.94dB), the antenna has multi-band characteristics.

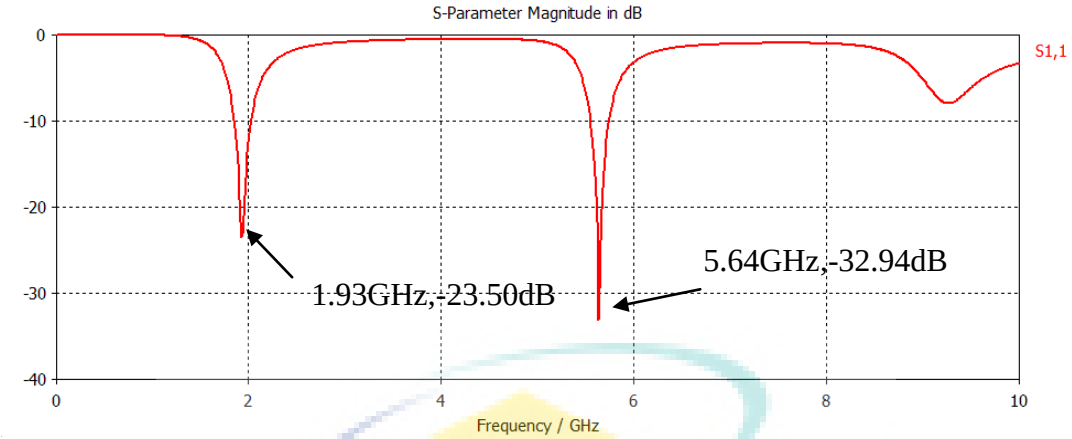

Figure 4.51: Return Loss S11 at 1.93 GHz and 5.64 GHz

Figure 4.52 shows the simulated VSWR from 0-10 GHz. VSWR is 1.14 at 1.93 GHz, 1.04 at 5.6 GHz.

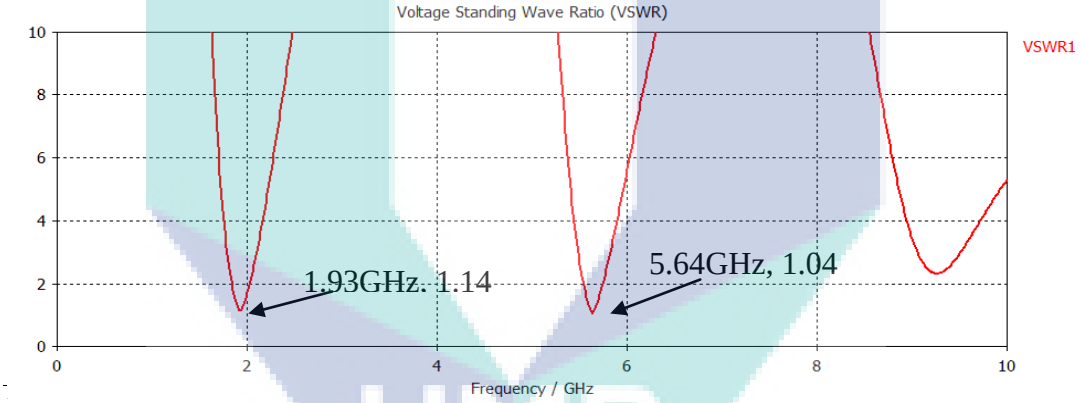

Figure 4.52: VSWR at 1.93 GHz and 5.64 GHz

Radiation Pattern and Antenna Gain

The radiation pattern at 1.93GHz in E-plane and H-plane is shown in Figure 4.53a and Figure 4.53b. The radiation pattern in 3D at frequency 1.93 GHz is shown Figure 4.54.

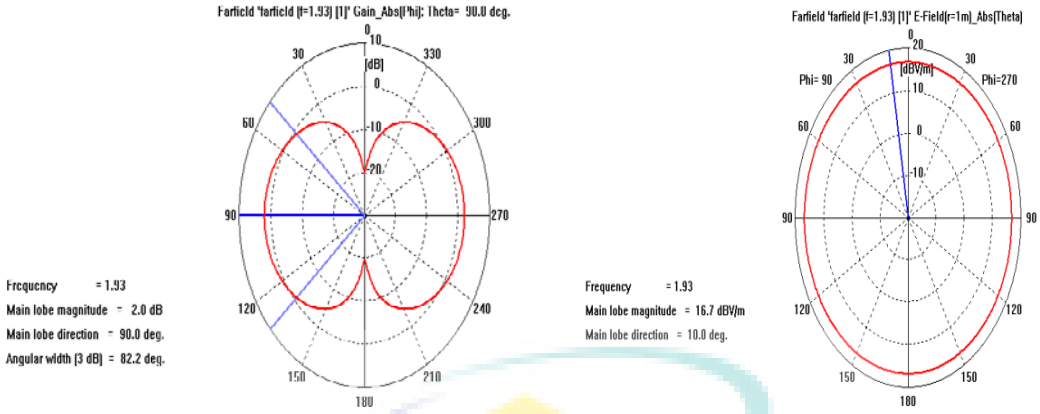

Figure 4.53: Radiation Pattern (a) E-Plane, and (b) H-Plane at 1.93 GHz

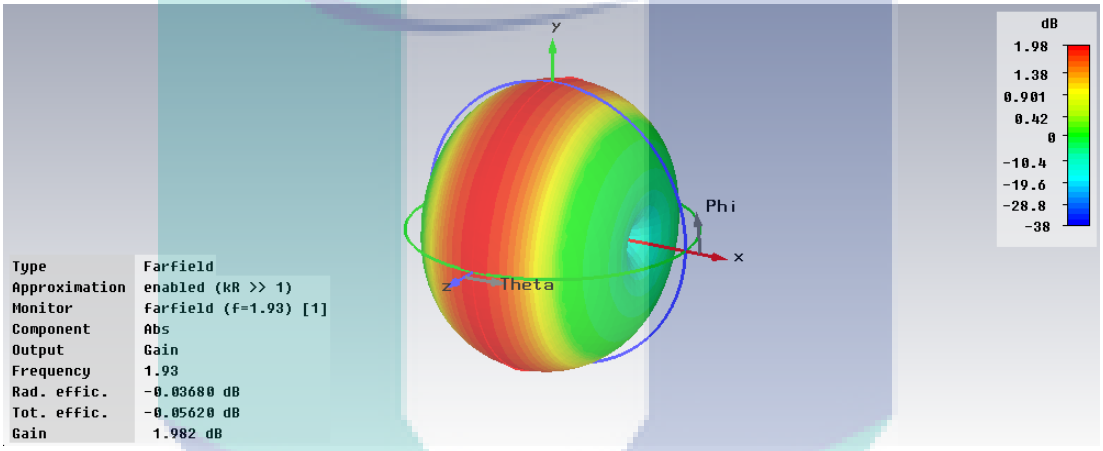

Figure 4.54: 3-D Radiation Pattern at 1.93 GHz

The radiation pattern in E-plane and H-plane is shown in Figure 4.55a and Figure 4.55b. The radiation pattern in 3D at frequency 4.64GHz is shown Figure 4.56.

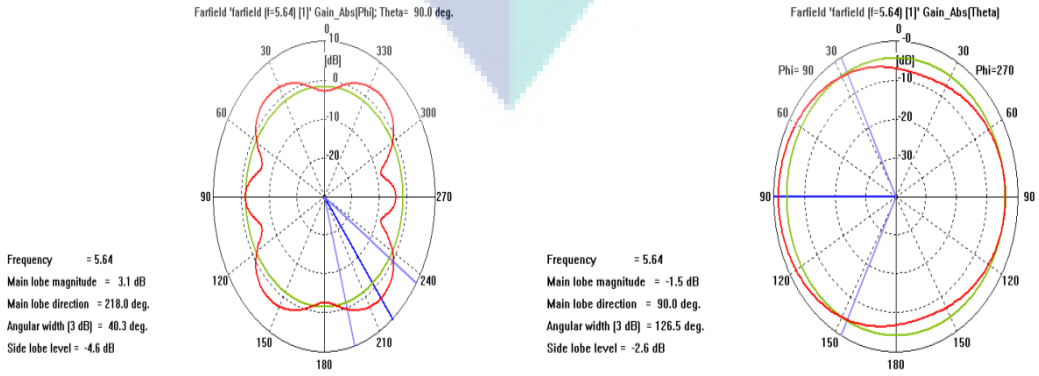

Figure 4.55: Radiation Pattern (a) E-Plane, and (b) H-Plane at 5.64GHz

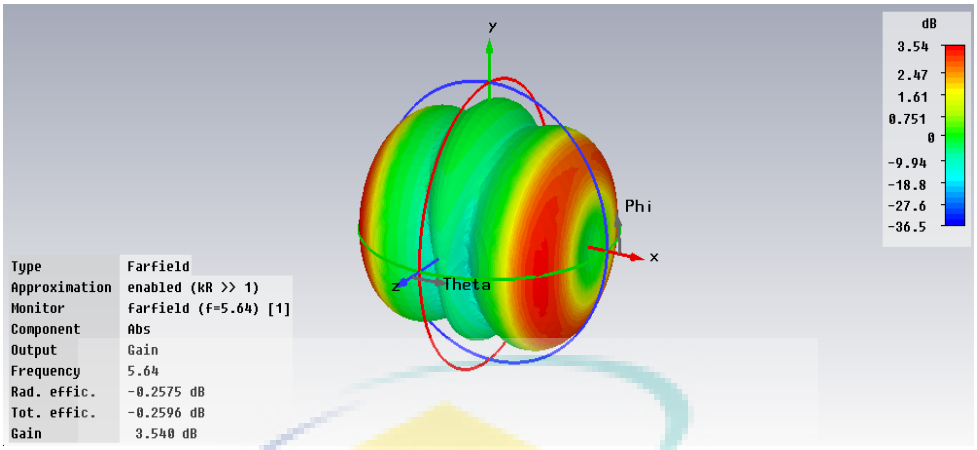

Figure 4.56: 3-D Radiation Pattern at 5.64 GHz

Table 4.16 shows the summary of results and Table 5.17 shows the summary of radiation patterns. Here, return losses and VSWRs are significantly worse as compared to Koch middle one-third antenna at iteration 2.

Table 4.16: 2nd Iteration, Koch Left One-Third Antenna

n-resonant frequency	F (GHz)	S11 (dB)	VSWR	%BW (fH-fL)/fC	Ratio of resonant freq. f-2/f-1
1	1.93	-23.50	1.14	8.8	2.29
2	5.64	-32.94	1.04	3.3	

Table 4.17: 2nd Iteration, Radiation Pattern of Koch Left One-Third Antenna

Frequency (GHz)	HPBW (degree)	Gain (IEEE) (dB)	Dir. (dBi)
1.93	82.2	1.982	2.01
5.64	40.3	3.548	3.79

4.4.3 Third Iteration

To design the Koch left one-third antenna at Iteration 3, coordinates and its design in CST are given in Appendix C3. Figure 4.57 shows the return loss (S11) for frequency swept from 0 GHz to 10 GHz for the Koch left one-third antenna at 3rd iteration. It can be seen that the shape works as antenna at three frequencies 1.66GHz

(with the return loss of -25.43dB), 4.72GHz (with the return loss of -11dB),and 7.39GHz (with return loss -16dB). The antenna has multi-band characteristics.

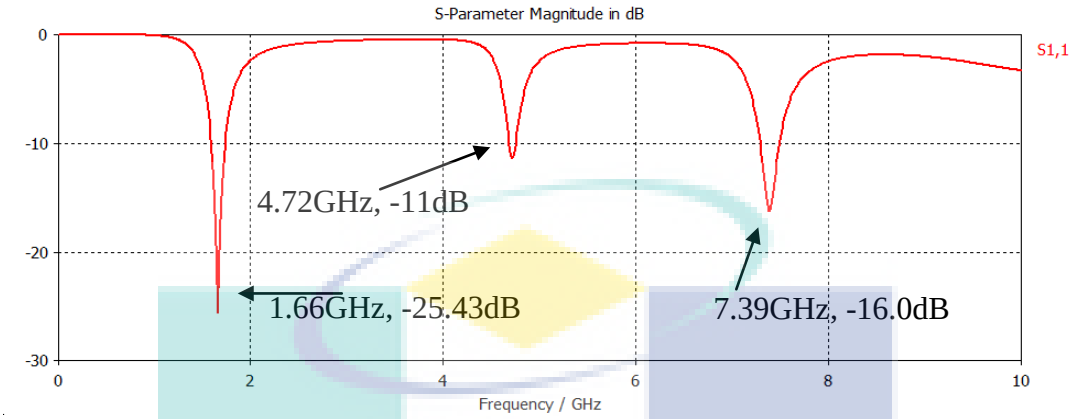

Figure 4.57: Return Loss S11 at 1.66, 4.72, 7.39 GHz

Figure 4.58 shows the simulated VSWR from 0-10 GHz. VSWR is 1.11 at 1.66 GHz, 1.73at 4.72 GHz and 1.36 at 7.39GHz.

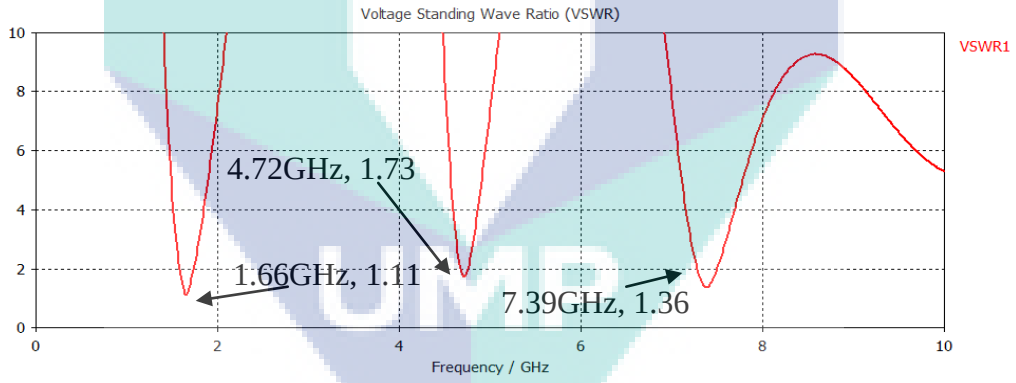

Figure 4.58: VSWR at 1.66, 4.72, 7.39 GHz

Radiation Pattern and Antenna Gain

The radiation pattern at 1.66GHz in E-plane and H-plane is shown in Figure 4.59a and Figure 4.59b. The radiation pattern in 3D at frequency 1.66 GHz is shown Figure 4.60

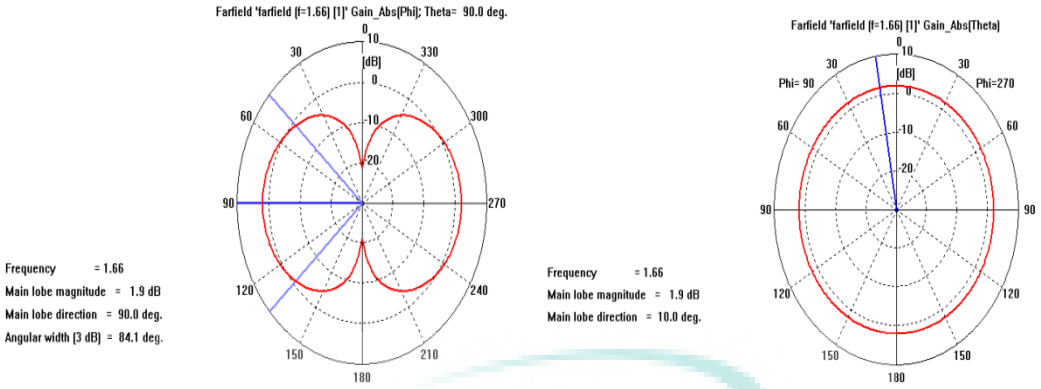

Figure 4.59: Radiation Pattern (a) E-Plane, and (b) H-Plane at 1.66GHz

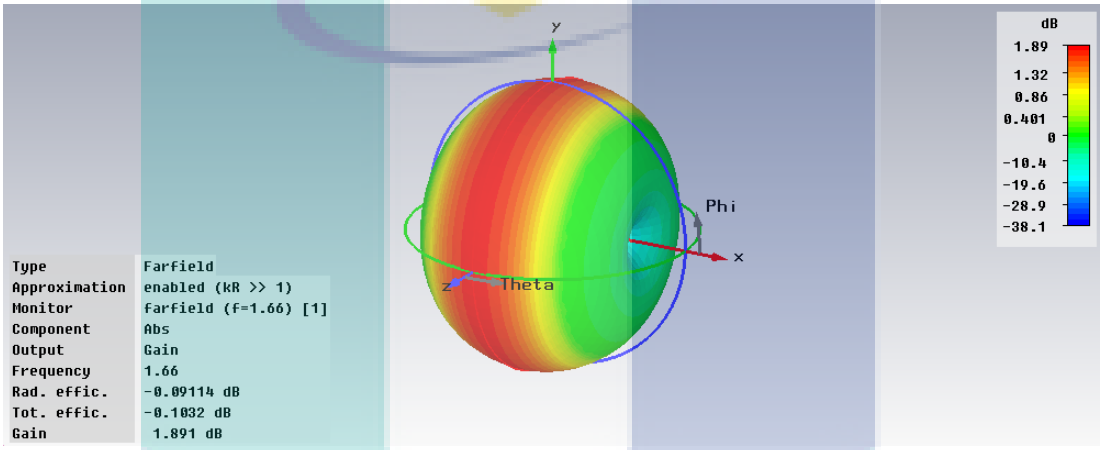

Figure 4.60: 3-D Radiation Pattern at 1.66 GHz

The radiation pattern at 4.72 GHz in E-plane and H-plane is shown in Figure 4.61a and Figure 4.61b. The radiation pattern in 3D at frequency 4.72 GHz is shown Figure 4.62.

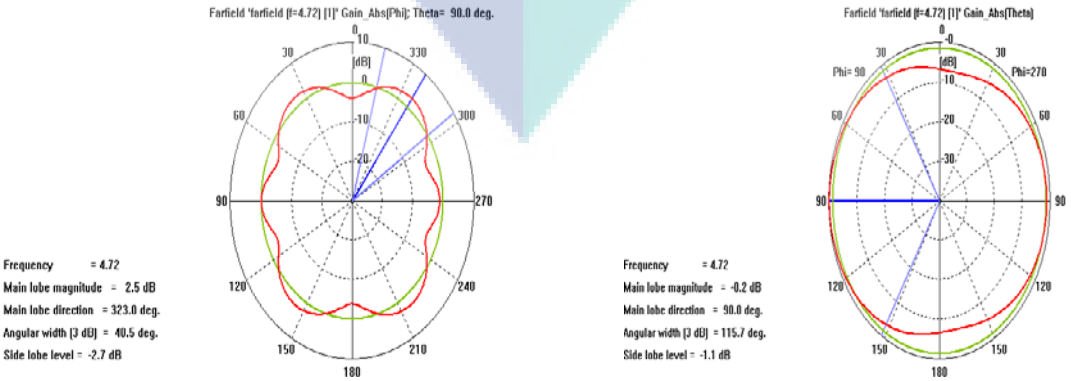

Figure 4.61: Radiation Pattern (a) E-Plane, and (b) H-Plane at 4.72 GHz

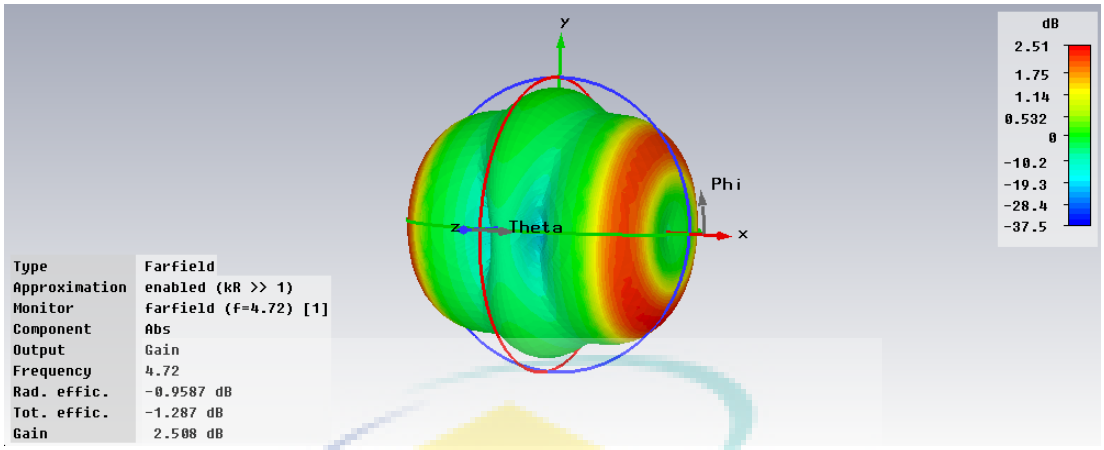

Figure 4.62: 3-D Radiation Pattern at 4.72 GHz

The radiation pattern at 7.39GHz in E-plane and H-plane is shown in Figure 4.63a and Figure 4.63b. The radiation pattern in 3D at frequency 7.39 GHz is shown Figure 4.64.

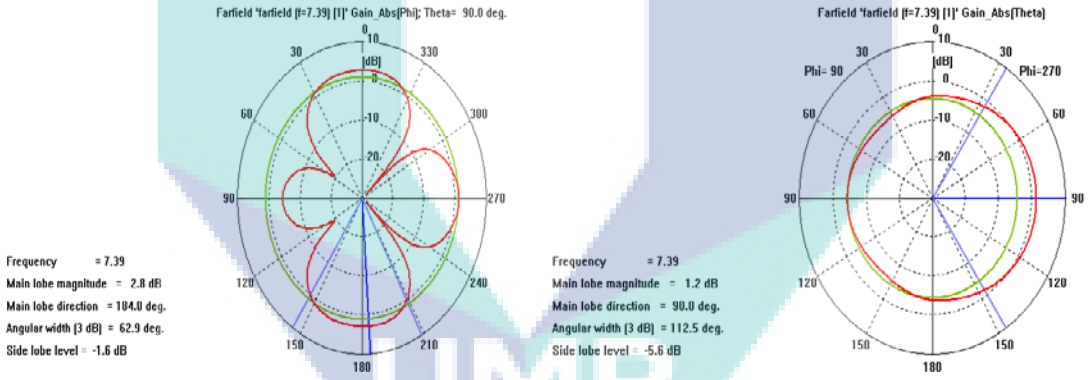

Figure 4.63: Radiation Pattern (a) E-Plane, and (b) H-Plane at 7.39GHz

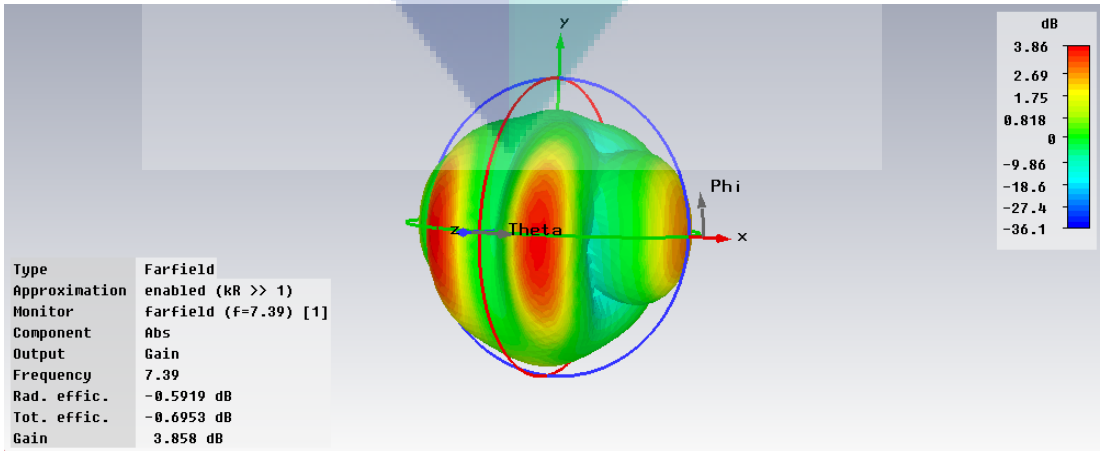

Figure 4.64: 3-D Radiation Pattern at 7.39GHz

Table 4.18 shows the summary of results and Table 4.19 shows the summary of radiation patterns. It can be compared that performance of antenna here is very much poor as compared to Koch middle one-third antenna at iteration 3.

Table 4.18: 3rd Iteration, Koch Left One-Third Antenna

n-resonant frequency	F (GHz)	S11 (dB)	VSWR	%BW (fH-fL)/fC	Ratio of resonant freq. f-2/f-1	Ratio of resonant eq. f-2/f-1
1	1.66	-25.43	1.11	8.4	2.84	1.56
2	4.72	-11.	1.73	1.4		
3	7.39	-16	1.36	2.7		

Table 4.19: 3rd Iteration, Radiation Pattern of Koch Left One-Third Antenna

Frequency GHz)	HPBW (degree)	Gain (IEEE) (dB)	Dir. (dBi)
1.66	84.1	1.891	1.98
4.72	40.5	2.508	3.46
7.39	62.9	3.858	4.45

4.4.4 Comparison of Antenna at All Three Iterations

Return loss comparison is shown for Koch left one-third iteration at Iteration 1, 2 and 3 in Figure 4.65. VSWR comparison graph for all the three iterations is shown in Figure 4.66.

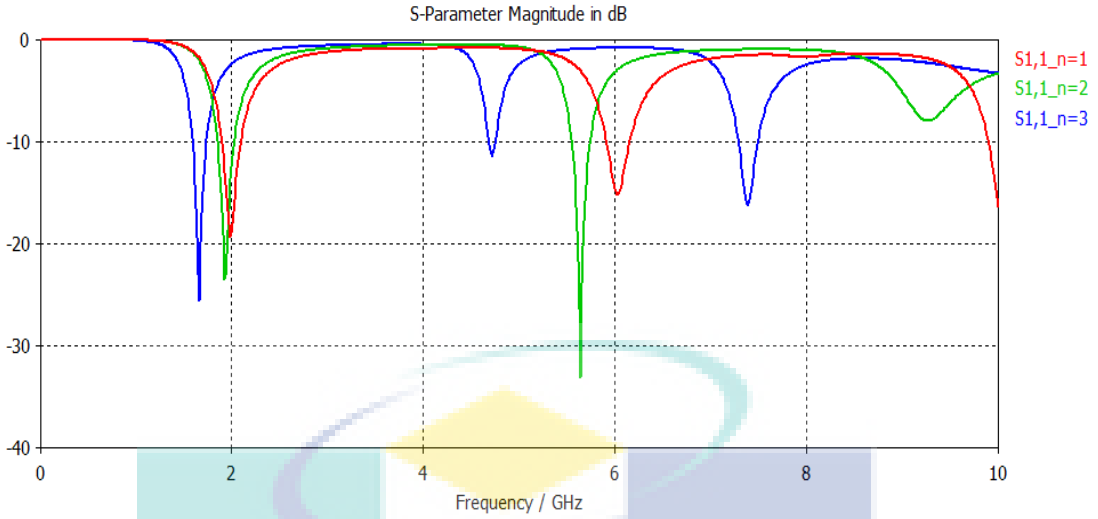

Figure 4.65: Return Losses at Iteration 1, 2 and 3

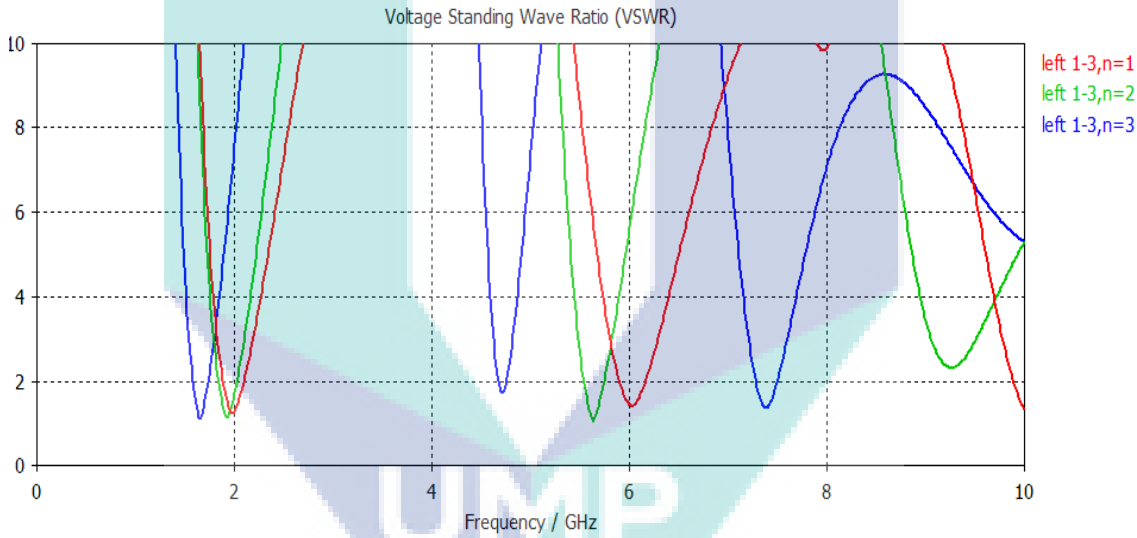

Figure 4.66: VSWRs at Iteration 1, 2 and 3

It can be observed from Figure 4.65 that overall return loss in the minimum at iteration 2. Also, Figure 4.66 shows that VSWR is not much affected by iterations. So, Koch left one-third antenna will perform its best when designed at iteration 2.

4.5 COMPARATIVE STUDY OF THE THREE ANTENNAS

Comparison of Koch middle one-third and Koch middle one-fifth antennas is given in Table 4.20

Table 4.20: Comparison of Koch middle one-third antenna and Koch middle one-fifth antenna

Iteration	**Koch middle one-third antenna**	**Koch middle one-fifth antenna**	**Remarks**
1 Frequency resonance (in GHz)	2.16 6.63	2.17 6.79	Almost similar performance
Return Loss (in dB)	-18.87 -13.44	-18.45 -13.60	+0.42 -0.16
VSWR	1.25 1.54	1.271 1.527	+0.021 -0.013
% of Bandwidth	10 3.5	9.8 3.7	-0.2 +0.2
Second Iteration			
2 Frequency resonance (in GHz)	2.01 5.90	2.13 6.45	Poor performance
Return Loss (in dB)	-35.842 -38.37	-23.33 -16.20	+12.512 +22.17
VSWR	1.032 1.02	1.146 1.366	+0.114 +0.346
% of Bandwidth	8.9 3.4	9.3 3.6	+0.4 +0.2
Third Iteration			
3 Frequency resonance (in GHz)	1.93 5.69 9.63	1.96 5.78 9.31	Overall significantly better performance
Return Loss (in dB)	-36.27 -14.86 -25.98	-45.44 -34.31 -13.81	-9.17 -19.45 +12.17
VSWR	1.03 1.43 1.105	1.01 1.039 1.51	-0.02 -0.391 +0.405
% of Bandwidth	8.8 3.5 2.2	9.8 13.8 2.6	+1.0 +10.3 +0.4

Generally, fractal antennas are designed for Iteration 3 or 4. From Table 4.20, it can be observed that at Iteration 3, in comparison of Koch middle one-third antenna, return loss of Koch middle one-fifth antenna decreases significantly for first two resonant frequencies by 9.17 dB and 19.45 dB respectively. VSWR also reduces for the first two resonant frequencies by 0.02 and 0.391 respectively. Further, there is increase in bandwidth at all the three frequencies, especially at second resonant frequency, where bandwidth increased by 10.3 %.

Thus, it is clear that the Koch middle one-fifth antenna performs better than the Koch middle one-third antenna. The result is, also, supported by the fact that since fractal dimension of the Koch middle one-fifth curve is lesser than the Koch middle one-third curve, therefore, Koch middle one-fifth curve will have better antenna properties.

Also, comparison of Koch middle one-third antenna and Koch left one-third antenna is given in Table 4.21. It can be seen in Table 4.21 that at Iteration 3, Koch left one-third antenna has more return loss and higher VSWRs than the Koch left one-third antennas. Thus, Koch left one-third antenna has poor performance than the Koch left one-third antenna. It can work efficiently only at first iteration.

Table 4.21: Comparison of Koch middle one-third antenna and Koch left one-third antenna

Iteration	Koch middle one-third antenna	Koch left one-third antenna	Remarks
1 Frequency resonance (in GHz)	2.16 6.63	1.99 6.03	Better performance
Return Loss (in dB)	-18.87 -13.44	-19 -15	-0.13 -1.56
VSWR	1.25 1.54	1.19 1.39	-0.06 -0.15
% of Bandwidth	10 3.5	10 3.9	0 +0.4
Second Iteration			
2 Frequency resonance (in GHz)	2.01 5.90	1.93 5.64	Poor performance
Return Loss (in dB)	-35.842 -38.37	-23.50 -32.94	+12.342 +5.43
VSWR	1.032 1.02	1.14 1.04	-0.108 +0.02
% of Bandwidth	8.9 3.4	8.8 3.3	-0.1 -0.1
Third Iteration			
3 Frequency resonance (in GHz)	1.93 5.69 9.63	1.66 4.72 7.39	Poor performance
Return Loss (in dB)	-36.27 -14.86 -25.98	-25.43 -11 -16	+10.84 +3.86 +9.98
VSWR	1.03 1.43 1.105	1.11 1.73 1.36	+0.08 +0.3 +0.255
% of Bandwidth	8.8 3.5 2.2	8.4 1.4 2.7	-0.4 -2.1 +0.5

4.6 SUMMARY

The three antenna geometries Koch middle one-fifth curve, Koch left one-third curve and conventional von Koch middle one-third curve have been simulated and performance of Koch middle one-fifth curve and Koch left one-third curve have been compared with the conventional von Koch middle one-third curve.

It was found that Koch middle one-fifth antenna performs better than the Koch left one-third antenna. Further, Koch one-third curves have same dimensions. But by changing the main antenna portion from middle to left degrades the performance of antenna.

CHAPTER 5

CONCLUSION AND FUTURE WORK

5.1 CONCLUSION

New variants of fractal Koch curve and Koch snowflakes have been designed by dividing the initiator, mainly, into three unequal parts. The new Koch curves belong to the gallery of superior fractals. Applying the same idea, many other variants of Koch models can be generated. So, there is a need to systematize them in literature. A classification of Koch curves is given for their systematic generation (Chapter 3).

Also, for systematic and easy generation of Koch curves via L-system, two general production rules have been given. Due to the change in method of generation, geometrical properties of the Koch fractals change. General formulas have been given for calculation of perimeter, area and fractal dimension of the Koch fractals. These new geometries, theoretically, prove that new Koch curves of lesser dimension will perform better as antenna in communication (Chapter 3).

To visualize the theoretical findings, three antennas have been simulated: Koch middle one-third antenna, Koch middle one-fifth antenna, and Koch left one-third antenna. Koch middle one-fifth antenna has lesser dimension than and Koch left one-third has equal dimension to the Koch middle one-third antenna. Both the new antennas were compared with the Koch middle one-third antenna and it was found that Koch middle one-fifth antenna performs better than the Koch middle one-third antenna.

Further, Koch one-third curves have same dimensions, but it was found that by changing the main antenna portion from middle to left degrades the performance of antenna.

5.2 LIMITATION OF THE STUDY

The antennas proposed by the method of unequal division in the study have following limitations:

(i) The antennas generated by further reduced scaling factors, e.g. 1/7, 1/8, 1/9, 1/10…. are converging to flat antenna. Though these antennas are further of lesser dimension, but due to the flattening tendency, they may not give the desired result.

(ii) Proposed Koch antennas are suitable where antenna is fabricated on circular space. It is not a good idea to fabricate Koch antennas on square or triangle antenna space as Koch antennas do not utilize the available space fully.

.

5.3 FUTURE WORK

Koch middle one-fifth curve, which has lesser dimension than the Koch middle one-third curve proves itself a better antenna. This result encourages to find the antenna characteristics of Koch middle one-sixth curve, which has further lesser dimension than the Koch middle one-fifth curve. Similarly, many curves of lesser dimensions can be obtained in Category 2, and tested as antenna.

Also, since change in location of main portion of antenna, changes its characteristics, therefore it is a matter of further investigation that how the performance changes with the change in location of main portion of antennas of the same dimension. For example,

I. The performance difference between Koch left one-fifth and Koch right one-fifth curves

II. The performance difference between Koch left one-sixth, Koch right one-sixth curves etc.

REFERENCES

Almong, Benyamin, Arie(IL), Beit, Habib, Laurent & Shapira(IL), Moshav. 2006. Fractal dipole Antenna. US patent, US2006/0170604A1.

Baliarda, C. P, Romeu, J. & Cardama, A. 2000. The Koch monopole: A small fractal antenna. *IEEE Trans. Antennas Propag.*, 48: 1773-1781.

Baliarda, C. P., Romeu, J., Pous, R., Ramis, J. & Hijazo, A. 1998. Small but long Koch fractal monopole. *Electron. Lett.*, 34: 9-10.

Barcellos, Anthony. 1984. The fractal geometry of Mandelbrot. *The College Mathematics Journal*, 15(2): 98-114.

Barnsley, M. F. 2006. *Superfractals*. UK: Cambridge University Press.

Barnsley, Michael F. & Rising, Hawley. 1993. *Fractals Everywhere.* 2nd ed. Boston: Academic Press Professional.

Best, S. R. 2005. The Koch Fractal Monopole Antenna: The Significant of Fractal Geometry in Determining Antenna Performance. Technical Report. Manchester, NH: Cushraft Corporation.

Briggs, J. 1992. *Fractals: The Patterns of Chaos.* London: Thames and Hudson.

Bunde, Armin & Havlin, Shlomo (Eds.). 1994. *Fractals in Science*. Berlin, Heidelberg: Springer-Verlag.

Chandra, M. & Rani, M. 2009. Categorization of fractal plants. *Chaos, Solitons, Fractals*, 41(3): 1442-1447.

Chang, Hung-Yue, Fang, Chen-Hsing, Cheng, Wei-Li & Chen, Chih-Lung. 2007. Multi-band antenna and design method thereof. US patent. 7209081B2.

Cohen, N., 1996. Fractals' new era in military antenna. http://mobiledevdesign.com/hardware_news/radio_fractals_new_era/

Cohen, N. 1997. Fractal antenna applications in wireless telecommunications. *IEEE Proc. of Electronics Industries Forum*, 43-49.

Cohen, Nathan. 2006. Fractal antenna ground counterpoise, ground planes, and loading elements and microstrip patch antennas with fractal structure. US patent.7019695B2.

Crilly, A. J., Earnshaw, R. A. & Jones, H. 1991. *Fractals and Chaos*. New York: Springer-Verlag

Crownover, Richard M. 1995. *Introduction to Fractals and Chaos*. Boston, London: Jones & Barlett Publishers.

Dietel, Paul & Dietel, Harvey. 2005. *C++ How to Program*. 5th ed. New Jersey: Prentice Hall.

Edgar, Gerald A. 1990. *Measure, Topology and Fractal Geometry*. New York: Springer-Verlag.

Elkamchouchi, Hassan & Mustafa, Abu Nasr. 2007. 3D fractal rectangular Koch dipole and Hilbert dipole antennas. *IEEE Int. Conf. on Microwave and Millimeter Wave Technology*, 1 - 4.

Epstien, M. & Adeeb, Sameer M. 2008. The stiffness of self-similar fractals. *Int. J. Solids Struct.*, 45: 3238-3254.

Falconer, K. 2003. *Fractal Geometry: Mathematical foundations and applications.* Second edition. Hoboken, NJ: John Wiley & Sons.

Fractus, S. A. 2000. New fractal antennas for compact and versatile telecommunication service. *Microw. J.*, 43(1): 1, 196, 198, 200, 202, 204.

Garcia, E. 2005. Fractal Patterns, L-Systems and Semantics. The Fractal Nature of Semantics. Islita.com material.

Ghatak, Rowdra, Poddar, Dipak R. & Mishra, Rabindra K. 2009. A moment-method characterization of V-Koch fractal dipole antennas. *Int. J. Electron. Commun. (AEU)*, 63: 279-286.

Gottfried, Byron. 1996. *Programming with C.* 2nd ed. New York: McGraw-Hill.

Harish, A. R. & Joshi, R. K. 2007. Studies on application of fractal based geometries in printed antenna structures. in: IEEE Proc. Applied Electromagnetics Conference (AEMC) 2007. 1 – 4.

Hohlfeld R. & Cohen, N. 1999. Self-similarity and the geometric requirements for frequency independence in antenna. *Fractals*, 7(1): 79-84.

Jackson, William. 2004. Fractals in Indian architecture. http://classes.yale.edu/fractals/panorama/Architecture/IndianArch/IndianArch.html

Kanetker, Yashwant P. 2008. *Let Us C*. New Delhi: Jones & Bartlett.

Kordzadeh, A. & Kashani, F. Hojat. 2009. A new reduced size microstrip patch antenna with fractal shaped defects. *Prog. Electrom. Res.*, 11: 29-37.

Krishna, D. D., Gopikrishna, M., Anandan, C. K, Mohanan, P. & Vasudevan, K. 2009. Compact wideband Koch fractal printed slot antenna. *IET Microw. Antennas Propag*, 3(5): 782-789.

Kumar, Sandeep. 2010. *A New Approch to Fractal Graphics and Their Application*. Lucknow, India: Uttar Pardesh Technical University.

Mandelbrot, B. B. 1982. *The Fractal Geometry of Nature*. New York: W. H. Freeman and Co.

Mann, W. R. 1953. Mean value methods in iteration. *Proc. Amer. Math. Soc.*, 4: 506-510

McClure, M. 2008. Images of a vibrating Koch drum. *Computers & Graphics*, 32: 711-715.

Mirzapour, B. & Hassani, H. R. 2009. Size reduction and bandwidth enhancement of snowflake fractal antenna. *IET Microw. Antennas Propag.*, 2(2): 180-187.

Patwardhan, K. S., Naimpally, S. A. & Singh, S. L, 2001. *Lilavati of Bhaskaracharya.* Delhi, India: Motilal Banarsidass.

Peitgen, H. O., Henriques, J. M. & Penedo, L. F. (Eds.). 1991. *Fractals in the Fundamental and Applied Sciences*. Amsterdam: North Holland.

Peitgen, H. O., Jürgens, H. & Saupe, D. 2004. *Chaos and Fractals: New frontiers of science*. New York: Springer-Verlag.

Peitgen, H. O. & Richter, P. H. 1986. *The Beauty of Fractals*. Heidelberg: Springer-Verlag.

Peitgen, H. & Saupe, D. (Eds). 1988. The *Science of Fractal Images*. New York: Springer-Verlag.

Prasad, Sanjeev. 2009. *Superior Cantor Sets and Superior Devil's Staircases in Fractal Graphics*. Lucknow, India: Uttar Pardesh Technical University.

Rani, M. 2005. Fractals in Vedic heritage and fractal carpets. *Proc. National seminar on History, Heritage and Development of Mathematical Sciences*, 110-121.

Rani, M. 2002. *Iterative Procedures in Fractals and Chaos*. Ph. D. Thesis. Haridwar, India: Gurukula Kangri Vishwavidyalaya.

Rani, M. & Agarwal, R. 2010. Effect of stochastic noise on superior Julia sets. *J. Math. Imaging & Vis*., 36: 63-68.

Rani, M. & Goel, S. 2009. Categorization of new fractal carpets. *Chaos, Solitons, Fractals*, 41(2): 1020-1026.

Rani, M. & Kumar,V. 2002. A fractal hedgehog theorem. *J. Korea Soc. Math. Educ. Ser. B; Pure & Appl. Math*., 9(2): 91-105.

Rani, M. & Kumar, V. 2004a. New fractal carpets. *Arab. J. Sci. Eng.*, Sect. C Theme Issues, 29(2): 125-134.

Rani, M. & Kumar, V. 2004b. Superior Julia set. J. *Korea Soc. Math. Educ., Ser. D; Res. Math. Educ*., 8(4): 261-277.

Rani, M. & Kumar, V. 2004c. Superior Mandelbrot set. *J. Korea Soc. Math. Educ., Ser. D; Res. Math. Educ*., 8(4): 279-291.

Rani, M. & Prasad, S. 2010. Superior Cantor sets and superior Devil's staircases. *Int. J. Artif. Life Res*., 1(1): 78-84.

Schroeder, M. 1991. *Fractals, Chaos, Power Laws: Minutes from an infinite paradise*. New York: W. H. Freeman and Company.

Sengufta, Kaushik. 2005. Influence of fractal lacunarity on the performance of dipole antennas with generalized Koch curves. Proc. *18th Int. conf. Applied Electromagnetic sand Communication, IECCom*, 1-4.

Song, X. D., Fu, J. M. & Wang, W. 2008. Design of a miniaturized dual band Koch fractal boundary microstrip antenna. *IEEE Microwave Conference*, 282 – 284.

Stevens, R. T. 1989. *Fractal Programming in C*. Redwood City, CA: M&T Books.

Strycek, M. & Hertl, I. 2007. Fractal log-periodic Antenna. *in: IEEE Proc. RadioElektronika, 17th international conference*. 1-3.

Tang, Philip Wan Sing. 2002. *Fractal Antennas*. Ph. D. Thesis. Orlando, USA: University of Central Florida.

Varadan, Vijay K., Vinoy, Kalarickaparambil J., Jose, Kollakompil A., Varadan, Vasundara V. 2003. Miniaturized conformal wideband fractal antennas on high dielectric substrates and chiral layers. US patent. 6525691B2.

Veerasamy, Vijayen S., 2003. Vehicle windshield with fractal antenna.US patent. 6552690B2.

Vinoy, K. J. 2002. *Fractal Shaped Antenna Elements for Wide-Band Wireless Application*. Ph. D. Thesis. Pennsylvania: The Pennsylvania University.

Vinoy, K. J., Abraham J. K. & Varadan, V. K. 2003. On the relationship between fractal dimension and the performance of multi-resonant dipole antennas using Koch curves. *IEEE Trans. Ant. Propag.*, 51: 2296-2303.

Vinoy, K. J., Jose, K. A., & Varadan, V. K. 2004. Impact of fractal dimension in the design of multi-resonant fractal antennas. *Fractals*. 12: 55-66.

Vinoy, K. J., Jose, K. A, & Varadan. 2002. Multi-band characteristics and fractal dimension of dipole antennas with Koch curve geometry. *Antennas and Propagation Society International Symposium*, 4: 106-109.

Vinoy, K. J., Jose, K. A., Varadan, V. K & Varadan, V. V. 2001. Hilbert curve fractal antenna: a small resonant antenna for VHF/UHF applications. *Microwave Optical Technol. Lett.*, 29: 215-219.

Werner, Douglas H. & Ganguly, Suman. 2003. An overview of fractal antenna engineering research. *IEEE Antennas Propag. Mag*., 45(1): 38-57.

Werner, Douglas H., Haupt, R. L. & Werner, P. L. 1999. Fractal antenna engineering: The theory and design of fractal antenna arrays. *IEEE Ant. Propag. Mag.*, 41(5): 37-59.

Wohlberg, B. & Jager, G. De. 1999. Review of the fractal image coding literature. *IEEE. Trans. Image Process.*, 8(12): 1716-1729.

Zhang, Yizhe & Kishk, Ahmed A. 2006. Analysis of dually polarized fractal antennas. *in: Proc. Antennas and Propagation Society International Symposium*, 2041 – 2044.

PUBLICATIONS

(1) Superior Fractal Antennas, Malaysian Technical Universities Conference on Engineering and Technology, Melaka, Malaysia, Jun 28-29, 2010, 23-26.

(2) Categorization of superior Koch fractal antennas, in: IEEE Proc. International Conference on Intelligence and Information Technology, ICIIT 2010, Lahore, Pakistan, Oct 28-30, 2010, vol. 6, 551-554.

(3) New Koch Curves and Their Classification, Chaos & Complexity Letters, 6(3), 2011.

(4) Koch Curves: Rewriting System, Geometry and Application, Journal of Computer science, 7(9), 2011, 1358-1362.

APPENDIX A1

KOCH MIDDLE ONE-THIRD CURVE, 1ST ITERATION

Coordinates

No	X	Y
1	.125	.05
2	9.333	.05
3	14	8.132
4	18.666	.05
5	28	.05
6	28	0.0
7	18.66	0.0
8	14	8.132-.05
9	9.333	0
10	.125	0

Design in CST

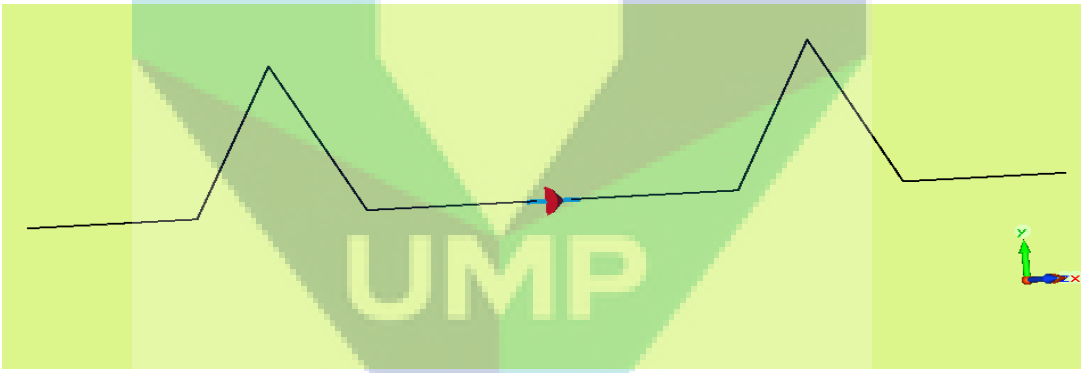

APPENDIX A2

KOCH MIDDLE ONE-THIRD CURVE, 2nd ITERATION

Coordinates

No	X	Y	No	X	Y
1	.125	-.05	18	28	-0.1
2	3.111	-.05	19	24.96	-.1
3	4.66	-.146	20	23.33	-.292
4	6.22	-0.05	21	21.77	-.1
5	9.33	-.05	22	18.66	-.242
6	10.88	-.146	23	17.11+.05	-.146
7	9.33	-.242	24	18.66	-.242
8	12.44	-.242	25	15.55	-.242
9	14	-.338	26	14	-.338
10	15.55	-.242	27	12.44	-.242
11	18.66	-.242	28	9.33	-.242
12	17.11	-.146	29	10.38	-.146
13	18.66	-.05	30	9.33	-.05
14	21.77	-.05	31	6.22	-.05
15	23.33	-.146	32	4.66	-.146
16	24.96	-.05	33	3.11	-.05
17	28	-.05	34	.125	-.1

Design in CST

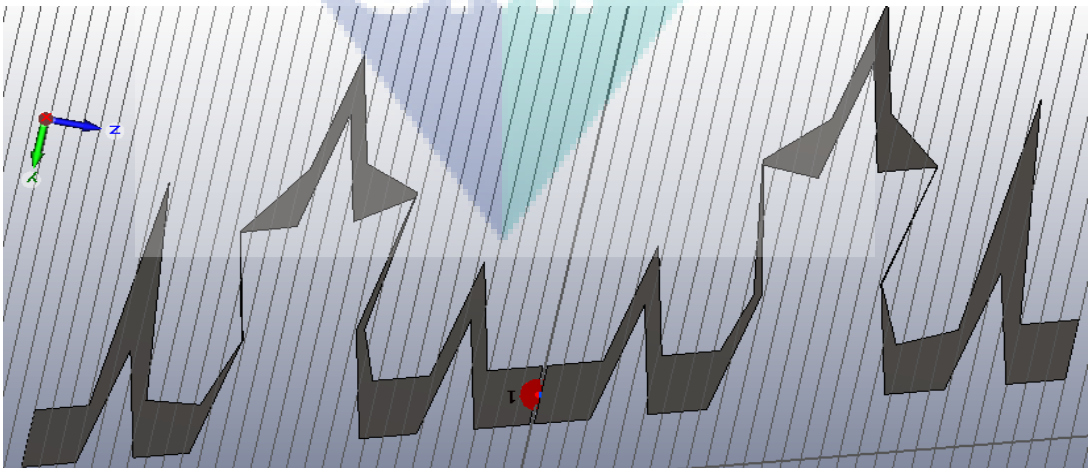

APPENDIX A3

KOCH MIDDLE ONE-THIRD DESIGN, 3rd ITERATION

Coordinates

No	X	Y	No	X	Y	No	X	Y
1	0.125	0.05	51	20.222	.082	101	12.962+0.005	0.274
2	1.037	0.05	52	20.74	.05	102	12.444	0.242-0.01
3	1.5	.082	53	21.777	.05	103	11.407	0.242-0.01
4	2.074	0.05	54	22.296	.082	104	10.888	0.274-0.01
5	3.111	0.05	55	21.777	.114	105	10.37	0.242-0.01
6	3.629	.082	56	22.814	.114	106	9.333+0.005	0.242-0.0001
7	3.111	.114	57	23.333	.146	107	9.851+0.005	0.21
8	4.27	.114	58	23.851	.114	108	9.333+0.005	0.178+0.0002
9	4.666	.146	59	24.888	.114	109	10.37	0.178+0.01
10	5.185	.114	60	24.37	.082	110	10.888+0.005	0.146
11	6.222	.114	61	24.888	0.05	111	10.37	0.114-0.01
12	5.703	.082	62	25.925	0.05	112	9.333+0.005	0.114-0.0001
13	6.222	0.05	63	26.44	0.082	113	9.851+0.002	0.082
14	7.259	0.05	64	26.962	0.05	114	9.333	0.05-0.01
15	7.777	.082	65	28	0.05	115	8.296	0.05-0.01
16	8.296	0.05	66	28	0.05-0.01	116	7.777	.082-0.01
17	9.333	0.05	67	26.962	0.05-0.01	117	7.259	0.05-0.01
18	9.851	.082	68	26.44	0.082-0.01	118	6.222	0.05-0.01
19	9.333	.114	69	25.925	0.05-0.01	119	5.703-.002	0.082
20	10.37	.114	70	24.888	0.05-0.01	120	6.222-0.003	0.114-0.0001
21	10.888	.146	71	24.370-0.0002	0.082	121	5.185	0.114-0.01
22	10.37	.178	72	24.888-0.005	0.114-0.00015	122	4.666	0.146-0.01
23	9.333	.178	73	23.851	0.114-0.01	123	4.27	0.114-0.01
24	9.851	.210	74	23.333	0.146-0.01	124	3.111+0.002	0.114-0.00004
25	9.333	.242	75	22.814	.114-0.01	125	3.629+0.003	0.082
26	10.37	.242	76	21.777+0.005	0.114-0.00015	126	3.111	0.05-0.01
27	10.888	.274	77	22.296+0.005	0.082	127	2.074	0.05-0.01
28	11.407	.242	78	21.777	0.05-0.01	128	1.5	0.082-0.01
29	12.444	.242	79	20.74	0.05-0.01	129	1.037	0.05-0.01
30	12.960	.274	80	20.222	0.082-0.01	130	0.125	0.05-0.01

31	12.444	.306	81	19.703	0.05-0.01			
32	13.481	.306	82	18.666	0.05-0.01			
33	14	.338	83	18.148-0.005	0.082			
34	14.518	.306	84	18.666-0.0005	0.114-0.000015			
35	15.555	.306	85	17.629	0.114-0.01			
36	15.037	.274	86	17.111-0.05	0.146			
37	15.555	.242	87	17.629	0.21+0.01			
38	16.592	.242	88	18.666-0.005	0.178+0.00022			
39	17.11	.274	89	18.148-0.005	0.21			
40	17.629	.242	90	18.666-0.005	0.242-0.00015			
41	18.666	.242	91	17.629	17.629			
42	18.148	.21	92	17.111	0.274-0.01			
43	18.666	.178	93	16.592	0.242-0.01			
44	17.629	.21	94	15.555	0.242-0.01			
45	17.111	.146	95	15.037-0.005	0.274			
46	17.629	.114	96	15.555-0.005	0.306-0.00015			
47	18.666	.114	97	14.518	0.306-0.01			
48	18.148	.082	98	14	0.338-0.01			
49	18.666	.05	99	13.481	0.306-0.01			
50	19.703	.05	100	12.444+0.005	0.306-0.0001			

Design in CST

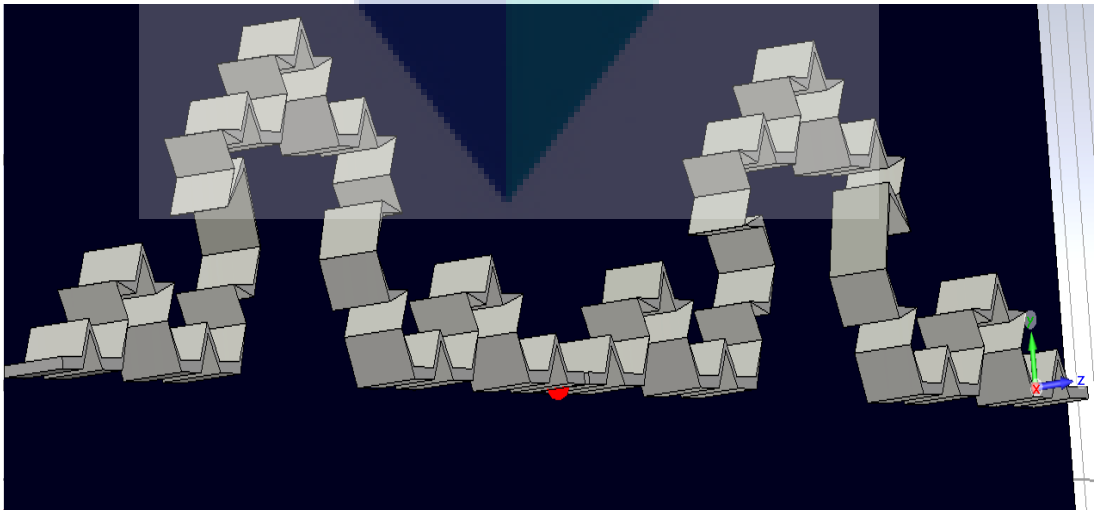

APPENDIX B1

MIDDLE ONE-FIFTH CURVE, 1ST ITERATION

Coordinates

No	X	Y
1	0.125	.05
2	11.2	0.05
3	14	4.89
4	16.8	0.05
5	28	0.05
6	28	-0.05
7	16.8	-0.05
8	14	4.7996
9	11.2	-0.05
10	.125	-0.05

Design in CST

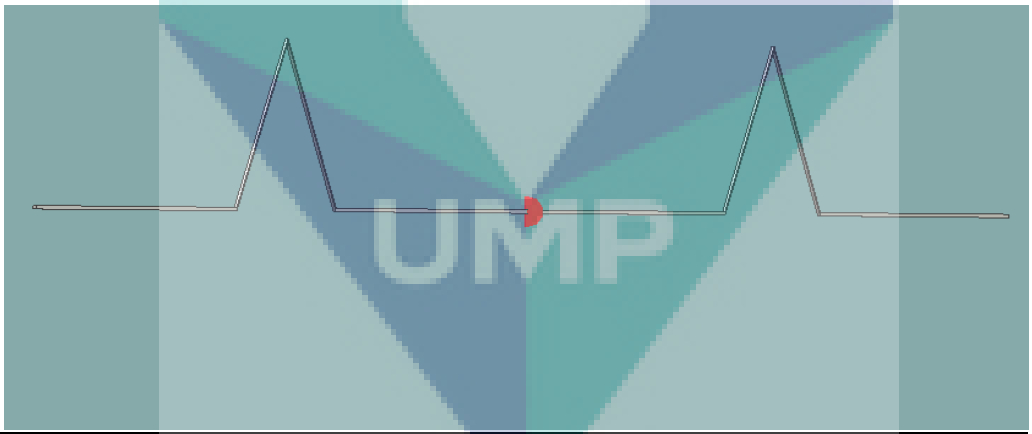

APPENDIX B2

MIDDLE ONE-FIFTH CURVE, 2ND ITERATION

Coordinates

No	X	Y	No	X	Y
1	.125	0.05	18	28	-0.05
2	4.48	0.05	19	23.52	-0.05
3	5.6	1.98	20	22.4	1.93-0.05
4	6.72	0.05	21	21.28	-0.05
5	11.2	0.05	22	16.8	-0.05
6	12.32	1.98	23	15.68-0.07	1.9876-0.02
7	11.76	2.959	24	16.24-0.13	2.959-0.1
8	12.88	2.959	25	15.12	2.959-0.1
9	14	4.899	26	14	4.899-0.05-0.05
10	15.12	2.959	27	12.88	2.959-0.05-0.02
11	16.24	2.959	28	11.76+0.05+.05	2.959-0.05-0.02
12	15.68	1.9876	29	12.32+0.05	1.98
13	16.8	0.05	30	11.2+0.05	-0.05
14	21.28	0.05	31	6.72-0.05	-0.05
15	22.4	1.98	32	5.6	1.98-0.05-0.05
16	23.52	0.05	33	4.48+0.05	-0.05
17	28	0.05	34	.125	-0.05

Design in CST

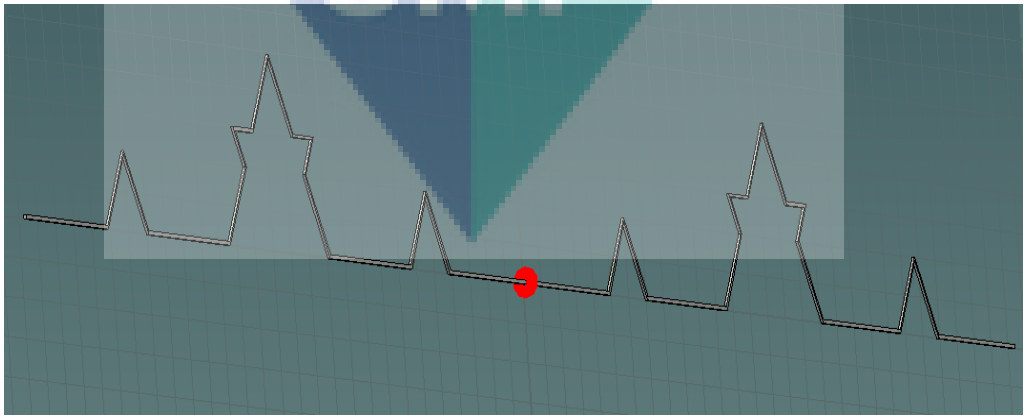

APPENDIX B3
MIDDLE ONE-FIFTH CURVE, 3RD ITERATION

Coordinates

No	X	Y	No	X	Y	No	X	Y
1	.125	0.05	51	19.04	.077	101	13.32+0.02	.181
2	1.79	0.05	52	19.48	0.05	102	12.88	.153-0.01
3	2.44	0.077	53	21.28	0.05	103	12.43	.153-0.005
4	2.68	0.05	54	21.72	0.077	104	12.32	.160-0.005
5	4.48	0.05	55	21.50	.091	105	12.20	.153-0.005
6	4.92	0.077+.0001	56	21.95	.091	106	11.76+0.02	.153-0.0005
7	4.70	0.091	57	22.4	.119	107	11.984+0.01	.140
8	5.15	.091	58	22.84	.0915	108	11.87+0.02	11.87+0.02
9	5.6	.119	59	23.29	.0915	109	12.096-.006	.133+0.0006
10	6.04	0.091	60	23.07	0.077	110	12.32+0.007	.1192
11	6.49	.091	61	23.52	0.05	111	11.872-.002	.091-0.002
12	6.27	.077	62	25.31	0.05	112	11.424+.001	.091-.00015
13	6.72	0.05	63	25.76	.077	113	11.648	.0777-.0001
14	8.15	0.05	64	26.20	0.05	114	11.2	0.05-0.005
15	8.96	.077	65	28	0.05	115	9.408-0.008	0.05-0.003
16	9.40	0.05	66	28	0.05-0.02	116	8.96	0.077-0.004
17	11.2	0.05	67	26.20	0.05-0.02	117	8.512-0.36	0.05-0.003
18	11.64	0.077+.0006	68	25.76	.077-0.02	118	6.72	0.05-0.003
19	11.42	.091	69	25.31	0.05-0.02	119	6.27-0.0003	.077-.00002
20	11.87	.091	70	23.52	0.05-0.02	120	6.496-0.025	.0915-.0009
21	12.32	.119	71	23.07-0.05	0.077	121	6.048-0.008	.091-0.0025
22	12.09	.133	72	23.29-0.02	.091-.0002	122	5.6	.1192-0.002
23	11.87	.133	73	22.84	.091-0.005	123	5.152	.0915-0.005
24	11.98	.140	74	22.40	.119-0.01	124	4.704+0.008	.0915-.0008
25	11.76	.153	75	21.95	.091-0.01	125	4.92+0.005	.077
26	12.20	.153	76	21.50+0.05	.091-.0015	126	4.48	0.05-0.003
27	12.32	.16	77	21.728-.002	.077	127	2.68	.05-0.003

28	12.43	.153	78	21.28	0.05-0.01	128	2.24+0.2	2.24+0.2
29	12.88	.153	79	19.48	0.05-0.01	129	1.79	0.05-0.003
30	13.32	.181	80	19.04	0.077-0.01	130	.125	.05-0.003
31	13.104	0.195	81	18.59	0.05-0.01			
32	13.552	.195	82	16.80	0.05-0.01			
33	14	0.223	83	16.35-0.003	0.077			
34	14.44	.195	84	16.57-0.01	.091-.0003			
35	14.89	.195	85	16.128-.008	.091-0.007			
36	14.67	.181-0.002	86	15.68-0.03	.119-0.001			
37	15.12	.153	87	15.904-.004	.113+0.005			
38	15.56	0.153	88	16.12-0.002	.113+.00025			
39	15.68	0.16	89	16.016-0.02	.140-0.0001			
40	15.79	.153	90	16.24-0.007	.153-0.0002			
41	16.24	.153	91	15.792-.002	.153-0.006			
42	16.01	.140	92	15.68	.16-0.004			
43	16.12	.113	93	15.568-.008	.153-0.004			
44	15.90	.113	94	15.120	.153-0.005			
45	15.68	.119-0.002	95	.153-0.005	.181-0.002			
46	16.12	.091	96	14.89-0.05	.195-0.002			
47	16.57	.091	97	14.44	.195-0.003			
48	16.35	.077	98	14	.223-0.002			
49	16.80	0.05	99	13.55	.195-0.003			
50	18.59	0.05	100	13.104+0.04	.195-0.001			

Design in CST

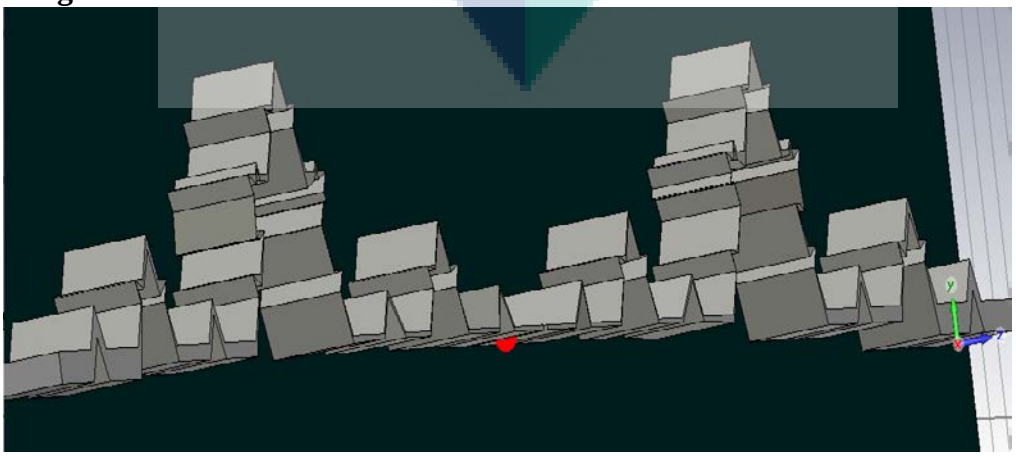

APPENDIX C1

KOCH LEFT ONE-THIRD, 1st ITERATION

Coordinates

No	X	Y
1	.125	0.05
2	4.66	8.132
3	9.333	0.05
4	28	0.05
5	28	-0.05
6	9.33	-0.05
7	4.66	8.132-0.05
8	.125	-0.05

Design in CST

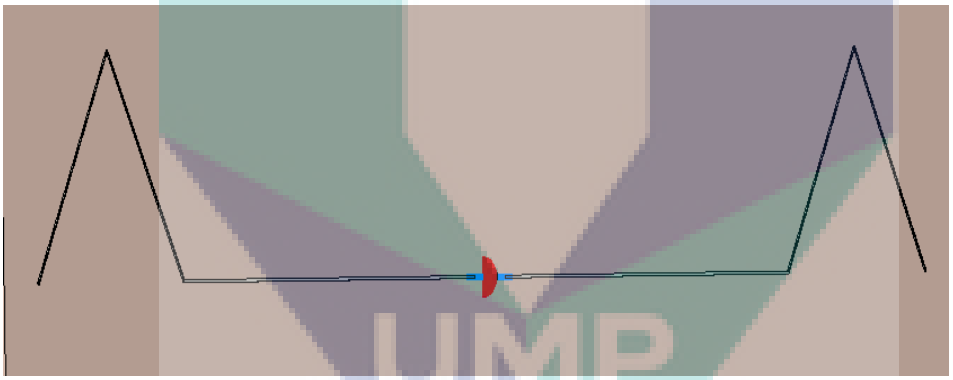

APPENDIX C2

KOCH LEFT ONE-THIRD CURVE, 2ND ITERATION

Coordinates

No	X	Y	No	X	Y
1	.125+.5	0.05	14	28+.5	0.05
2	-1.55+.5	2.7443	15	21.777+.5	-0.05
3	1.55+.5	2.744	16	20.22+.5	2.7443-0.01
4	4.666+.5	8.132	17	18.66+.5	-0.05
5	7.777+.5	8.132	18	12.44+.5	-0.05
6	6.22+0.5	5.4386	19	10.88+.5	2.7443-0.01
7	9.333+0.5	0.05	20	9.33+.5	-0.05
8	10.88+.5	2.7443	21	6.22+.5-.05	5.4386
9	2.7443	0.05	22	7.777+.5-.07	8.132-.05
10	18.66+0.5	0.05	23	4.666+0.5	8.132-0.05-0.05
11	20.22+.5	2.7443	24	1.55+.5	2.744-0.05-0.05
12	21.777+.5	0.05	25	-1.555+.5+.0	2.7443-0.05
13	28+.5	0.05	26	.125+.5-0	.05+.05

Design in CST

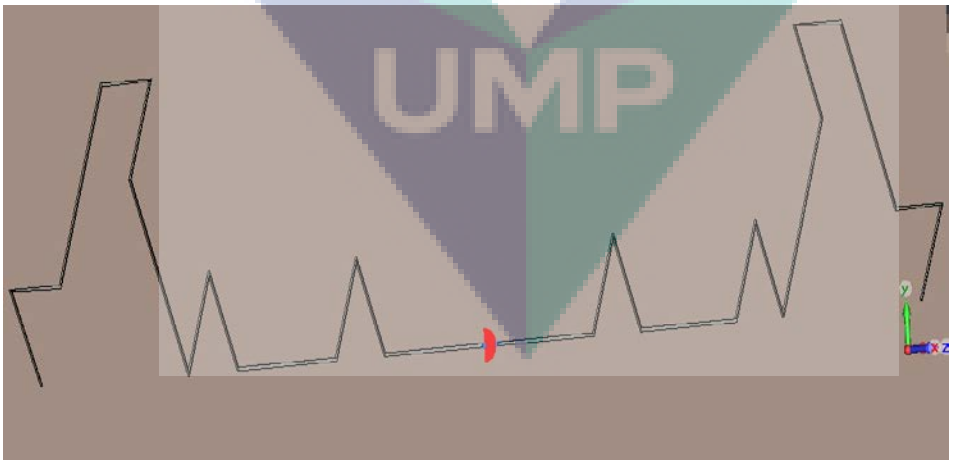

APPENDIX C3

KOCH LEFT ONE-THIRD CURVE, 3RD ITERATION

Coordinates

No	X	Y	No	X	Y
1	.125	0.05	50	22.814	-0.05
2	-1.1	0.05	51	22.296	.082-0.05
3	-.518	.1137	52	22.296	.082-0.05
4	-1.555	0.1	53	21.777	-0.02
5	-2.59	.128	54	20.7	.114
6	-0.518	0.146	55	21.2	.146-0.002
7	1.555	0.146	56	20.222	.146-0.02
8	1.039	.128-0.0042	57	19.185	.082-0.02
9	2.074	.128	58	18.18	.082-0.0008
10	3.111	.242	59	18.68	0.05+0.001
11	2.592	.274	60	16.59	0.03
12	3.629	.274	61	16.07	.082-0.02
13	5.185	.370	62	15.55	0.05-0.02
14	5.703	.33	63	13.481	0.05-0.02
15	7.777	.33	64	12.96	0.082-0.02
16	8.296	.306	65	12.444	0.05-0.02
17	7.259	.306	66	11.3	.114-0.02
18	6.233	.235	67	11.8	.146-0.005
19	7.259	.242	68	10.88	.146-0.02
20	6.740	.20	69	9.851	.082-0.05
21	7.777	.146	70	9.333	0.05-0.02
22	8.814	.146	71	8.2	.114-0.01
23	8.296	.114-0.01	72	8.7	.146-0.004
24	9.33	0.05	73	7.777	.146-0.01
25	9.851	.0820	74	6.68	.210-0.01
26	10.88	.146	75	7.2	.242-0.002
27	11.925	.146	76	6.15	.242-0.01
28	11.43	.10	77	7.26	.31
29	12.444	0.05	78	8.25	.3075
30	12.962	.082	79	7.777	.333-0.01
31	13.481	0.05	80	5.703	0.333-0.02
32	15.555	0.05	81	5.185	.370-0.02
33	16.07	0.082	82	3.62	3.62
34	16.59	0.05	83	2.599	.274-0.00015
35	18.66	0.051	84	3.125	.242+0.0005
36	18.148	0.082	85	2.075	.128-0.01
37	19.185	.082	86	1.025	.128-0.0045
38	20.222	.146	87	.128-0.0045	.145
39	21.259	.146	88	-0.518	.146-0.01
40	20.740	.114-0.002	89	-2.074	.125
41	21.77	0.05	90	-1.55	.11

42	22.296	.082	91	-.50	0.115
43	22.814	0.05	92	-1.0	0.055
44	24.888	0.05	93	.125	0.05+0.02
45	25.407	.082			
46	28	0.05			
47	28	-0.05			
48	25.407	.082-0.05			
49	24.888	-.05			

Design in CST